EXPLORING TWO NEW MODALITIES OF TOPOISOMERASE II-TARGETING DRUGS TO ENHANCE SPECIFICITY FOR CANCER CELLS

By

Lorena Infante Lara

Dissertation

Submitted to the Faculty of the

Graduate School of Vanderbilt University

in partial fulfillment of the requirements

for the degree of

DOCTOR OF PHILOSOPHY

in Biochemistry

January 31st, 2019

Nashville, Tennessee

Approved:

Neil Osheroff, Ph.D.
Martin Egli, Ph.D.
David Cortez, Ph.D.
Emily Hodges, Ph.D.
Katherine Friedman, Ph.D.

Dedication

To those whose life circumstances prevent them from reaching their dreams.

I have worked hard, but I have also been incredibly lucky.

Acknowledgements

First thanks go to my advisor, Neil Osheroff. As all his current and former students know, he is equal parts scientific genius, great educator, funny guy, and pain in the neck. Neil constantly pushed me to improve myself, both in my science and in my writing, and it all came together to make me a better scientist. Thanks to his coaching, I have two solid papers. And even with all that, he still gave me room to explore other interests. While in his lab, I took extra-curricular classes, volunteered as a translator and interpreter for local middle and high schools, exchanged pen pal letters with middle schoolers, sat on the ASPIRE Advisory Committee for three years to help determine the progress and future path of the program, worked both as vice president and president of the Biochemistry Student Association, took a 3-month leave of absence so I could participate in the AAAS Mass Media Science and Engineering Fellows Program, traveled to three conferences (presenting at one by invitation from the organizers), and chaired the 2018 Gordon Research Seminar on DNA Topoisomerases in Biology and Medicine. It was because he understands that not all of us graduate students want to sell our souls to industry or age into sensible sweater vests in academia (heh) that I was able to find a career that I can already tell will make me happier than being at the bench, and that's saying something.

I am grateful to my dissertation committee. Starting with my pre-qualifying exam, they have needled me with endless questions that have forced me to think things through. The gall. Special thanks to Dave Cortez and Kathy Friedman: precision of language is my new way of life.

Big thanks to the Cellular, Biochemical and Molecular Sciences NIH training grant, which funded me for two years.

Thank you to my lab mates, current and former. Thank you to Katie A., for teaching me the ropes way back when I came to rotate; to MaryJean, for always being friendly and for teaching me how to not get everything hot when working with radioactivity; and to Kendra, for helping out

with pretty much whatever I needed help with, and for loving Belcourt Taps as much as I do. Thanks to Rachel, for being my bay mate, helping to answer my sometimes ridiculous questions, putting up with my music, and for being a trusty vice-president when I was BSA president. Her help was invaluable to me, both in the lab and outside. To Elizabeth, who is one of my best friends. I enjoyed sharing all those experiences both in and out of lab. From ranting about failed experiments or torn gels, troubleshooting, having fun at conferences, and standing by as Jamie and I executed a last-minute poster retrieval at the airport (oops), to running 5Ks (why on earth did we do that?), rock climbing, the Irish Festival, St. Patty's Day (remember those White Russians? Oh, Manny.), bubble soccer, and so many more. Finally, thanks to the kiddos, Esha and Alexandria, who are really not kiddos, but I pretend like I'm old and they're younger than I am, so they're kiddos. They make lab time especially fun. Pew pew.

No lab-related thanks could end without thanks to Jo Ann. With her accumulated experience, 4 times out of 5, she'll know the answer to the question you just thought of. Thanks also for the chair booties (because they're cute), the waffle shop goodies (because they're delicious), and the random chips and queso that would sometimes appear in lab (because awesome).

Thanks as well to all my friends who have come, gone, or who have stayed with me throughout my time in grad school. First, to Michael, who has been one of my closest friends for the past 13 or so years. Him I thank for his continued friendship and support, even though we don't see each other that frequently anymore. Thanks to Casey, one of my oldest Nashville friends and one of the biggest cinephiles I've ever met. To Aaram, that crazy dude I befriended mostly by chatting with at 2 or 3am the night before a Bioreg. assignment was due, with whom I loved to play soccer, hang out, and just spend time with. A thank you to all my other friends, as they all made my time here much more entertaining. Thanks to Sam, Kathleen, Callie, Leif, Cherie, Kristin, Adrian, Denise, all my teammates on all the soccer, volleyball, and ultimate

frisbee teams I've played on, and to anyone else I'm currently forgetting. I promise I'm not intentionally leaving anyone out (no, not even you).

Thank you to my dear friends Ph.Doctor Loseph and Jonathon. Those guys are awesome – the kind of friends who will drop what they're doing and come running when you need them.

I'd like to formally acknowledge and thank the ASPIRE program here at Vanderbilt. There is no way I would be where I am today were it not for it. ASPIRE exposed me to 30 different varieties of things I could do with my Ph.D., and I struck gold when I found out about science writing. They gave me the opportunity to learn about it through their Ph.D. Career Connections and through the Biomedical Research and the Media module. That 6-session class got me started down this road to writing. Thank you to Wayne Wood, for teaching the course, and to Bill Snyder, for putting up with my inexperience as I kept writing for the VUMC Reporter after the course was over. Thank you to Ashley Brady, who has been my champion in this ride. She's been a boon, answering questions about resumes, CVs, and putting me into contact with people who might be helpful for me to know; a colleague, working tirelessly to put out issue after issue of the BRET Results and Discussion Newsletter; and best of all, a friend. Thanks also to Kate Stuart, another boon and a friend, and to the rest of the BRET Office/ASPIRE staff, who I know is incredibly dedicated and passionate about helping all of us trainees find a place for ourselves in this world. Special thanks to Kathy Gould, without whom I literally would not have this job I'm about to jump into. I thank her for trusting me and for pitching me as the best fit for the role.

Thanks to AAAS and to the Mass Media Fellows program. This immersive experience was, as it has been for so many others before me, life changing. Gracias a mi editora, Eulimar Núñez, de quien aprendí muchas cosas, y a mis demás compañeros en Univisión.

Thank you to the IMSD program – an incredible asset for those of us lucky enough to be in it. Thanks especially to Linda Sealy, who always works for the betterment of her students.

And now, the last of my personal acknowledgements.

Thank you to Jamie, who has been a part of my life for the past four years. They've been four years filled with fun, with tears, with late nights chatting about existentialism and early mornings chasing sunrises. I cherish our time together, and while I cannot possibly wait to spend dozens of more years with her, I also am content to let the time go by slowly, so I can enjoy each moment.

Tied to Jamie is His Highness Lord Pupperbutt (Dante), who cannot read so it doesn't matter if I call him names. To the Fuzzbuttimus, who is a jerk sometimes but who gives me snuggles.

Finally, to my family. Gracias a todos ustedes que han estado conmigo, apoyándome, desde que nací. Gracias a los chistosísimos y cariñosos Topiles. A mis abuelitas y a mi Madrina, quienes siempre han visto por mi y a quienes quiero y adoro con todo mi corazón. Y gracias, sobre todo, a mis papás. Con ellos he pasado todo tipo de aventura – desde tener un hermanito a vivir en Europa y casi morir haciendo deporte extremo (cruzar las calles) en el Cairo. Ellos me han dado todo lo que he necesitado y todo lo que he querido. Gracias a ellos tuve acceso a la mejor educación que estuvo a nuestra disposición. Pero principalmente, lo que mis papás me dieron fue una crianza donde aprendí a dar las gracias por lo que tengo, a siempre tratar de ser buena persona, a ser determinada y fuerte, a ser independiente y a pensar por mí misma. Los quiero mucho y espero siempre enorgullecerlos.

Table of Contents

List of Tables

Page

List of Figures

Page

List of Abbreviations

-SC	Negatively supercoiled DNA
2′-MOE	2′-*O*-methoxyethyl-modified oligonucleotides
X-mer	X-length oligonucleotide
Acr	Acridine
ADP	Adenosine diphosphate
AML	Acute myeloid leukemia
Amsa	Amsacrine
APL	Acute promyelocytic leukemia
ATP	Adenosine triphosphate
BCR	Breakpoint cluster region
Cbz	Carboxybenzyl
CC_3	Level of compound required to triple baseline levels of cleavage complexes
cEt	2’-*O*-constrained ethyl-modified nucleotides
CR	Cooling rate
DEPT	4'-Demethylepipodophyllotoxin
DMSO	Dimethyl sulfoxide
Doxo	Doxorubicin
dsDNA	Double-stranded DNA
DTT	Dithiothreitol
EDTA	Ethylenediaminetetraacetic acid
EGCG	Epigallocatechin gallate
EGTA	Ethylene glycol-bis(β-aminoethyl ether)-N,N,N′,N′-tetraacetic acid
EtBr	Ethidium bromide

Etop	Etoposide
GSK	GlaxoSmithKline
HPMA	*N*-(2-Hydroxypropyl)methacrylamide
hTIIα	Human topoisomerase IIα
hTIIβ	Human topoisomerase IIβ
LNA	Locked nucleic acids
Mitox	Mitoxantrone
MLL	Mixed lineage leukemia
MS	Multiple sclerosis
Na_2EDTA	Disodium EDTA
OTI	Oligonucleotide-linked topoisomerase II inhibitor
PAMAM	Polyamidoamine
PDB	Protein Data Bank
PEG	Polyethylene glycol
PLGA	Polylactic-co-glycolic acid
PML	Promyelocytic leukemia
PNA	Peptide nucleic acids
PNK	Polynucleotide kinase
R	Reference
RARA	Retinoic acid receptor α
Rel	Relaxed DNA
S Temp	Starting temperature
SDS	Sodium dodecyl sulfate
SNP	Single-nucleotide polymorphism

ssDNA	Single-stranded DNA
t-AML	Therapy-associated AML
t-APL	Therapy-associated APL
TBTA	Tris(benzyltriazolylmethyl)amine
THF	Tetrahydrofuran, abasic site analog
TLC	Thin layer chromatography
Trifluoromethylated 9-amino acridin-1(2H)-ones	Trifluoromethylated 9-amino-3,4-dihydroacridin-1(2H)-ones
WHD	Winged helix domain
WT	Wild type
εdC	3,N^4-ethenodeoxycytidine
εdG	1,N^2-ethenodeoxyguanosine
εrC	3,N^4-etheno-2'-ribocytidine

Chapter 1: Introduction and Scope of the Dissertation

DNA Topology

Every living organism on this planet has its genetic information coded in long strands of deoxyribonucleic acids (DNA)[1], which have an alphabet of four bases that pair in predetermined ways: adenine (A) pairs with thymine (T) and cytosine (C) pairs with guanine (G)[2, 3]. The bases on one strand of DNA form hydrogen bonds with their complementary bases on the other strand, thus forming the rungs of a ladder whose backbone is made up of a repeating pattern of a sugar (deoxyribose) and a phosphate group that are joined together through a phosphodiester bond[2]. The way that the bases pair and stack on top of one another, however, introduces a twist into the structure, such that the flat ladder is converted into a double-stranded helix[2]. This plectonemic coiling gives rise to an assortment of topological relationships and problems[4-8]. As a result, although the information contained in DNA is represented by its sequential array of bases, access to it is controlled by the three-dimensional structure of the double helix[4-8]. Different cellular processes – such as DNA replication, recombination, and transcription – require the opening of DNA[4, 5, 7, 9-11], but this creates torsional stress both ahead and behind the bubble of open genetic material[8].

James Watson and Francis Crick, Nobel Prize winners for correctly inferring the structure of DNA, followed up their seminal paper[2] with another publication that explored these very issues[3]. How, they wondered, do cells access the information within the stable structure of the double helix “without everything getting tangled”[3]?

Globally, cells maintain their DNA in an underwound state, which facilitates its opening during necessary cell processes such as DNA replication[10, 12]. Because the number of turns of the double helix remains invariant (so long as the ends of DNA are not allowed to swivel, which can be considered to be the case in all cells[8]), as the replication (or other DNA tracking) machinery melts the DNA, it accumulates positive supercoils (associated with overwinding of the double

helix) ahead of replication forks and negative supercoils (associated with underwinding) behind the fork[8, 10, 12-14]. The problem with this situation becomes evident when we envision what happens if we were to grab each of two intertwined strings and pull from the middle: as we open the middle, we tighten the coils around the ends. When the strings are long enough, the tightness in the coils at each end of the open "bubble" is so strong that we cannot pull the strings apart anymore. This is exactly what happens with DNA; without a means of dealing with this torsional stress, cells cannot carry out processes that require the helix to be opened.

Another topological problem associated with DNA during replication is catenation. The nature of semiconservative DNA replication[15-17]means that the generated products are catenated daughter chromosomes that must be separated (decatenated) for proper segregation into daughter cells during mitosis[12, 18-21].

These topological problems are exacerbated by the fact that DNA is a large molecule that be compacted by thousands of fold, which often results in tangling. The (haploid) human genome contains 3 billion base pairs and is approximately 1 m long and 2 nm in diameter, but the average human nucleus is only about 10 microns (μm) in diameter. That is roughly equivalent to taking a rope 0.2 mm in diameter that spans the distance between Nashville and Mt. Juliet (~22 km) and trying to make it fit into a space the size of a soccer ball (about 22 cm). DNA must be compacted in such a way that its information is easily accessible so as to facilitate efficient cell function. But in much the same way that you can perfectly wrap a pair of headphones into neat coils only to find them a tangled mess after a couple of hours in your pocket, DNA will form knots and tangles despite the best efforts of a cell to prevent them[22-24].

DNA Topoisomerases

If you could grab a rope-sized, double-stranded, linear molecule of DNA with your hands, you could access the information it contained on the inside by pulling the strands apart, starting at one end of the molecule and pulling until slowly you were left with one strand in each hand. In

doing so, you would notice that as you pulled the strands apart the ends would twist about one another to relieve the torsional stress you were creating. The reality of DNA in a cell does not allow the ends to rotate, however[6-8, 19]. On the one hand, circular genomes (e.g. those in bacteria or mitochondria) do not have ends at all and cannot relieve torsional stress through end rotation. On the other hand, linear genomes are constrained through attachments to the chromosome scaffold and thus cannot rotate to relieve the tension that arises from opening the double helix[8, 19, 21].

The cellular response to knots, tangles, and torsional stress is DNA topoisomerases. This family of enzymes is ubiquitous through all of life, and interconverts different DNA topoisomers by making a transient cut on one (type I topoisomerases) or both strands (type II topoisomerases) of the double helix[8, 18, 19, 21, 25, 26]. As a result of their activity, topoisomerases can alleviate torsional stress generated by the movement of DNA replication forks and transcription complexes, and can resolve DNA knots and tangles generated during recombination and replication, respectively[8, 18, 19, 21, 25, 26]. Although type I and type II topoisomerases vary in the number of DNA strands they cleave and in their specific mechanism of action, they all function by using tyrosine residues that act as nucleophiles when catalyzing the DNA cleavage reaction[8, 18, 19, 21, 25, 26]. This scission reaction results in covalent bonds formed between the tyrosine residues and the cleaved DNA, which protects the newly formed ends from DNA repair enzymes and keeps them in close proximity for religation[8, 18, 19, 21, 25, 26]. At the conclusion of their catalytic cycles, all topoisomerases return the DNA to its previous chemical state, leaving its sequence and chemical nature unaltered and changing only its topological state[8, 18, 19, 21, 25, 26].

Type I Topoisomerases

There are three types of type I topoisomerases: type IA, IB, and IC[8, 12, 25]. Type IA topoisomerases cut one strand of the DNA, pass the second strand through the break, and

reseal the cleaved strand[8, 12, 25]. This action reduces the number of supercoils in the DNA by 1, and thus is said to relax the DNA. Most type IA enzymes relax negative supercoils, but reverse gyrase, which is found exclusively in thermophilic bacteria and archaea, actively introduces positive supercoils into the DNA[25, 27, 28]. Interestingly, type IA enzymes can also decatenate single-stranded DNA[12, 25, 29]. Unlike type IA enzymes, type IB topoisomerases do not employ a strand passage mechanism and instead cut one strand of the DNA and swivel the other about the intact phosphodiester bond. This rotation is controlled by the amount of friction and torque contained in the molecule[30]; the tighter the supercoils and the higher the tension, the more supercoils that the enzyme relaxes in one cycle. Type IB enzymes can function on under- or overwound substrates[25, 31]. The third type, type IC, has only been found in a single archaeal genus. It behaves in a manner similar to type IB enzymes, but has little structural similarity to them[32]. Except for reverse gyrase, type I topoisomerases act without a high-energy cofactor such as ATP[25, 28].

Humans have several type I topoisomerases. These are topoisomerase I (a type IB enzyme), which relaxes negative supercoils and is essential for relieving the torsional stress generated during the replication and transcription of nuclear and mitochondrial DNA[25, 33-35]; topoisomerase IIIα (a type IA enzyme), which primarily resolves single-stranded DNA tangles that sometimes arise during replication, repair and recombination[36-38]; topoisomerase IIIβ (a type IA enzyme[39]), which is an RNA topoisomerase[40] that can carry out RNA cleavage[41] and strand passage reactions[42]; and mitochondrial topoisomerase I (a type IB enzyme), which has functions that are very similar to those of topoisomerase I but is localized exclusively in the mitochondria[25, 35].

Topoisomerase I is essential in metazoans; complete loss of the enzyme results in lethality[43-45]. Its function has traditionally been thought to be limited to DNA nicking and closing, resulting in the release of topological stress associated with replication, transcription,

repair, and recombination[5, 14, 45]. Recent studies, however, suggest that topoisomerase I has pleiotropic functions in cells, playing a role in genomic stability, gene-specific transcription, and response to various anticancer agents[45].

Type II Topoisomerases

There are two types of type II topoisomerases, type IIA and IIB, and both detangle, unknot, and relax DNA by carrying out strand passage reactions. Although type IIA topoisomerases were originally discovered in 1976[46], it was not until 1997 that the first type IIB was identified[47]. Type IIA enzymes have been found in every domain of life and in viruses, but to date, type IIB topoisomerases are confined mostly to archaea and plants[48]. Both types of enzymes relax positive and negative supercoils, share similar ATPase and DNA-cleavage domains, and undergo similar catalytic cycles[25, 47], but their primary and tertiary structures differ greatly[25, 48]. Given the focus of my dissertation, type IIA enzymes will be referred to as type II topoisomerases and type IIB enzymes will not be covered further.

Unlike type I topoisomerases, type II topoisomerases transiently cleave both strands of the DNA, creating a staggered cut with 5' overhangs (Figure 1). To maintain genomic integrity during this process, active site tyrosine residues covalently attach to the 5'-termini at each scissile bond; these covalent enzyme-cleaved DNA complexes are referred to as cleavage complexes[8, 18, 19, 21, 25, 26]. It is notable that the two cleavage steps, while coordinated, do not occur simultaneously[49-51].

Type IIA topoisomerases are composed of various subfamilies, including the eukaryotic type II topoisomerases (present in all eukaryotes), DNA gyrases (present in all bacteria, some archaea, and eukaryotes with endosymbionts of bacterial origin) and topoisomerases IV (specific to bacteria)[48]. Most bacteria have both a DNA gyrase and a topoisomerase IV[52, 53], which work in coordination to regulate DNA supercoiling and decatenation[53]. The primary roles of DNA gyrase are to remove the positive supercoils that accumulate ahead of replication forks

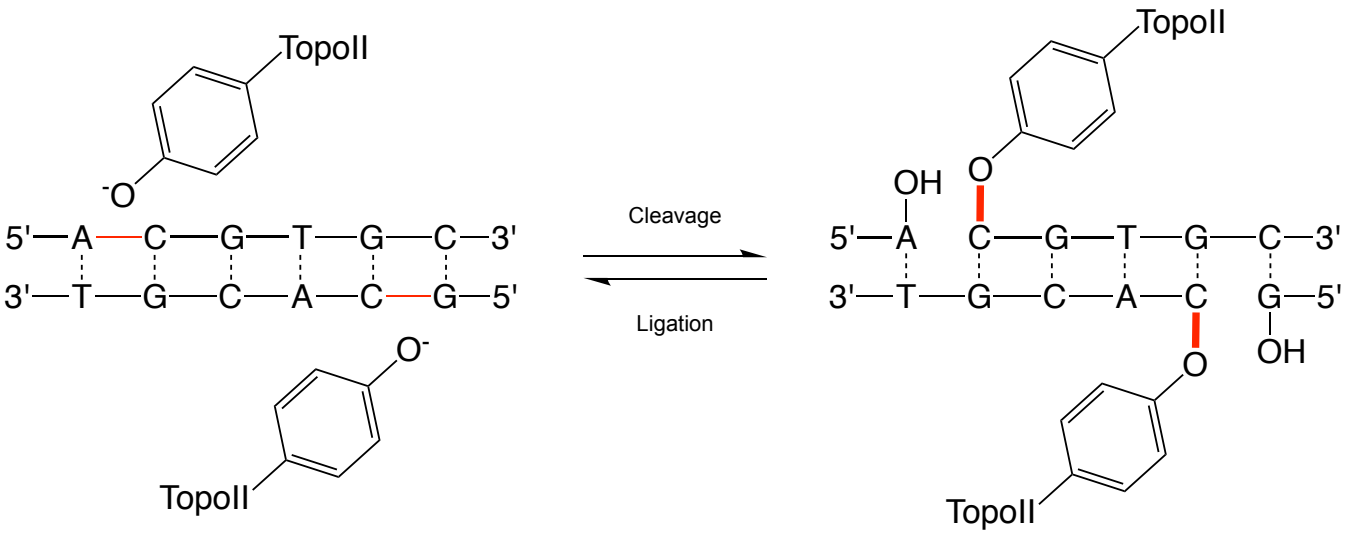

Figure 1. Nucleophilic attack by tyrosine residues catalyzes the double-stranded break characteristic of type II topoisomerases. Each topoisomerase II subunit (TopoII) has a catalytic tyrosine residue that undergoes a transesterification reaction with the DNA backbone, resulting in two single-stranded DNA breaks that are 4-base pairs away and that are stabilized through covalent interactions with the enzyme.

and to introduce negative supercoils into the DNA[52]. Topoisomerase IV, in turn, removes the catenanes that form behind replication forks[52]. Some bacteria, like *Mycobacterium tuberculosis*, have a single type II topoisomerase[31] that behaves as a "hybrid" as it is responsible for the tasks that are normally carried out by DNA gyrase and topoisomerase IV[54-56].

Eukaryotic type II topoisomerases, referred henceforth as type II topoisomerases, are homodimers. Each protomer subunit can be broken down into three defined domains: the N-terminal domain, the catalytic core, and the C-terminal domain (Figure 2)[19, 57]. The N-terminal domain contains the ATPase domain, which binds and hydrolyzes the high-energy cofactor that is necessary for the catalytic cycle of the enzyme[19]. The catalytic core is composed of the TOPRIM and DNA breakage-reunion domains, the latter of which contains a winged helix domain (WHD)[19, 57]. The catalytic core of the enzyme is sufficient (when dimerized) to carry out DNA cleavage and religation, but not strand passage[58]. The C-terminal domain of the enzyme contains a nuclear localization signal and sites of phosphorylation[18, 19, 59], and although it is not necessary for catalytic activity, it aids in the recognition of the geometry of the DNA substrate strand passage[58]. Unlike the N-terminal domain and the catalytic core of type II topoisomerases, the C-terminal end is not evolutionarily conserved[19] and imparts the enzymes with different characteristics. For example, the C-terminal domain of both isoforms of type II topoisomerases expressed in humans (discussed below) provides each one with differing abilities to recognize DNA geometry (the three-dimensional arrangement of the helices)[58].

The holoenzyme interconverts DNA topoisomers through the coordination of three separable dimerization interfaces or gates: the N-gate, the DNA-gate, and the C-gate (Figure 2)[57, 60]. Through their coordinated action, type II topoisomerases pass a "transport segment" of DNA, captured through the clamp-like closing of the N-gate, through a break they generate on a "gate segment" of DNA (Figure 3)[19, 57]. Before any cleavage can take place, the enzyme must be

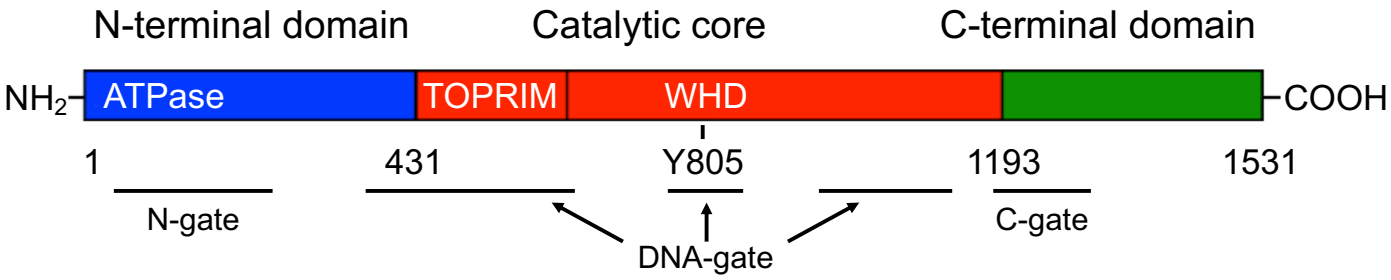

Figure 2. Domain structure of human topoisomerase IIα. The N-terminal domain is shown in blue, the catalytic core in red, and the C-terminal domain in green. The N-gate, DNA-gate, and C-gate are the dimerization interfaces of the holoenzyme, which act to coordinate the capture, cleavage, and release of the DNA segments. The position of the catalytic tyrosine (Y805) within the winged helix domain (WHD) is indicated.

able to bend the gate segment ~150º[60-62]. Following bending, the enzyme utilizes two tyrosine residues in the WHD to create a single-stranded DNA break on each strand of the gate segment, resulting in a double-stranded break with a 4-base pair stagger stabilized by phosphotyrosyl bonds[8, 18, 19, 62, 63]. As the energy of the phosphodiester bond is conserved by the formation of the phosphotyrosyl bond, no energy input is needed for cleavage and religation of the DNA, but two divalent metal ions – Mg^{2+} probably fulfills this role in a physiological setting – are required[18, 19, 21, 63, 64]. Although binding of ATP facilitates the capture of the T segment and closing of the N-gate[63, 65], hydrolysis is needed to facilitate the conformational changes in the enzyme needed for the strand passage step that brings the transport segment through DNA-gate formed by the cleaved gate segment[19, 31, 63, 66]. Following strand passage, the gate segment is religated and the transport segment is released through the C-gate[57]. Hydrolysis of a second ATP molecule helps the enzyme release the gate segment and reset for a new round of the catalytic cycle[19, 63, 67], although it is possible to skip the second hydrolysis step and catalyze strand passage of a new transport segment without dissociating from the initial gate segment[19].

Although most lower eukaryotes express only one type II topoisomerase, human cells express two closely related isoforms, topoisomerase IIα and IIβ[18]. These isoforms are related but are coded for by different genes[6, 14, 68-72] and differ in their molecular weight (170 kDa for topoisomerase IIα and 180 kDa for topoisomerase IIβ)[73, 74]. Despite their similarities, however, conditional knockout experiments have shown that the β isoform cannot complement for a deficiency in α, which is essential for the survival of proliferating cells[19]. The concentration of topoisomerase IIα increases over the cell cycle (peaking in G2/M)[75] and plays essential roles in DNA replication and chromosome segregation[18, 19, 21]. For this reason, its presence is undetectable in quiescent cells[19, 76, 77].

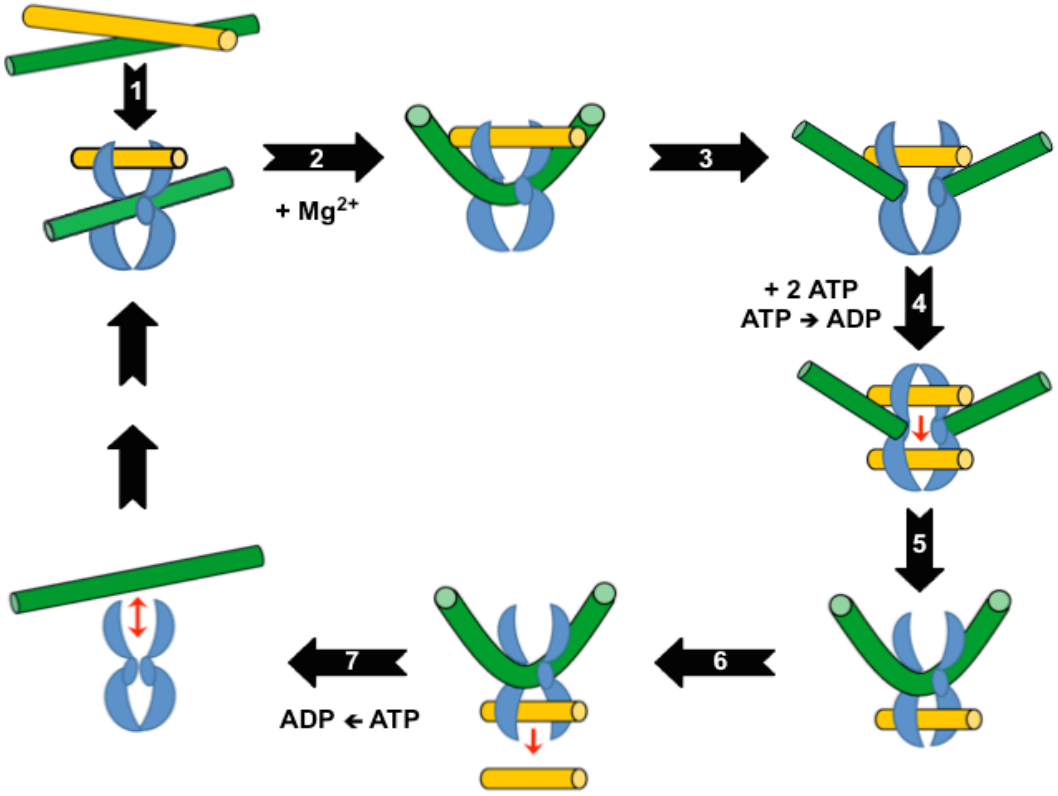

Figure 3. Catalytic cycle of type II topoisomerases. A type II topoisomerase first binds to two DNA segments, a gate (green) and a transport (yellow) segment (**1**). The enzyme bends the gate segment (**2**) and then creates a transient double-stranded break that is stabilized by a covalent bond between a catalytic tyrosine residue and the 5' phosphate of the DNA (**3**). Following the hydrolysis of an ATP molecule, the transport segment is then passed through the break (**4**), and the gate segment is religated (**5**). Next, the transport segment is released (**6**). Hydrolysis of a second ATP molecule releases the gate segment (**7**) and readies the enzyme for a new round of the cycle.

Topoisomerase IIβ maintains a steady concentration irrespective of proliferative state or stage of the cell cycle[75] but reaches its highest levels in post-mitotic cells[78]. Although the precise cellular function of topoisomerase IIβ is not well defined, it appears to play an important role in transcription[79-81] and the expression of hormonally regulated genes[8, 18, 19, 25, 26]. Unlike topoisomerase IIα, topoisomerase IIβ is not essential at the cellular level, but its function is critical during neural development[82, 83].

Type II topoisomerases are inherently dangerous enzymes due to the fact that they cut DNA as part of their normal catalytic process[18, 21, 63, 84-87]. To minimize the potential for DNA damage, topoisomerases covalently bind to the cleaved DNA ends; this prevents the ends from becoming separated within the cell and masks them from DNA repair machinery[18, 21, 63, 86]. In addition, the cleavage-ligation equilibrium strongly favors ligation, and cleavage complexes are short-lived and readily reversible[18, 59, 66, 88-92]. Yet even with these protections in place, the action of type II topoisomerases can result in non-transient DNA damage. If a DNA tracking system (such as a replication fork) encounters a cleavage complex, the helicase associated with the tracking system can displace the single-stranded DNA that is not covalently attached to the type II topoisomerase, preventing the topoisomerase from returning the DNA to its original state[93].

Most of the time, the DNA damage response can handle low levels of topoisomerase II-generated DNA damage. However, when the concentration of cleavage complexes in a cell is too high, it can overwhelm the repair responses and eventually trigger cell death pathways[18, 21, 59, 63, 86, 94, 95]. In addition, even the “successful” attempts of a cell at dealing with the damage can result in inaccurate repair and damaged chromosomes that can ultimately lead to cancer (discussed below)[18, 59, 87, 96-100].

Topoisomerase II Poisons

Certain kinds of compounds and DNA structures increase the concentration of cleavage complexes, which in turn increases the probability that these covalent complexes will be converted into double-stranded DNA breaks that require repair[18, 59, 86, 87, 93, 95, 101]. Because these agents convert the type II enzymes into cellular toxins that fragment the genome, they are called topoisomerase II poisons to distinguish them from catalytic inhibitors that impair the overall catalytic activity of the type II enzymes without increasing the concentration of cleavage complexes.

Although topoisomerase II poisons technically inhibit their target – by trapping the cleavage complex they impair the completion of the catalytic cycle – they exert their cellular effects by inducing or stabilizing cleavage[102]. Conversely, catalytic inhibitors of type II topoisomerases can act at any step of the catalytic cycle but their actions result in a decrease in the levels of cleavage complexes[102]. Thus, while both classes of drugs rob the cell of the proper functioning of type II topoisomerases, poisons lead to an increase in double-stranded DNA breaks[102].

Drugs as Topoisomerase II Poisons

Type II topoisomerases are important cytotoxic targets for anticancer drugs (Figure 4). Despite the fact that all human cells express one or both topoisomerase II isoforms, topoisomerase II-targeting drugs are efficacious against cancer cells primarily for three reasons. First, because cancer cells are generally highly proliferative, they express high levels of topoisomerase IIα[19, 75, 87], leading to the creation of more drug-stabilized cleavage complexes. Second, because of the high metabolic rate of cancer cells, replication forks and transcription complexes constantly move along the DNA, making it more likely that they will convert cleavage complexes to permanent DNA breaks[103]. Third, due to impaired cell cycle checkpoints and DNA damage repair pathways in many cancers, malignant cells often are more susceptible to the DNA damage caused by topoisomerase II-targeted drugs[87, 104].

Anticancer drugs

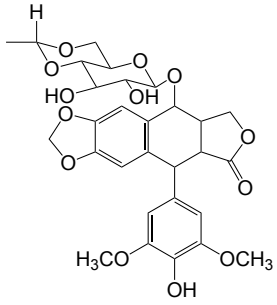

Etoposide

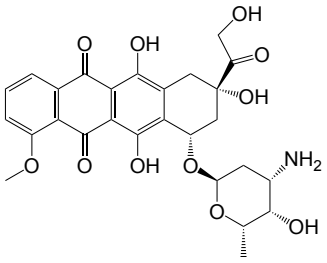

Doxorubicin

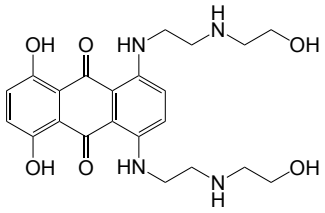

Mitoxantrone

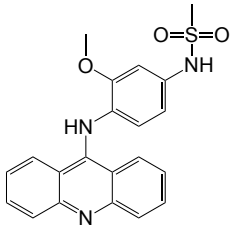

Amsacrine

Dietary poisons

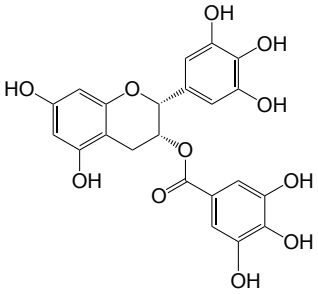

EGCG

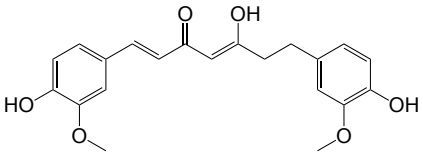

Curcumin

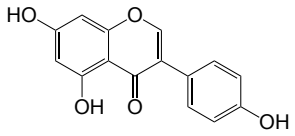

Genistein

Figure 4. Structure of compounds that act as topoisomerase II poisons.

Topoisomerase II poisons are amongst the most widely prescribed anticancer drugs in the world[8, 18, 86, 87, 95, 105]. Etoposide, for example, is used to treat testicular, ovarian, and lung cancers among others[18, 86, 87, 95, 106, 107]. Doxorubicin is prescribed for treatments against breast, bladder, stomach, and thyroid cancers, as well as a variety of other disseminated neoplastic conditions[18, 87, 108]. Mitoxantrone is prescribed against a variety of cancers, such as breast, prostate, and laryngeal cancers, non-Hodgkin's lymphoma, and chronic myeloid leukemia[18, 87, 98, 109], but its primary use is against acute myeloid leukemia (AML) and against the autoimmune disorder multiple sclerosis (MS). This compound has FDA approval for its ability to reduce neurologic disability and the frequency of clinical relapses in patients with secondary progressive, progressive relapsing, or worsening relapsing-remitting MS[110]. Amsacrine, the last of the examples listed here, is used to treat relapsed acute myeloid leukemias and malignant lymphomas[18, 111].

Amsacrine was the first anticancer agent shown to act by poisoning topoisomerase II[112]. The drug is composed of an acridine ring coupled to a 4'-amino-methane-sulfon-*m*-anisidide head group. Structure-activity studies suggest that the poisoning activity of amsacrine is embodied in the head group, while the acridine moiety enhances drug activity primarily by promoting strong interactions with DNA[113]. A number of other topoisomerase II-targeting agents also utilize an acridine or related aromatic core[8, 18, 86, 87, 95, 105, 114]. Although most of these drug cores are attached to an aromatic head group, some agents (such as mitoxantrone) lack a head group altogether (Figure 4).

Etoposide, in particular, has been well studied. It is a derivative of podophyllotoxin, a substance naturally found in plants such as the American Mayapple (*Podophyllum peltatum*), which has been used as an anticancer agent in traditional and folk medicine for over a millennium[115]. When purified, however, podophyllotoxin and its derivatives in the Mayapple demonstrated high toxicities that precluded their use in the clinic[116]. It was later determined

that podophyllotoxin bound to tubulin, the monomeric component of microtubules, leading to mitotic arrest. The observed toxicities led to a search for synthetic derivatives that retained their anticancer activity but that were not as toxic as the natural podophyllotoxins[115, 117-119].

Among the compounds synthesized during the search were 4'-demethylepipodophyllotoxin (DEPT) and its derivatives etoposide and teniposide (Figure 5). The latter two have a glucoside moiety that prevents their interaction with tubulin[120], completely changing the mechanism of action of the compounds and making them less toxic to cells[119]. Etoposide and teniposide were finally approved by the FDA as anticancer agents in 1983[119] and 1992, respectively. Since its approval, etoposide has been a front-line treatment for many cancers[115], and was one of the first anticancer drugs shown to target human type II topoisomerases[115], the first being amsacrine[112].

Etoposide affects the activity of human type II topoisomerases through enzyme-drug interactions, not through drug-DNA interactions[89, 121, 122], and stabilizes both single- and double-stranded cleavage complexes[50]. As determined by saturation transfer difference nuclear magnetic resonance spectroscopy, the sugar group does not appear to interact with topoisomerase II in the enzyme-DNA complex[123, 124]. In fact, compared to etoposide, DEPT induces similar levels of human topoisomerase IIα-mediated DNA cleavage and prevents the religation of cleaved DNA to a similar extent[123, 124]. For these reasons, it is reasonable to call DEPT the "active core" of etoposide.

Outside of the clinic, topoisomerase II poisons make frequent appearances in our diet. For example, epigallocatechin gallate (EGCG) is the main active bioflavonoid in green tea[125, 126], genistein is an isoflavone present in soy products[125, 127], and curcumin is the main flavoring and coloring component of turmeric[128]. Screens of natural products consistently turn up new topoisomerase II poisons, including a variety of metabolites from olive plants[129], black seed[130], and various fruits and vegetables.

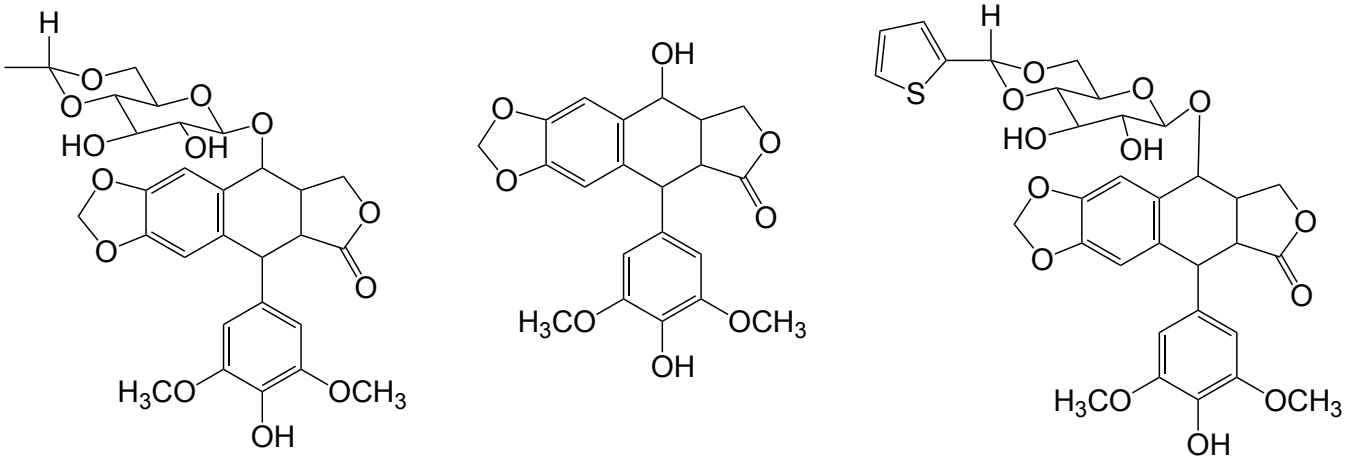

Figure 5. Structure of related podophyllotoxins. Rings A-D on etoposide are labeled. The sugar group on etoposide is attached at the C4 position.

Many dietary poisons are reported to be chemopreventive[131] when consumed as part of a regular diet[132], but can also have harmful effects. For example, Asian populations consume 20-80 mg of genistein per day compared to 1-3 mg in the United States, and have comparatively lower rates of breast and prostate cancers[132, 133]. When regularly consumed during pregnancy, however, genistein increases the risk of infant leukemias[134]; rates of incidence in Japan, for example, are in fact two to three times higher than in the United States[87, 135]. Topoisomerase II poison-associated leukemias are discussed in more detail below.

As widespread as they are, topoisomerase II poisons do not all induce enzyme-mediated DNA cleavage the same way. Compounds can be split into interfacial or covalent poisons based on their mechanism of action. The differences between these two types of poisons are summarized in Table 1.

Interfacial poisons act non-covalently at the interface between the enzyme and the DNA. These compounds physically block the religation of cleaved DNA by wedging themselves into the cleaved DNA scissile bonds[49, 102, 136]. Unlike covalent poisons, they are unaffected by reducing agents and increase the amount of type II topoisomerase-mediated DNA cleavage regardless of whether they are added to cleavage reactions first or last. Prominent examples of interfacial poisons include etoposide, amsacrine, and doxorubicin.

Covalent poisons were originally referred to as redox-dependent poisons because some of these compounds undergo redox cycling to enact their effect on the type II topoisomerases[102, 137]. They act by adducting topoisomerase II at cysteine (and potentially other) residues outside of the DNA cleavage-ligation active site of the enzyme[18, 129, 131, 138-140]. Adduction results in the cross-linking of both protomers of the enzyme and prevents the N-gate from opening[141, 142]. Although closing the N-gate does not mechanically increase DNA cleavage, it increases the concentration of DNA in the active site of the enzyme and results in higher levels of cleavage[143].

Interfacial poisons	Covalent poisons
• Act non-covalently at the active site and physically block religation • Unaffected by reducing agents • Enhance enzyme-mediated DNA cleavage when added to the enzyme-DNA complex • Enhance DNA cleavage when incubated with the enzyme prior to the addition of DNA • Examples: etoposide, doxorubicin	• Covalently adduct topoisomerase II at sites distal to the active site • Lose activity when incubated with reducing agents • Enhance DNA cleavage only when added to the enzyme-DNA complex • Inhibit topoisomerase II when incubated with the enzyme prior to the addition of DNA • • Examples: curcumin, EGCG

Table 1. Differences between interfacial and covalent poisons of type II topoisomerases.

Covalent poisons display several hallmark characteristics that distinguish them from interfacial poisons[58, 128-130, 138, 142, 144]. First, reducing agents abrogate the activity of these agents[128-130, 144, 145], as redox-cycling is required for the actions of the compounds[18, 102]. Furthermore, because covalent poisons act by altering the N-terminal portion of the enzyme, they do not enhance DNA cleavage by topoisomerase II constructs that lack this domain[58]. Finally, although covalent poisons enhance DNA scission when added to the topoisomerase II-DNA complex, they inhibit enzyme-mediated cleavage when incubated with the protein prior to the addition of DNA[144, 146]. The adduction of covalent poisons to the enzyme and the resulting closure of the N- gate likely contribute but cannot wholly account for the inhibition of the enzyme, as closing the N-terminal gate does not prevent binding to linear DNA molecules[146] nor does it prevent cleavage[143]. Examples of covalent poisons include curcumin and EGCG (Figure 4).

Topoisomerase II poisons tend to have aromatic rings as a headgroup or core[102, 130, 132, 144], but it is not a requirement. As covalent poisons act by modifying their target enzymes rather than by interacting as “ligands” (as interfacial poisons do), they can tolerate a greater range of structural alterations[128, 130, 138, 140, 142, 144, 145, 147, 148]. Interfacial poisons tend to have planar ring systems that are DNA-interacting and side chains that are enzyme-interacting[94, 149, 150], and may or may not be DNA intercalators[151].

DNA Lesions as Topoisomerase II Poisons

The last type of topoisomerase II poison I will cover are DNA lesions and unusual DNA structures. As part of their catalytic cycle, type II topoisomerases first test the bendability of the DNA substrate. If they can bend the DNA, they can cut at that site[60, 62]. DNA lesions and structures that increase the flexibility/bendability of the double helix tend to be good cleavage substrates and facilitate the forward rate of cleavage, thereby leading to an increased number of cleavage complexes in a cell[18, 92, 152-159]. The Osheroff lab has previously characterized

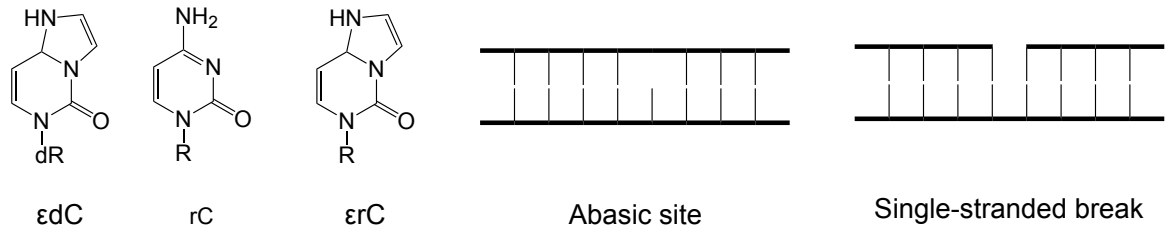

Figure 6. Structures of DNA lesions that act as topoisomerase II poisons. εdC, 3,*N*4-ethenodeoxycytidine; rC, 2′-ribocytidine; εrC, 3,*N*4-etheno- 2′-ribocytidine.

a wide variety of DNA lesions as topoisomerase II poisons, including abasic sites[157, 160] and exocyclic lesions such as 3,N^4-ethenodeoxycytidine (εdC), 3,N^4-etheno-2'-ribocytidine (εrC), and 1,N^2-ethenodeoxyguanosine (εdG)[159] (Figure 6). Although the only way to determine whether or not a particular lesion will induce topoisomerase II-mediated DNA cleavage is to test it experimentally, lesions that are small, that do not create kinks or distort the DNA, or that do not increase the flexibility of the double helix tend not to act as topoisomerase II poisons[157]. Examples of such lesions are N^6-methyladenine, 8-oxoguanine, and 8-oxoadenine (Figure 7)[157].

Type II Topoisomerases and Cancer

Although topoisomerase II poisons are extremely useful in treating cancers and other diseases such as multiple sclerosis, their use can unfortunately lead to a variety of mechanism-induced (i.e., topoisomerase II-generated) toxicities. These arise because of the difficulty of targeting drugs such as etoposide specifically to cancer cells[18, 86, 87, 106] and because all cell types express one or both topoisomerase II isoforms[21, 25].

Shortly after etoposide and teniposide were first introduced into the clinic in the 1980s, physicians began observing a new form of secondary leukemias that was characterized by balanced chromosomal translocations[161, 162]. Over 10% of patients treated with etoposide went on to develop therapy-associated acute myeloid leukemias (t-AML)[84, 87, 163-166]. Thankfully, once the high-risk regimens were identified[84, 167], the number of affected patients dropped to ~2-3%[87].

A variety of translocations or mutations can give rise to the highly heterogeneous AML, the most common acute leukemia in adults[168]. t-AMLs associated with topoisomerase II-targeting drugs display a balanced translocation that includes the mixed lineage leukemia (*MLL*) gene on chromosomal band 11q23[84, 87, 169], which codes for a histone methyltransferase[170]. *De novo* AMLs have an 8.3-kb breakpoint cluster region (BCR) in *MLL*[84, 87], but the chromosomal

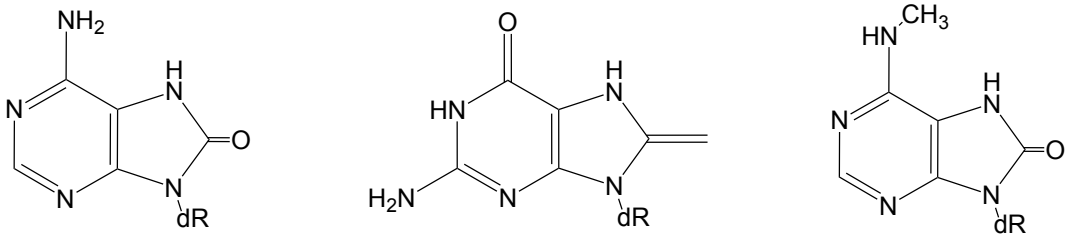

8-oxoadenine 8-oxoguanine N^6-methyladenine

Figure 7. Structures of DNA lesions that do not act as topoisomerase II poisons.

breakpoints associated with t-AMLs are concentrated on the 1-kb telomeric end of the *de novo* BCR[87, 171]. Over 80 translocation partners have been described for *MLL*, but *AF4* and *AF9* are the most prevalent partners associated with topoisomerase II-targeting drugs[171]. Whether or not the translocation sites in *MLL* or its partner are located within a BCR, they are located within a few base pairs of drug-induced topoisomerase II DNA cleavage sites[169, 172] and are hypothesized to arise directly as a result of illegitimate repair following cleavage by a type II topoisomerase[172-174],[175, 176].

Another important type of topoisomerase II poison-related leukemia, therapy-associated acute promyelocytic leukemia (t-APL), arises from a balanced translocation between intron 6 of the promyelocytic leukemia (*PML*) gene on chromosome 15 and intron 2 of the retinoic acid receptor α (*RARA*) gene on chromosome 17. t-APL is associated with the use of mitoxantrone in treating breast cancers and MS; in fact, MS patients account for ~16% of t-APL patients[87, 177, 178]. The remarkable feature of t-APLs is that ~60% of patients display breakage in *PML* within an 8-bp BCR, whereas *de novo* APLs have a BCR that is about 1 kb in length[87, 98, 177]. In contrast, the breakpoints at *RARA* occur at a variety of locations along the 17-kb-long intron 2[98, 99, 177, 179]. As with AML, the breakage sites on the translocation partners (*PML* and *RARA* for APL) are located on or in close proximity to drug-induced (mitoxantrone, etoposide, and epirubicin, an analog of doxorubicin) type II topoisomerase cleavage sites[87, 98, 99, 177, 180]. Although the specific mechanism by which drug-induced topoisomerase II-mediated DNA cleavage triggers the leukemic translocation is controversial, considerable circumstantial evidence suggests that sites cleaved by the enzyme go on to generate the translocation breakpoint[81, 87, 162, 176, 177].

Specifically, topoisomerase IIβ has been implicated in this process. Some of the first indications of the involvement of the β isoform came from experiments using skin-specific *top2b*$^{-}$ knockout mice, which had a lower incidence of secondary malignancies compared to wild-type

(WT) mice after treatment with etoposide[181]. As discussed above, topoisomerase IIβ plays a larger role in transcription than topoisomerase IIα. Recent insights on transcription suggest that genes are transcribed in “factories”, or hubs of transcription machinery that are clustered with others that are engaged on different templates[182]. Given that *MLL*, *AF9*, and *AF4* are transcribed in the same factory, it has been suggested that illegitimate repair and recombination between these genes can occur following transcription-associated topoisomerase IIβ cleavage that has been stabilized by topoisomerase II poisons[87, 171]. Combined with the fact that topoisomerase IIβ has also been implicated in the cardiotoxicity associated with anthracyclines like doxorubicin[86, 183, 184], developing drugs that display strong activity and higher specificity for the α isoform is a desirable goal.

Scope of the Dissertation

Many anticancer drugs have very undesirable side effects because they oftentimes affect non-cancer cells almost as much as they affect cancerous cells[59, 87, 162, 181, 185]. Because all cells express at least one isoform of human type II topoisomerases[18, 19, 86, 87], all cells are at least somewhat susceptible to the effects of topoisomerase II poisons, especially proliferative tissues (hair, skin, gastrointestinal tract, etc.) with high cell turnover[186]. Such widespread susceptibility to this and other classes of cytotoxic anticancer drugs necessitates the generation of new or improved drugs or delivery systems that are better targeted to cancer cells.

An example of drug modifications designed to target cancer cells are polyamine-containing etoposide derivatives. As many cancers upregulate the polyamine transport system[187, 188], cancer cells preferentially uptake the polyamine-modified derivatives compared to non-cancer cells[188-190]. Other examples of polymer conjugates include polyethylene glycol (PEG), N-(2-Hydroxypropyl) methacrylamide (HPMA), polylactic-co-glycolic acid (PLGA), and polyamidoamine (PAMAM)[191]. An example of an improved drug delivery system is the nanoparticle, a non-toxic polymer shell that can be designed to encapsulate anticancer drugs

and to release its cargo only when it reaches its cancer cell targets[192-194]. Additional drug delivery approaches include drug-loaded hydrogels[195], receptor-based targeting[194], and antibody-drug conjugates[196]. This dissertation describes two other approaches to reducing off-target effects and improving cancer-cell specificity of topoisomerase II poisons.

Chapter 1 of the dissertation covers the background literature, and sets the stage for discussion of two approaches for improving the specificity of topoisomerase II-targeting anticancer drugs. Chapter 2 discusses the materials and methods employed for all the experiments in the dissertation. Chapter 3 delves into whether novel trifluoromethylated 9-amino-3,4-dihydroacridin-1(2H)-one derivatives could serve as a scaffold for new topoisomerase II-targeting drugs. It explores whether the compounds increase DNA cleavage mediated by topoisomerase IIα, and, if they do, whether those compounds act as covalent or interfacial topoisomerase II poisons. This material has been published in *Bioorganic & Medicinal Chemistry Letters*[197]. Chapter 4 describes the ability of topoisomerase IIα and IIβ to mediate DNA cleavage on duplexes containing oligonucleotide-linked topoisomerase II poisons (OTIs). These drug-DNA hybrids are designed to target specific DNA sequences, and are therefore proposed as a new approach to targeting cancer cells while reducing the cytotoxicity of treatment. The majority of data in this chapter have been published in *Nucleic Acids Research*[198]. Chapter 5 provides an overview of the results and an outlook on the next steps for these and for related research avenues.

Chapter 2: Materials and Methods

Biology

Enzymes

Recombinant wild-type human topoisomerase IIα and topoisomerase IIβ and wild-type yeast topoisomerase II and the etoposide-resistant H1011Y mutant yeast type II enzyme were expressed in *Saccharomyces cerevisiae* JEL-1Δtop1 and purified as described previously[153, 199-201]. This mutation was originally published as H1012Y[201]. The numbering of the mutation was changed to H1011Y in 2001[202] to accommodate a reported error in the original amino acid sequence of *S. cerevisiae* topoisomerase II[203]. The catalytic core of human topoisomerase IIα (residues 431−1193) was a gift from J. Deweese (Lipscomb University College of Pharmacy) and was expressed and purified as described previously[153, 199, 200]. Human enzymes were stored at -80 °C as 1.5 mg/mL stocks in 50 mM Tris-HCl, pH 7.9, 0.1 mM ethylenediaminetetraacetic acid (EDTA), 750 mM KCl, and 40% glycerol, and yeast enzymes were stored as 2 mg/mL stocks in 10 mM Tris-HCl, pH 7.7, 1 mM ethylene glycol-bis(β-aminoethyl ether)-N,N,N′,N′-tetraacetic acid (EGTA), 1 mM EDTA, 750 mM KCl, 30% glycerol, and 0.5 mM dithiothreitol (DTT). The residual concentration of DTT was <2 μM in final reaction mixtures. Calf thymus topoisomerase I was obtained from Invitrogen.

Materials

Analytical grade etoposide was purchased from Sigma-Aldrich and stored at room temperature as a 40 mM stock solution in 100% dimethyl sulfoxide (DMSO). Negatively supercoiled pBR322 DNA was prepared from *Escherichia coli* using a Plasmid Mega Kit (Qiagen) as described by the manufacturer. Analytical grade etoposide was purchased from Sigma-Aldrich. Amsacrine and acridine were a gift from Dr. David Graves (University of Alabama at Birmingham).

Oligonucleotides and OTIs

Three DNA sequences were used to create a series of oligonucleotide duplexes. The first sequence was a 50-mer that encompassed bases 1461-1510 of intron 6 of *PML*, and contained a previously identified, 8-base pairs-long topoisomerase II cleavage hotspot (bases 1482-1489) associated with the generation of t-APLs[98]. The hotspot contains a strong topoisomerase II-mediated cleavage site that is represented in position 24-25 on the top (or target) strand of the oligonucleotide and to 26-27 on the bottom strand (either an unmodified oligonucleotide or an OTI). Top strand: 5'-CTTTGTTCCTCATTCTGACTGAGCCCTAGCCTTGGTCACACACTGAGCAG-3'. Bottom strand: 5'-CTGCTCAGTGTGTGACCAAGGCTAGGGCTCAGTCAGAATGAGGAACAAAG -3'. OTI28, OTI29, OTI33, and OTI23 had the same sequence as the *PML* 50-mer bottom strand, except that the active core of etoposide (4'-demethylepipodophyllotoxin, DEPT) was linked to the oligonucleotides at positions 28, 29, 33, and 23, respectively. A 50-mer bottom strand that contained the linker with no attached drug (LIN28) or a tetrahydrofuran abasic site analog (AP28) at position 28 also were synthesized.

The second sequence utilized was a 50-mer that spanned a previously identified translocation between *PML* and *RARA* in a patient with t-APL[99]. Top strand: 5'-CTTTGTTCCTCATTCTGACTGAGCCCTA/GTCTGCCATCCTAACCTTCCAT-3', made up of bases 1461-1488 of intron 6 of *PML* (before the slash) and bases 12039-12060 of intron 2 of *RARA* (after the slash) The bottom strand was fully complementary. Bottom strand: 5'-ATGGAAGGTTAGGATGGCAGAC\TAGGGCTCAGTCAGAATGAGGAACAAAG-3'.

Sequences from *RARA* are located to the left of the backslash and sequences from *PML* are located to the right of the backslash. A 50-mer OTI with the bottom strand sequence was synthesized and contained a linked DEPT at position 29. Two additional OTIs based on the same sequence, a 30-mer (5'-TAAGACTGACTCGGGATCAGACGGTAGGAT-3') and a 20-mer

(5-CTGACTCGGGATCAGACGGT-3'), were synthesized. These sequences contained 10 or 15 fewer bases from each of the 5'- and 3'-termini of the 50-mer, respectively, but had the linked DEPT at the same nucleotide as the 50-mer.

The third oligonucleotide was a 50-mer that corresponded to bases 12011-12060 of intron 2 of the parental *RARA* sequence that spanned a patient-derived translocation breakage point (at 12038-12039, corresponding to 28-29 on the oligonucleotide) observed in a patient[99]. Top strand: 5'- CAGAAAGGGGCAACTTCATCAGACACCCGTCTGCCATCCTAACCTTCCAT-3'. All the non-OTI oligonucleotides were synthesized by Sigma-Aldrich unless specified.

Six oligonucleotides were designed that contained a single-base difference in the WT *PML* top strand sequence such that, when annealed to a WT *PML* bottom strand, OTI28, OTI29, OTI33, or OTI23, each duplex would contain a single mismatch. The oligonucleotides were named using the convention X#Y, where X is the WT base, # is the position of the changed base (5'-3'), and Y is the new base. Thus, the six "mismatch" oligonucleotides were C19G, G23A, C24G, C24A, C24T, and C25G. Duplexes containing a mismatch are referred to simply by the name of the mismatch oligonucleotide. The mismatch oligonucleotides were designed such that the mismatches were the most disruptive as measured by DNA breathing. For example, the WT base pair at position 19 on a *PML* duplex is C:G. Since the base pair that would generate the highest amount of breathing is G:G[204], the base at position 19 on the top strand was changed from C to G. Three base changes, resulting in G:G, A:G, and T:G mismatches, were generated for position 24.

Oligonucleotides were synthesized by our collaborators at GlaxoSmithKline (GSK), except for AP28, which was obtained from Eurofins MWG Operon, and the mismatch oligonucleotides, which were obtained from Sigma-Aldrich.

Cleavage of Plasmid DNA

DNA cleavage reactions were carried out using the procedure of Fortune and Osheroff[205]. Reaction mixtures contained 10.6 nM negatively supercoiled pBR322 plasmid DNA and 290 nM human topoisomerase IIα or 850 nM human topoisomerase IIα catalytic core in a final volume of 20 µL of human DNA cleavage buffer[10 mM Tris-HCl, pH 7.9, 5 mM $MgCl_2$, 100 mM KCl, 0.1 mM EDTA, and 2.5% (v/v) glycerol]. Reactions were carried out in the presence of 0-1000 µM trifluoromethylated 9-amino acridin-1(2H)-one derivatives or acridine, 0-50 µM amsacrine, or 0-200 µM etoposide. Mixtures were incubated for 6 min at 37 ºC and enzyme-DNA cleavage complexes were trapped by the addition of 2 µL of 5% sodium dodecyl sulfate (SDS) followed by 2 µL of 250 mM Na_2EDTA, pH 8.0. Proteinase K (2 µL of a 0.8 mg/mL solution) was added, and samples were incubated for 30 min at 45 ºC to digest the enzyme. Samples were mixed with 2 µL of agarose loading dye [60% sucrose (w/v), 10 mM Tris-HCl, pH 7.9, 0.5% bromophenol blue, 0.5% xylene cyanol], heated for 2 min at 45 ºC, and subjected to electrophoresis using 1% agarose gels in 40 mM Tris-acetate, pH 8.3 and 2 mM EDTA (TAE) containing 0.5 µg/mL ethidium bromide. DNA bands were visualized by UV light and quantified using an Alpha Innotech digital imaging system. Double-stranded DNA cleavage was monitored by the conversion of supercoiled plasmid to linear molecules.

To examine the effects of reducing agents on the activity of the trifluoromethylated 9-amino acridin-1(2H)-one derivatives, 0.5 mM DTT was included in DNA cleavage reactions that were carried out in the presence of 1 mM compound. Reactions were stopped, processed, and analyzed as described above.

To assess the effects of the trifluoromethylated 9-amino acridin-1(2H)-one derivatives on human topoisomerase IIα prior to the addition of DNA, 220 nM enzyme was incubated in the presence of 1 mM compound for 0-5 min at 37 ºC in a total volume of 18 µL of cleavage buffer. DNA cleavage was initiated by the addition of 10.6 nM negatively supercoiled pBR322 DNA

(final concentration) to reaction mixtures (final volume of 20 µL), and samples were incubated for 6 min at 37 ºC. Reactions were stopped, processed, and analyzed as described above.

Cleavage of Oligonucleotides

DNA cleavage reactions were carried out by a modification of the procedure of Deweese *et al.*[92]. The top (target) strand of each double-stranded oligonucleotide was labeled on its 5'-terminus in 30 µL reactions containing 200 pmol of oligonucleotide, 1 µL of T4 polynucleotide kinase (PNK) (New England BioLabs), 3 µL of T4 PNK buffer as supplied by the manufacturer, and 2 µL of [γ-^{32}P]ATP (~5000 Ci/mmol, Perkin Elmer). The cpm/µL of each labeled oligonucleotide was adjusted so that the intensity of bands on the polyacrylamide gel was reflective of topoisomerase II-mediated DNA cleavage and not differences in labeling efficiency. Reactions were incubated at 37 ºC for 60 min, with an additional 1 µL of T4 PNK added after the first 30 min. Radiolabeled oligonucleotides were purified with Qiagen Mini Quick Spin columns according to the manufacturer's instructions. Top/target and bottom/OTI oligonucleotides were annealed by incubating them at a 1:1 ratio (0.5 pmol/µL) at 70 ºC for 10 min, followed by a gradual cool down (-4 ºC/min) to 37 ºC.

DNA cleavage reaction mixtures contained 2 pmol of double-stranded oligonucleotides and 440 nM human topoisomerase IIα, 415 nM human topoisomerase IIβ, 600 nM wild-type yeast topoisomerase II, or 1,340 nM H1011Y mutant yeast topoisomerase II in a final volume of 20 µL of human or yeast[50 mM Tris-HCl pH 7.9, 25 mM $MgCl_2$, 500 mM NaCl, 0.5 mM disodium ethylenediaminetetraacetic acid (Na_2EDTA), pH 8.0, 12.5% (v/v) glycerol] cleavage buffer. (Levels of yeast enzymes in DNA cleavage assays were adjusted to yield similar levels of background DNA cleavage.) Reactions were initiated by the addition of enzyme. Samples were incubated at 37 ºC for 10 min (topoisomerase IIα and yeast topoisomerase II) or 1 min (topoisomerase IIβ), and reactions were stopped by the addition of 2 µL of 10% SDS and 2 µL of 250 mM Na_2EDTA. Samples were incubated with proteinase K for 30 min at 37 ºC to digest

the type II enzyme. DNA cleavage products were precipitated with ethanol, mixed with 5 µL of 80% (v/v) formamide, 100 mM Tris-borate and 2 mM EDTA (TBE), and 10% agarose loading dye, and heated to 75 ºC for 2 min. DNA samples were resolved on 14% denaturing polyacrylamide gels and were visualized and quantified using a Bio-Rad Molecular Imager.

All double-stranded oligonucleotides contained unmodified (non-OTI) top/target strands that were radiolabeled at the 5' end. Bottom strands were either unmodified (non-OTI) or contained a linked DEPT (OTI), linker alone (LIN28), or a tetrahydrofuran (AP28). In some cases, unmodified double-stranded oligonucleotides (non-OTI duplexes) were treated with 0-500 µM etoposide.

Intercalation of Compounds into Plasmid DNA

DNA intercalation reactions were carried out using the protocol of Fortune *et al*.[206] Calf thymus DNA topoisomerase I (0.4 U) and 5.3 nM pBR322 were incubated in 20 µL of cleavage buffer that contained 175 mM rather than 100 mM KCl. Reactions were carried out in the absence or presence of 1 mM trifluoromethylated 9-amino acridin-1(2H)-one derivatives. Ethidium bromide (10 µM), amsacrine (500 µM), and acridine (500 µM), which are well-characterized intercalators, were used as positive controls, and etoposide (500 µM), a non-intercalative topoisomerase II poison, was used as a negative control. Mixtures were incubated for 15 min at 37 ºC, and reactions were stopped by the addition of 3 µL of 0.77% SDS and 77.5 mM Na_2EDTA, pH 8.0. Samples were extracted using 23 µL of phenol:chloroform:isoamyl alcohol (25:24:1), and the aqueous layer was mixed with 2 µL of agarose loading dye. Intercalation products were resolved on a 1% agarose gel in TBE. Gels were stained for 30 min using 1 µg/mL ethidium bromide and rinsed in deionized water for 10 min, and DNA bands were visualized as described above. DNA intercalation was monitored by the conversion of relaxed to supercoiled plasmid molecules.

Ligation of Cleaved Plasmid DNA

DNA ligation mediated by human topoisomerase IIα was monitored according to the procedure of Byl *et al*.[207] DNA cleavage-ligation equilibria were established for 6 min at 37 ºC as described above in the absence or presence of 1 mM trifluoromethylated 9-amino acridin-1(2H)-one derivative, 50 μM amsacrine, or 50 μM etoposide. Ligation was initiated by placing the reaction mixtures on ice. The temperature shift allows ligation but prevents the formation of new cleavage complexes[208]. Reactions were terminated after 0-15 s by the addition of 2 μL of 5% SDS followed by 2 μL of 250 mM Na_2EDTA, pH 8.0. Samples were processed, resolved on 1% agarose gels in TAE with ethidium bromide, and analyzed as described above. Ligation was monitored by the loss of linear DNA.

Ligation of Cleaved Oligonucleotides

DNA ligation assays were carried out with topoisomerase IIα by a modification of the procedure of Byl *et al.*[207]. DNA cleavage/ligation equilibria were established as in the *Cleavage of Oligonucleotides* section. Reactions contained either an unmodified double-stranded oligonucleotide in the presence of 500 μM etoposide or an unmodified top (i.e. target) strand hybridized to an OTI28 bottom strand. Ligation was initiated by placing the reaction mixtures on ice and were stopped by the addition of 2 μL of 10% SDS followed by 2 μL of 250 mM Na_2EDTA. Samples were processed, resolved on denaturing polyacrylamide gels, and analyzed as described above. The percent DNA cleavage at time zero was set to 100%, and the rate of ligation was determined by quantifying the loss of cleaved DNA over time.

Persistence of Oligonucleotide-Enzyme Cleavage Complexes

DNA cleavage/ligation equilibria were established using topoisomerase IIα and oligonucleotide substrates as described above. Persistence reactions were carried out by modification of the procedure of Bandele and Osheroff[209]. Reactions contained either an unmodified double-stranded oligonucleotide in the presence of 500 μM etoposide or an unmodified top strand

hybridized to an OTI28 bottom strand. Assay mixtures were diluted 20-fold with cleavage buffer incubated at 37 ºC for up to 120 min. Reactions were stopped and samples were processed, resolved on denaturing polyacrylamide gels, and analyzed as described above. The percent DNA cleavage at time zero was set to 100%, and the stability of the cleavage complexes was determined by quantifying the loss of cleaved DNA over time.

Trifluoromethylated 9-Amino-3,4-Dihydroacridin-1(2H)-One Chemistry

The following procedures were carried out by Alexis Sledge and Amine Laradji from the laboratory of Dr. Cosmas Okoro, a collaborator at Tennessee State University.

The trifluoromethylated 9-amino-3,4-dihydroacridin-1(2H)-one derivatives (referred to as trifluoromethylated 9-amino acridin-2-ones) were prepared from the corresponding enaminobenzonitrile[210], following the procedure published by Gregory M. Shustske and coworkers[211]. All compounds were resuspended in 100% DMSO.

9-Amino-3-(trifluoromethyl)-3,4-dihydro-2H-acridin-1-one (Compound 1)

A 50-mL round-bottom flask fitted with a condenser and magnetic stirrer was flushed with nitrogen. 5-H-2-(3-oxo-5-(trifluoromethyl)cyclohex-1-enylamino)benzonitrile (1 mmol) was placed in the flask along with CuCl (0.0165 g, 0.167 mmol), anhydrous K_2CO_3 (0.046 g, 0.333 mmol), and toluene (10 mL), and the resulting mixture was refluxed for 6 h. The reaction was determined to be complete after 6 h as monitored by thin layer chromatography (TLC). The hot mixture was filtered into hexane, and the precipitate was separated and removed by filtration. The precipitate was washed with water and the filter cake was recrystallized from methanol.

9-Amino-6-methyl-3-trifluoromethyl-3,4-dihydro-2H-acridin-1-one (Compound 2)

A similar procedure described for the preparation of compound 1 was used, except that 4-methyl-2-(3-oxo-5-(trifluoromethyl)cyclohex-1-enylamino)benzonitrile replaced the 5-H compound and tetrahydrofuran replaced the toluene in the reaction mixture.

9-Amino-7-chloro-3-(trifluoromethyl)-3,4-dihydro-2H-acridin-1-one (Compound 3)

A similar procedure described for the preparation of compound 1 was used, except that 5-chloro-2-(3-oxo-5-(trifluoromethyl)cyclohex-1-enylamino)benzonitrile replaced the 5-H compound in the reaction mixture.

9-Amino-7-fluoro-3-(trifluoromethyl)-3,4-dihydro-2H-acridin-1-one (Compound 4)

A similar procedure described for the preparation of compound 1 was used, except that 5-fluoro-2-(3-oxo-5-(trifluoromethyl)cyclohex-1-enylamino)benzonitrile replaced the 5-H compound and tetrahydrofuran replaced the toluene in the reaction mixture.

9-Amino-7-nitro-3-(trifluoromethyl)-3,4-dihydro-2H-acridin-1-one (Compound 5)

A similar procedure described for the preparation of compound 1 was used, except that 5-nitro-2-(3-oxo-5-(trifluoromethyl)cyclohex-1-enylamino)benzonitrile replaced the 5-H compound and tetrahydrofuran replaced the toluene in the reaction mixture.

9-Amino-7-bromo-3-(trifluoromethyl)-3,4-dihydro-2H-acridin-1-one (Compound 6)

A similar procedure described for the preparation of compound 1 was used, except that 5-bromo-2-(3-oxo-5-(trifluoromethyl)cyclohex-1-enylamino)benzonitrile replaced the 5-H compound and tetrahydrofuran replaced the toluene in the reaction mixture.

3-(trifluoromethyl)-3,4-dihydro-2H-acridin-1-one (Compound 7)

Aqueous HCl (1 mL of 1 N) was added to a mixture of 2-aminobenzaldehyde (1 mmol) and 5-(trifluoromethyl)cyclohexane-1,3-dione (1 mmol). The resulting mixture was heated at 75 ºC for 2 h. The reaction was determined to be complete after 6 h as monitored by TLC, and the resulting suspension was neutralized with 1 mL of 1 M NaOH. The precipitate was filtered, washed thrice with 6 mL water, air-dried, and recrystallized from ethanol.

OTI Chemistry

The following procedures were carried out by Drs. Sabine Fenner, Steven Ratcliffe, Alberto Isidro-Llobet, and Michael Hann, collaborators at GSK.

A scheme for the synthesis of OTIs linked to the etoposide core is shown in Figure 8. On the basis of the molecular modeling results, an 8-carbon linker was utilized, which consisted of a terminal alkyne moiety attached to the C5 position of a cytosine or thymine residue to attach an azide-modified DEPT (1) via copper-catalyzed click chemistry.

Synthesis of the activated etoposide core, shown in the top portion of Figure 8, started with commercially available DEPT (**1**) (ABCAM Biochemicals). Compound **1** subsequently was protected with carboxybenzyl (Cbz) at the 4'-OH using benzyl chloroformate and triethylamine in dichloromethane[103]. The desired product **2** was obtained in 91% isolated yield. The 4-OH of **2** was reacted with monotosylated diethylene glycol[104] using boron trifluoride etherate in dichloromethane at -20 ºC to generate **3a-b** in 72% yield as a mixture of two epimers. Removal of the Cbz protecting group under hydrogenation reaction conditions with Pd/C in ethyl acetate resulted in **4a-b** in 94% yield. The tosyl group was displaced with sodium azide in dimethyl formamide at 60 ºC and generated **5a-b** in 67% yield as a mixture of two epimers. The desired azide coupling partner **5a** was purified as a single epimer by chiral chromatography.

The synthesis of OTIs, exemplified by **7**, is shown in the bottom portion of Figure 8. Oligonucleotide **6**, which included an alkyne-modified cytosine (purchased from Jena Biosciences) at position 28, was synthesized by well-established solid phase methods. Copper-catalyzed click chemistry was employed to synthesize OTI28 (**7**) using a preformed complex of copper bromide and Tris(benzyltriazolylmethyl)amine (TBTA) in a mixture of DMSO, tert-butanol and water. A final isolated yield of 46% was obtained after HPLC purification. Subsequent OTIs

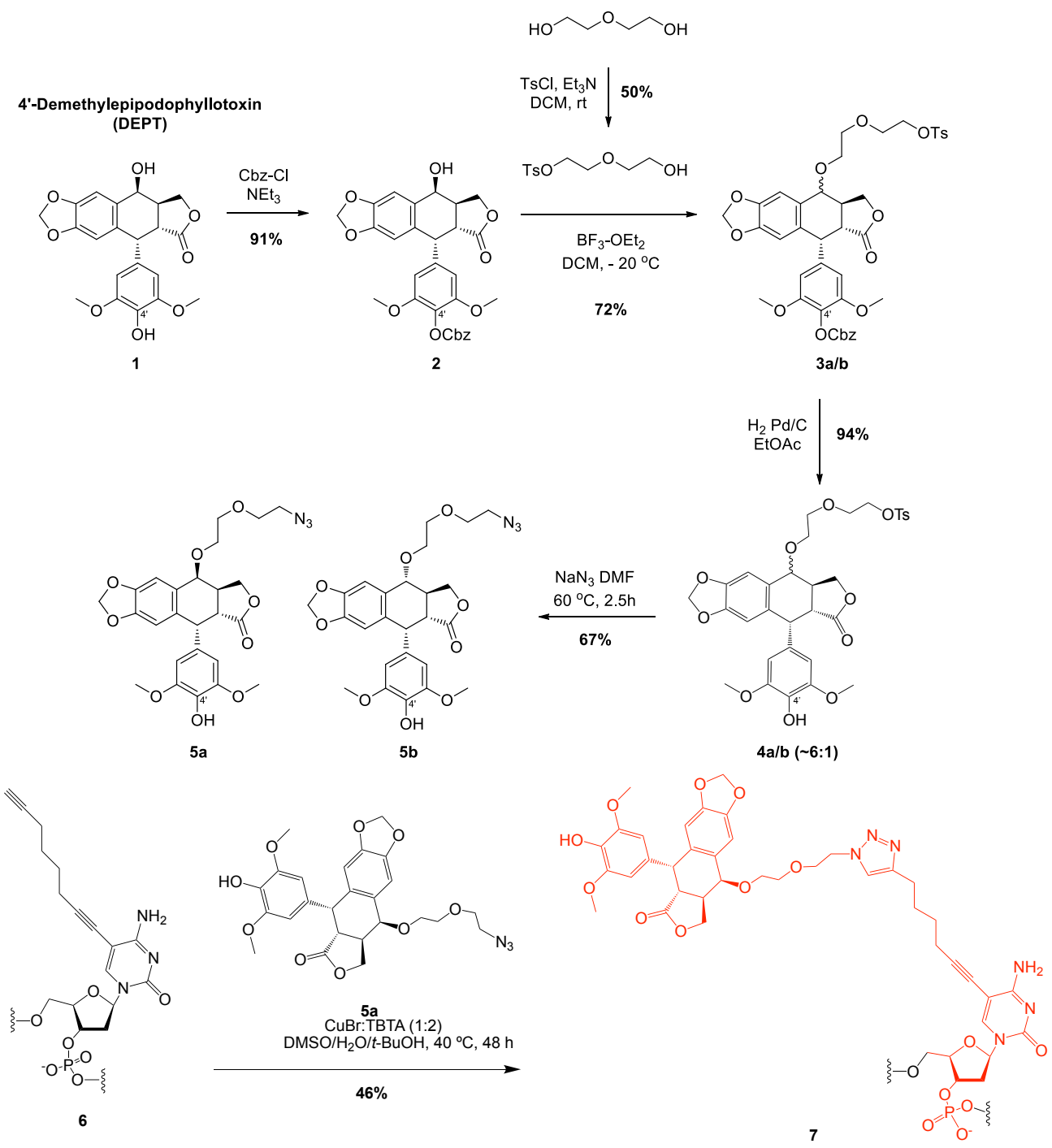

Figure 8. Schematic of the synthesis of OTIs. The synthesis of OTI28 (**7**) is shown as an example. DEPT (**1**) was protected with carboxybenzyl (Cbz) at the 4'-OH using benzyl chloroformate and triethylamine in dichloromethane to yield **2**. The 4-OH of **2** was reacted with monotosylated diethylene glycol using boron trifluoride etherate in dichloromethane at -20 ºC to generate **3a-b** as a mixture of two epimers. Removal of the Cbz protecting group under hydrogenation reaction conditions with Pd/C in ethanol resulted in **4a-b.** Continued next page.

The tosyl group was displaced with sodium azide in dimethyl formamide at 60 ºC to generate **5a-b** as a mixture of two epimers. The desired azide coupling partner **5a** was purified as a single epimer by chiral chromatography. Copper-catalyzed click chemistry was used to couple **5a** to oligonucleotide **6** (which included an alkyne-modified cytosine at position 28) to yield OTI28 (**7**).

were synthesized in a similar manner with an alkyne-modified thymine (Integrated DNA Technologies) at positions 23, 29, or 33 as the point of attachment for the linked DEPT, yielding OTI23, OTI29, and OTI33, respectively. Three additional OTIs of different lengths, a 50-mer, 30-mer, and 20-mer, were directed against a patient-derived *PML-RARA* breakpoint sequence (see below). The linked etoposide core in the 50-mer was positioned at the same base as OTI29.

Purity of all oligonucleotides ranged from 90% to 99.9%.

Molecular modeling

These procedures were carried out by Dr. Benjamin Bax at GSK.

To guide the placement and length of the chemical linker that joined the active DEPT core of etoposide to the modified base in the oligonucleotides, structures of OTI complexes were modeled using Coot[212], MOE[213], and Maestro (Schrödinger Release 2017-2: Maestro, Schrödinger, LLC, New York, NY, 2017). Models were based on the crystal structures of the human topoisomerase IIβ and topoisomerase IIα cleavage complexes with DNA and two etoposide molecules (one at each scissile bond) (PDB code: 3QX3[136] and PDB code: 5GWK[214], respectively), and the *Staphylococcus aureus* gyrase-DNA complex one etoposide molecule (PDB code: 5CDN)[215] (Figure 9). The positions of the etoposide molecules in the DNA complexes with human and bacterial enzymes are essentially the same (Figure 9).

With two etoposide molecules bound (one at each scissile bond), the DNA gate seems to be wedged open with a relatively small area buried between the two protein subunits at the DNA gate[136, 215] (Figure 10). However, a much larger area is buried between the two subunits at the DNA gate (Figure 10) in the *S. aureus* DNA gyrase with one etoposide bound, and the common CRsym conformation is observed[215]. Given that this conformation has also been observed with eukaryotic type IIA topoisomerases[64, 215], the subunits in our modeled topoisomerase IIβ complex with one etoposide were modeled in a CRsym conformation (Figure

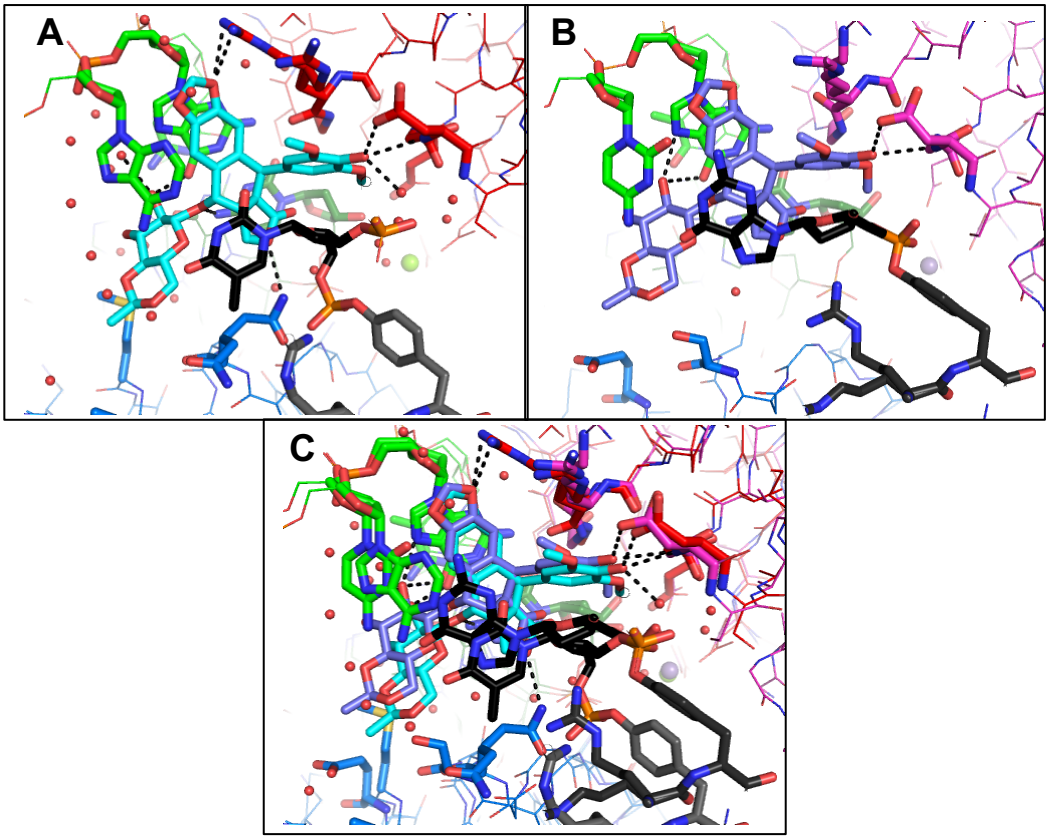

Figure 9. **Similarity of the etoposide binding site in crystal structures of DNA cleavage complexes formed with human topoisomerase IIβ and *S. aureus* gyrase.** (**A**) Structure of human topoisomerase IIβ (PDB code: 3QX3) with an etoposide molecule (cyan carbons) bound. One topoisomerase II protomer subunit has red carbons (TOPRIM domain) or blue carbons. Carbons from the DNA segment bound to this subunit are shown in green. The second topoisomerase II protomer subunit is shown in gray. Carbons from the DNA segment bound to this subunit are shown in black. Residues close to the etoposide are shown as sticks. (**B**) Structure of *S. aureus* gyrase (PDB code: 5CDN) with an etoposide molecule (marine carbons) bound. (**C**) Comparison of A and B. Note the difference in positions of the catalytic tyrosine from the subunits shown in blue and gray. These data were generated by collaborators at GSK.

11; notice the movement of the catalytic tyrosine residues between the complex with one and two etoposides relative to movement of the two subunits).

The alkyne moiety of the linker on the C5 position of the modified base projects ~2.6 Å further than the methyl on the C5 position of a thymine or a methylated cytosine (Figure 10). In modeling studies, the modified base was covalently attached to DEPT with a linker (Figures 11E,F and 8), and was modeled at four positions adjacent to the cleavage site on each strand (Figure 12): -2, -1, +1, and +2 on the cleaved strand, and +3*, +4*, +5*, and +6* on the non-cleaved (or OTI) strand. The rod-like alkyne moiety was observed to clash with protein residues when positioned on the cleaved strand at the -2, -1, +1, or +2 positions. However, modeling the rod-like alkyne moiety on the uncleaved strand at the +3*, +4*, +5*, or +6* position did not result in any clashes (Figure 12). These models indicate that cleavage is most likely to occur on the target strand rather than the OTI strand itself. Two different lengths of linkers were modeled, but a much longer linker (Figure 11E,F) was needed to enable the linked etoposide core to reach back to the binding site in the DNA from the +3*, +4*, +5*, or +6* positions.

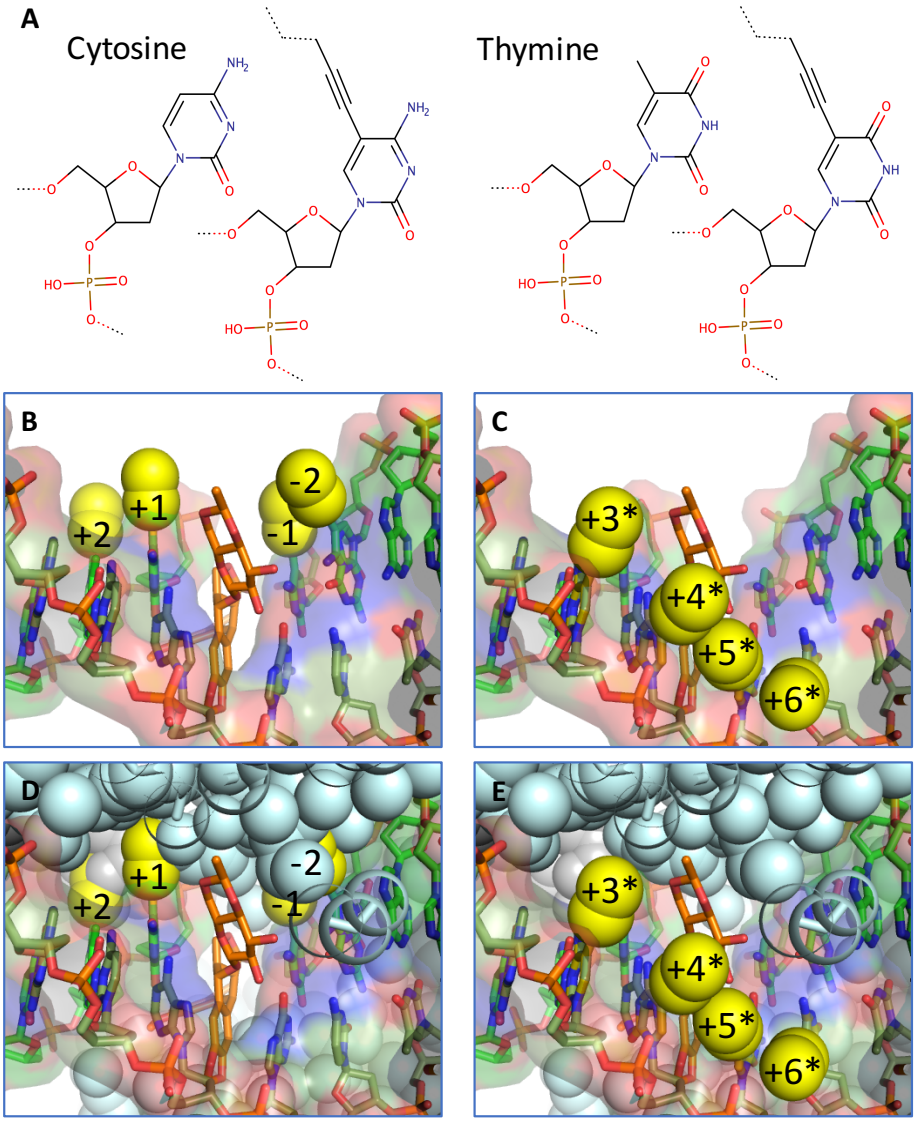

Figure 10. **Comparisons of etoposide crystal structures.** (**A**,**B**) Structure of human topoisomerase IIβ (PDB code: 3QX3) with a bound etoposide molecule. The colored subunit has been superimposed on the grey subunit in B (the complex displays C2 symmetry). DNA, orange; G DNA, gate DNA. (**C**,**D**) A 2.8 Å-crystal structure of *S. aureus* gyrase (PDB code: 5CDN) bound to one etoposide molecule. The colored subunit in D has been superimposed on the grey subunit. Note the relative shift in the subunit that was not superimposed (this complex is asymmetric). (**E**,**F**) A 2.45 Å-crystal structure of *S. aureus* gyrase (PDB code: 5CDP) with nicked DNA and one etoposide bound. The colored subunit in F has been superimposed on the grey subunit. Note that this complex is nearly C2 symmetric, apart from the ligand binding site. These data were generated by collaborators at GSK.

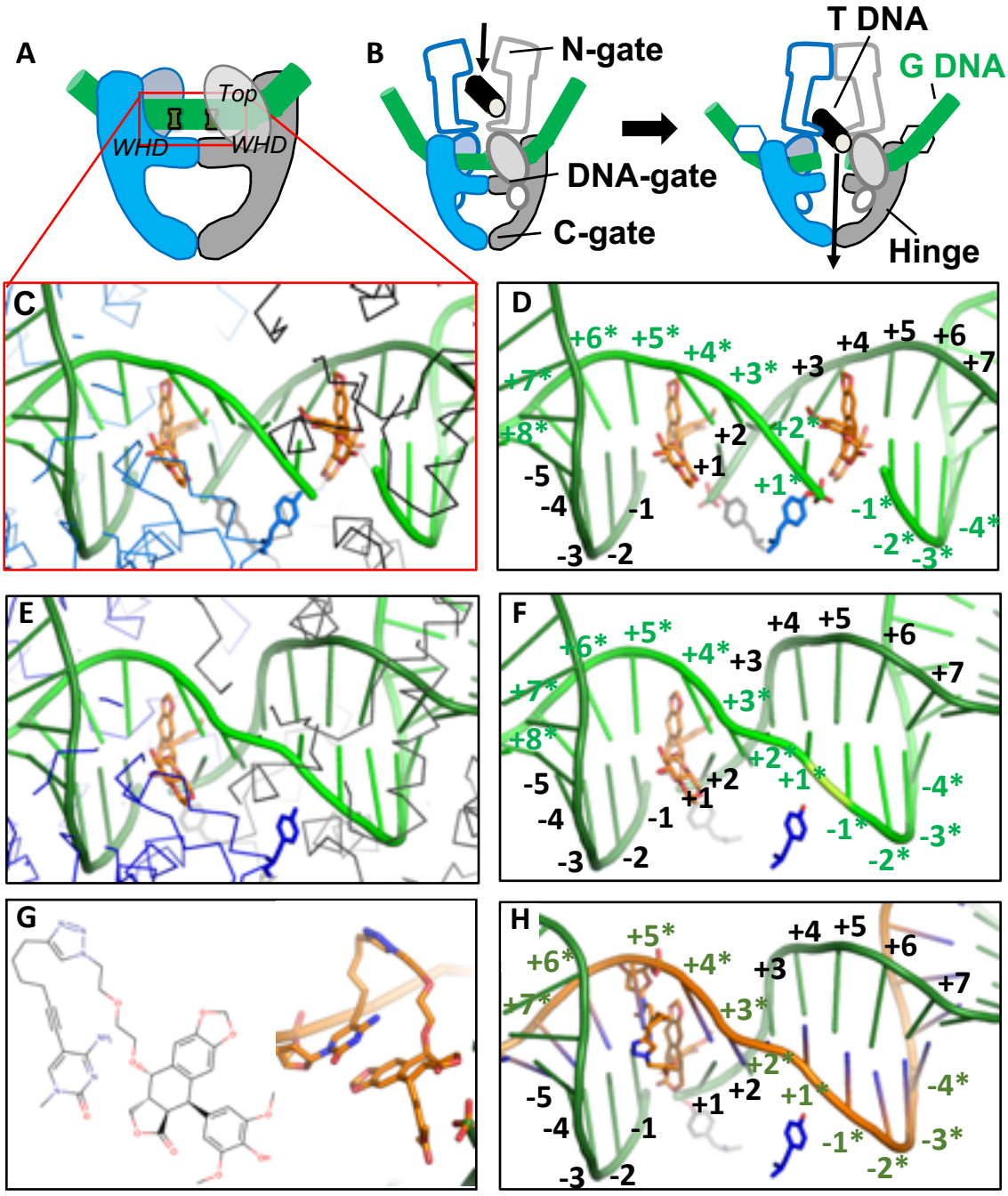

Figure 11. **Structure-guided design of an OTI.** (**A**) Schematic illustrating domains of type II topoisomerases used to determine the crystal structure of human topoisomerase IIβ covalently attached to DNA (green) in the presence of etoposide (orange). Domains pictured are TOPRIM (Top) and winged helix domain (WHD). (**B**) Schematic of topoisomerase II function. Protein protomer subunits are shown in blue and gray. T DNA, transport segment (black); G DNA, gate segment (green). (**C,D**) Detail from the crystal structure of a topoisomerase IIβ cleavage complex with two bound etoposide molecules (orange) stabilizing a double-stranded DNA (green) break (PDB code 3QX3). For clarity, in panel C, only the Cα trace of the protein subunits (blue and black lines) and catalytic tyrosine residues (blue and grey sticks) are shown. Continued next page.

In panel D, only the catalytic tyrosine residues that cleave the DNA are shown. The conventional numbering scheme used for DNA cleavage complexes formed by type II topoisomerases is shown. The enzyme cleaves between the -1 and the +1 on each strand. The numbering on the two strands in the double helix is differentiated by the presence or absence of asterisks. The catalytic tyrosine residues are covalently attached to the DNA at the +1 positions. (**E,F**) Model of a cleavage complex with one bound etoposide molecule stabilizing a single-stranded DNA break. The cleaved DNA strand is indicated by asterisks. The differences in the protein structure shown in E and F are the same as those in C and D. (**G**) Chemical (left) and modeled (right) structure of the etoposide core (DEPT) linked to the pyrimidine base. (**H**) OTI28 (orange strand) modeled with the modified cytosine base in the +5* position, stabilizing DNA scission at the 23-24 site (-1 to +1) on the cleaved target strand (green). These data were generated by collaborators at GSK.

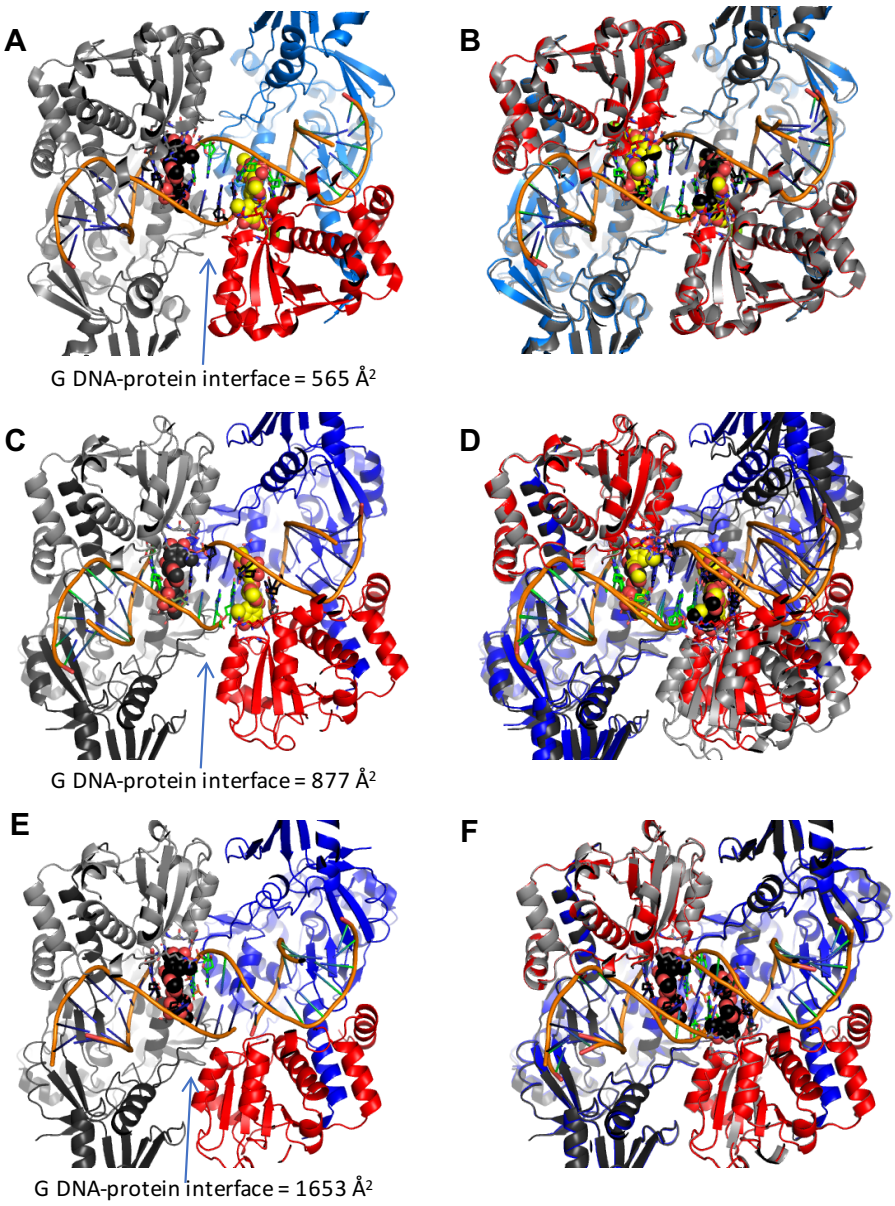

Figure 12. The alkyne moiety of the modified C or T is a rigid projection from the base. (**A**) Cytosine and thymine are compared with modified versions of the bases. Note that extra carbons project as a rigid rod-like group from the C5 position of the pyrimidines. The rest of the linker is flexible, indicated by dotted lines. (**B**,**C**) Etoposide (orange) and DNA (green) as seen in the cleavage complex of a 2.15 Å crystal structure of human topoisomerase IIβ (PDB code: 3QX3) with a molecule of etoposide. Modified bases have been superimposed on existing bases with the two extra carbons that protrude from the C5 position of the base shown in yellow. For clarity, the enzyme is not shown in B and C. (**D**,**E**) The same views as in B and C, but with the topoisomerase IIβ shown in cyan (space-filling model). Note that the protein clashes with the protruding acetylene group of the modified bases at positions -2, -1, +1 and +2, but not at positions +3*, +4*, +5*, and +6*. These data were generated by collaborators at GSK.

Chapter 3: Novel Trifluoromethylated 9-amino-3,4-dihydroacridin-1(2H)-ones Act as Covalent Poisons of Human Topoisomerase IIα

Introduction

A number of topoisomerase II-targeting anticancer drugs, including amsacrine, utilize an acridine or related aromatic core as a scaffold. Therefore, to further explore the potential of acridine-related compounds to act as topoisomerase II poisons, novel trifluoromethylated 9-amino-3,4-dihydroacridin-1(2H)-one derivatives (referred to as trifluoromethylated 9-amino acridin-1(2H)-ones) were synthesized and examined for their ability to enhance DNA cleavage mediated by human topoisomerase IIα.

Results indicate that many of the trifluoromethylated 9-amino acridin-1(2H)-ones are able to stabilize DNA cleavage mediated by topoisomerase IIα, but that they do not do so by intercalating into the DNA. Initial results suggested that the compounds do not act as interfacial topoisomerase II poisons, as they do not inhibit enzyme-mediated DNA religation. Further investigation suggests that their mechanism of action is closer to that of a covalent poison, as their activity is severely reduced by incubation with a reducing agent, they do not stabilize cleavage mediated by the catalytic core of human topoisomerase IIα, and they inhibit cleavage by the full-length enzyme when they are incubated together prior to the addition of DNA.

Results

Select Substituents Allow Novel Trifluoromethylated 9-Amino Acridin-1(2H)-ones to Stabilize Topoisomerase IIα-mediated DNA Cleavage

The structure of the seven trifluoromethylated 9-amino acridin-1(2H)-ones synthesized, as well as that of amsacrine for comparison, are shown in Figure 13. The trifluoromethyl group at C3 was included to provide additional H-bonding groups and because the presence of fluorine residues often provides improved pharmacological properties, such as increased membrane permeability, enhanced hydrophobic binding interactions, and improved metabolic stability

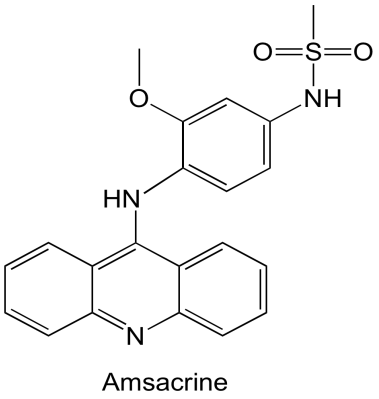

Amsacrine

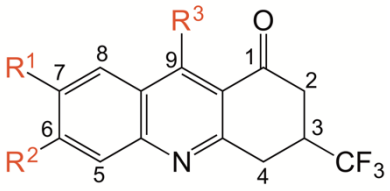

Compound	R_1	R_2	R_3
1	-H	-H	$-NH_2$
2	-H	$-CH_3$	$-NH_2$
3	-Cl	-H	$-NH_2$
4	-F	-H	$-NH_2$
5	$-NO_2$	-H	$-NH_2$
6	-Br	-H	$-NH_2$
7	-H	-H	-H

Figure 13. **Structures of amsacrine and the trifluoromethylated acridin-1(2H)-one derivatives used in the current study.** The trifluoromethylated acridin-1(2H)-one skeleton is shown (top right) and the substituents at positions R^{1-3} (red) for compounds **1-7** are listed in the table. Amsacrine is shown on the bottom left. The trifluoromethylated acridin-1(2H)-one derivatives were synthesized by collaborators at Tennessee State University.

(discussed in Fadeyi *et al.*[216]). The syntheses of these compounds started with the corresponding enaminobenzonitrile[216] utilizing the generalized scheme shown in Figure 14. The detailed syntheses are described in Chapter 2, and physical and chemical characterizations of the compounds can be found in the Supplementary Data of Infante Lara *et al.*[197].

As a first step toward analyzing the effects of the trifluoromethylated acridin-1(2H)-one derivatives on human topoisomerase IIα, I determined the ability of these compounds to enhance enzyme-mediated double-stranded cleavage of negatively supercoiled DNA (Figure 15). Several of the trifluoromethylated acridin-1(2H)-one derivatives induced high levels of enzyme-mediated DNA cleavage, although none were as potent as amsacrine or etoposide. Acridine, the aromatic core of amsacrine, did not enhance DNA cleavage. On the basis of the cleavage data (Figure 15), a number of structure-activity relationships among the compounds became evident.

First, the presence of the 9-amino moiety was critical for the activity of the trifluoromethylated acridin-1(2H)-one derivatives. Removal of this group (converting compound **1** to compound **7**) decreased cleavage enhancement from >8-fold to ~1.5-fold and increased the CC_3 (level of compound required to triple baseline levels of cleavage complexes; used as a measure of potency because this value is within the linear range of activity for the compounds examined) from 155 μM to ≫1000 μM. Second, the inclusion of either a methyl group at C6 (compound **2**) or a nitro moiety at C7 (compound **5**) was deleterious and decreased both the level of DNA cleavage and the potency of the compounds. Third, the inclusion of halogens at C7 affected the activity of the compounds against topoisomerase IIα. The presence of Cl, F, or Br (compounds **3**, **4**, or **6**, respectively) resulted in a modest reduction (<35%) in cleavage levels (at 1000 μM compound) compared to compound **1**. However, the chloro- and bromo-substituted compounds displayed an ~1.8-fold increase in potency. In contrast, the potency of the fluoro-substituted compound decreased ~3.4-fold.

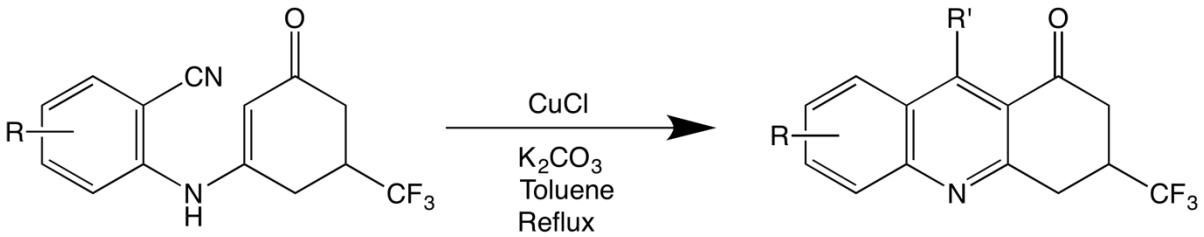

R = C6-H, C6-CH_3, C7-H, C7-Cl, C7-F, C7-NO_2, C7-Br
R' = C9-H, C9-NH_2

Figure 14. **Generalized scheme used to synthesize the trifluoromethylated acridin-1(2H)-one derivatives used in the current study.**

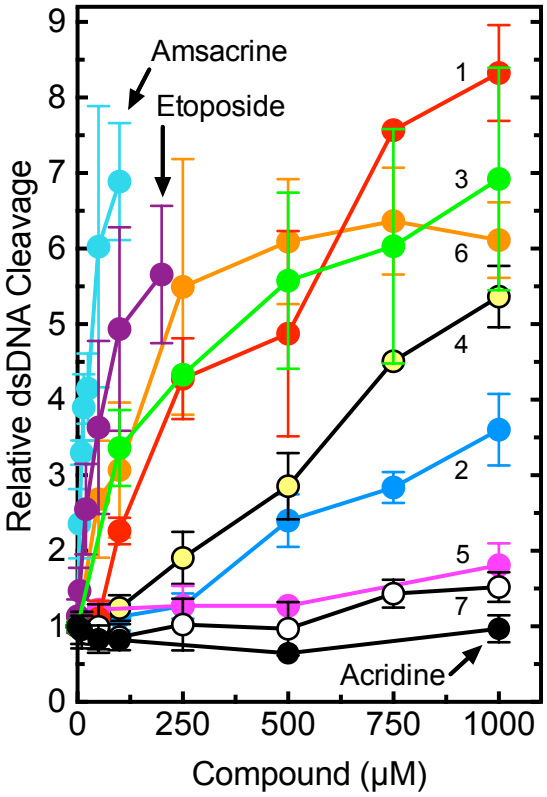

Compound	CC_3 (μM)
1	155
2	800
3	85
4	520
5	>>1000
6	90
7	>>1000
Acridine	>>1000
Amsacrine	8.5
Etoposide	32

Figure 15. **Effects of trifluoromethylated acridin-1(2H)-one derivatives on the DNA cleavage activity of human topoisomerase IIα**. Results with amsacrine, etoposide, and acridine are shown as controls. Activity is reported as the relative increase in double-stranded DNA (dsDNA) cleavage as compared to reactions carried out in the absence of compounds (left). Error bars represent the standard deviation of at least three independent experiments. The table (right) provides the concentrations (CC_3) of compounds **1–7**, acridine, amsacrine, and etoposide that are required to triple levels of cleavage complexes as compared to baseline levels generated in the absence of the compounds. These values are used as a measure of potency.

Trifluoromethylated 9-Amino Acridin-1(2H)-one Derivatives Do Not Intercalate Into the DNA

In some cases, enhanced interactions between topoisomerase II poisons and DNA leads to greater drug activity against the enzyme[113]. Therefore, the ability of the trifluoromethylated acridin-1(2H)-one derivatives to intercalate into DNA was assessed (Figure 16). In the concentration range examined, the compounds were weak intercalators at best (as determined by the shift in DNA topoisomer bands toward the position of negatively supercoiled DNA). Furthermore, there does not appear to be any correlation between the ability of the trifluoromethylated acridin-1(2H)-ones to intercalate and their activity against topoisomerase IIα. Compounds **2** and **4**, for example, displayed similar DNA cleavage enhancement but very different intercalation patterns. Furthermore, compound **5** displayed similar intercalation to compound **1**, but had a significantly lower potency against topoisomerase IIα. Because compounds **5** and **7** displayed virtually no activity against topoisomerase IIα, they were not subjected to further analysis.

Trifluoromethylated 9-amino Acridin-1(2H)-one Derivatives Do Not Inhibit Enzyme-Mediated Religation of DNA

Clinically relevant topoisomerase II-targeting drugs, such as amsacrine and etoposide, act as interfacial topoisomerase II poisons[94]. Therefore, to determine whether the trifluoromethylated 9-amino acridin-1(2H)-one derivatives act by a similar mechanism, the effects of these compounds on topoisomerase IIα-mediated DNA ligation were characterized (Figure 17). In marked contrast to amsacrine and etoposide, none of the trifluoromethylated 9- acridin-1(2H)-ones that enhanced DNA cleavage had any significant effect on rates of ligation. The lack of ligation inhibition does not preclude the possibility that the trifluoromethylated 9-amino acridin-1(2H)-one derivatives act as interfacial poisons. However, the finding suggests that these

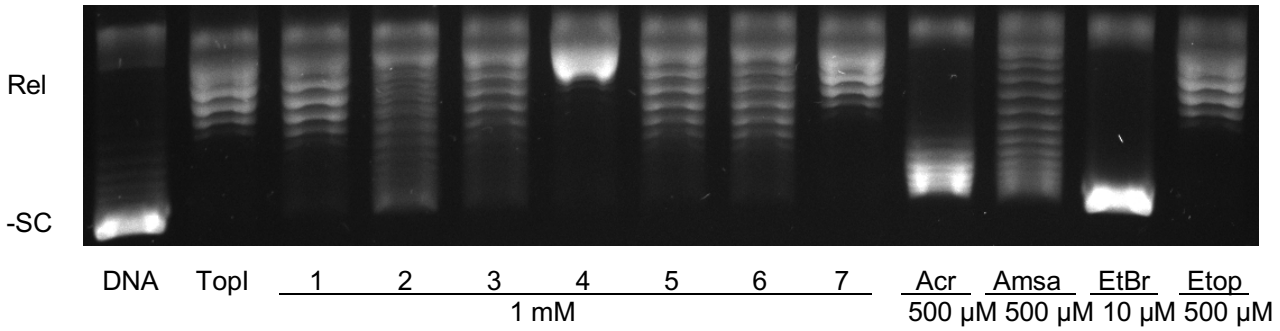

Figure 16. Intercalation of trifluoromethylated acridin-1(2H)-one derivatives into negatively supercoiled DNA. Results of a topoisomerase I-DNA relaxation assay are shown. Intercalation is indicated by the shift in the position of the plasmid from that of relaxed (Rel) DNA, which is generated upon incubation of negatively supercoiled DNA (-SC) with topoisomerase I. Each lane is labeled with the number of the trifluoromethylated acridin-1(2H)-one compound that was tested. Three intercalators, acridine (Acr, 500 μM), ethidium bromide (EtBr, 10 μM), and amsacrine (Amsa, 500 μM), and a non-intercalator, etoposide (Etop, 500 μM), are shown as positive and negative controls, respectively. Assays that contained only -SC DNA (DNA) or -SC DNA and topoisomerase I with no compound (TopI) are shown. Gel is representative of three independent experiments.

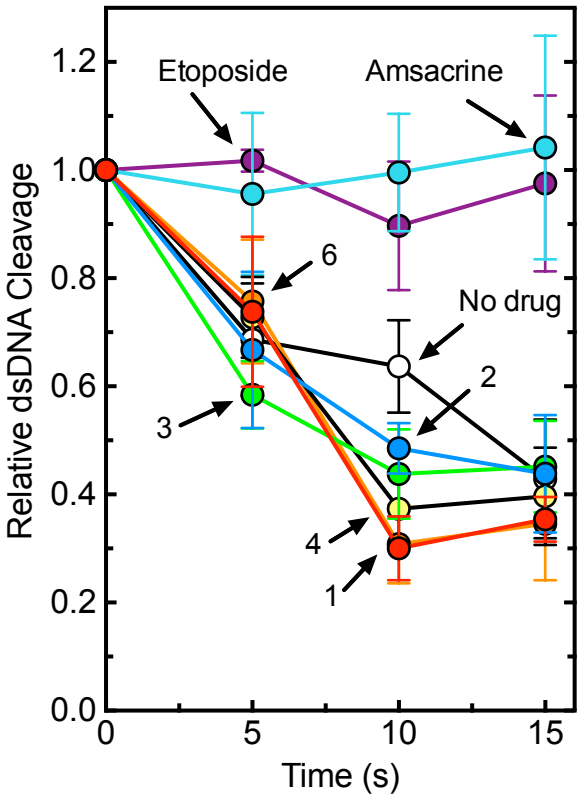

Figure 17. Effects of trifluoromethylated 9-amino acridin-1(2H)-one derivatives on DNA ligation mediated by topoisomerase IIα. Reaction mixtures were carried out in the absence (No drug) or presence of 1 mM compound. Reactions that contained 50 μM amsacrine or etoposide are shown as positive controls. Error bars represent the standard deviation of at least three independent experiments.

compounds may instead increase levels of topoisomerase IIα-DNA cleavage complexes through covalent interactions with the type II enzyme.

Trifluoromethylated 9-Amino Acridin-1(2H)-ones Display Characteristics of Covalent Topoisomerase II Poisons

In order to discern which mechanism the trifluoromethylated 9-amino acridin-1(2H)-one derivatives utilize to alter topoisomerase II function, I first determined the effects of DTT on the ability of these compounds to enhance topoisomerase IIα-mediated DNA cleavage (Figure 18). The reducing agent dramatically decreased levels of trifluoromethylated acridin-1(2H)-one-induced DNA cleavage. In contrast, DTT had no effect on the activity of the interfacial poison amsacrine. These results strongly suggest that the trifluoromethylated 9-amino acridin-1(2H)-one derivatives alter topoisomerase IIα-mediated DNA cleavage by acting as covalent poisons. Therefore, two additional experiments were carried out to confirm this mechanism.

I assessed the effects of the trifluoromethylated 9-amino acridin-1(2H)-one derivatives on the catalytic core of topoisomerase IIα, a construct that lacks both the C- and N-terminal domains (Figure 19). Interfacial poisons such as amsacrine maintain their activity against the catalytic core since their activity is dependent on interactions with the enzyme and DNA at the active site, but the trifluoromethylated 9-amino acridin-1(2H)-one derivatives did not induce enzyme-mediated DNA cleavage above background levels. As a final experiment, the trifluoromethylated 9-amino acridin-1(2H)-one derivatives were incubated with topoisomerase IIα prior to the addition of DNA (Figure 20). All of the compounds rapidly inhibited the DNA cleavage activity of the enzyme.

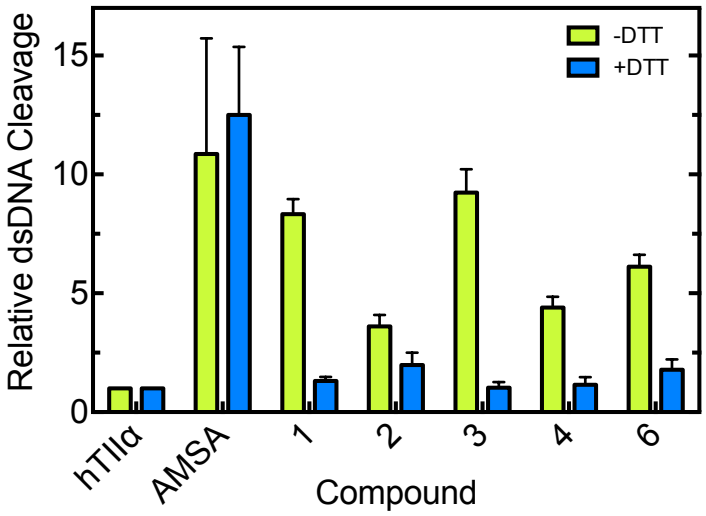

Figure 18. **Effects of a reducing agent on trifluoromethylated acridin-1(2H)-one- induced DNA cleavage mediated by topoisomerase IIα.** DNA cleavage reactions were carried out in the presence of 1 mM trifluoromethylated 9-amino acridin-1 (2H)-one derivatives in the absence (green) or presence (blue) of 0.5 mM DTT. Reactions carried out in the absence of compounds (hTIIα) or in the presence of 50 μM amsacrine (AMSA) are shown as controls. Error bars represent the standard deviation of at least three independent experiments.

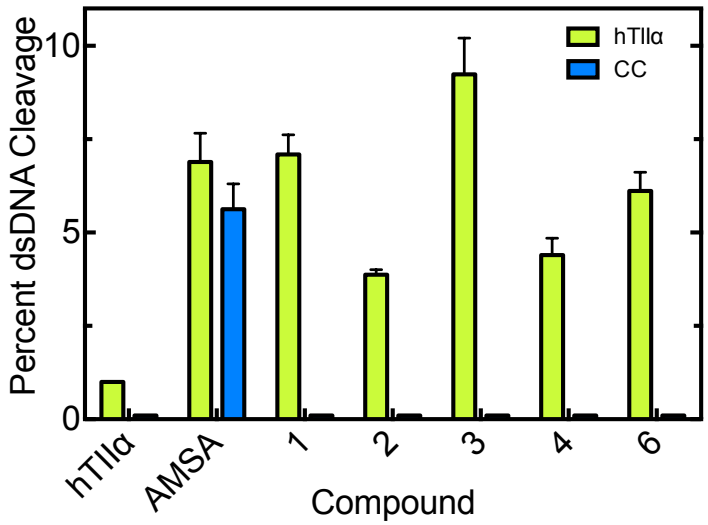

Figure 19. **Effects of trifluoromethylated 9-amino acridin-1(2H)-one derivatives on DNA cleavage mediated by the catalytic core of topoisomerase IIα.** DNA cleavage reactions using full-length topoisomerase IIα (green) or the catalytic core of the enzyme (blue) were carried out in the presence of 1 mM trifluoromethylated acridin-1(2H)-one derivatives. Reactions carried out in the absence of compounds (hTIIα) or in the presence of 50 μM amsacrine (AMSA) are shown as controls. Baseline levels of DNA cleavage mediated by the catalytic core are lower than those observed for the intact enzyme. Error bars represent the standard deviation of at least three independent experiments.

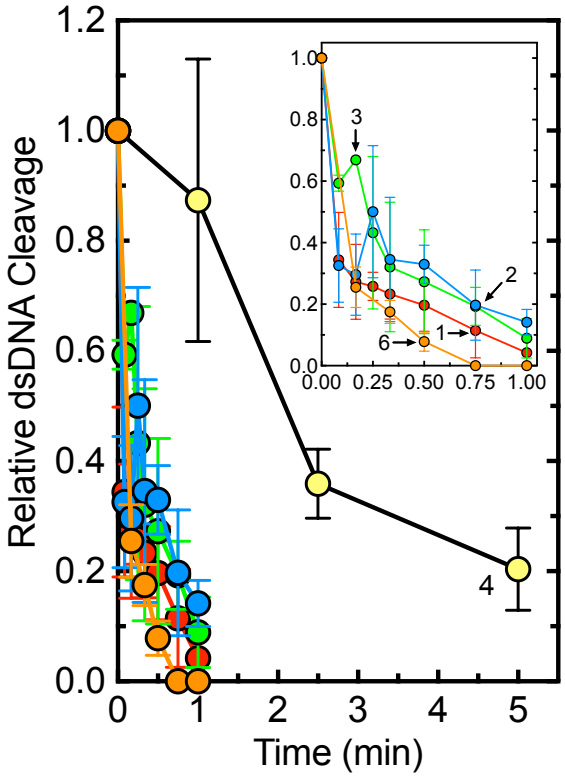

Figure 20. **Effects of trifluoromethylated 9-amino acridin-1(2H)-one derivatives on DNA cleavage mediated by topoisomerase IIα when incubated with the enzyme prior to the addition of DNA.** Cleavage reactions were initiated after topoisomerase IIα was incubated with 1 mM derivatives for 1-5 min. The inset displays an expansion of time points between 0-1 min for compounds **1**, **2**, **3**, and **6**. Error bars represent the standard deviation of at least three independent experiments.

Discussion

Taken together, the above experiments strongly suggest that the trifluoromethylated 9-amino acridin-1(2H)-one derivatives enhance topoisomerase IIα-mediated DNA cleavage by acting as covalent topoisomerase II poisons. The chemistry that underlies the adduction of topoisomerase IIα by the trifluoromethylated acridin-1(2H)-ones is not immediately apparent. However, given the essential nature of the 9-amino moiety for the activity of these compounds, it may involve amino-imino tautomerism or the hydrolysis of the amino group to form a more reactive species.

It is notable that the 4'-amino-methane-sulfon-*m*-anisidide head group of amsacrine (which also includes a primary aromatic amine) displays the ability to act as a covalent topoisomerase II poison[113]. On the basis of comparisons to amsacrine, it will be interesting to determine whether the addition of a head group to the trifluoromethylated acridin-1(2H)-one derivatives at the 9-amino position will convert these compounds to interfacial poisons that could act as scaffolds for the development of novel topoisomerase II-targeting drugs.

Chapter 4: Coupling the Core of the Anticancer Drug Etoposide to an Oligonucleotide Induces Topoisomerase II-mediated Cleavage at Specific DNA Sequences

Introduction

Etoposide and other topoisomerase II-targeting drugs are important anticancer therapeutics. Unfortunately, the safe usage of these agents is limited by their indiscriminate induction of topoisomerase II-mediated DNA cleavage throughout the genome[217] and by a lack of specificity toward cancer cells[18, 21, 25, 86, 87, 106].

A number of cancers are associated with the presence of a driver oncogene that is generated by a mutation or translocation in the DNA[218-220]. The ability to rapidly sequence patients' DNA affords a potential opportunity to develop new generations of topoisomerase II poisons that specifically target the driver mutations in cancer cells of affected individuals. This could introduce DNA strand breaks specifically in the oncogene or could generate cleavage complexes that act as roadblocks for transcription. In either case, disruption of the driver oncogene or interference with its transcription could potentially kill malignant cells that are dependent on the resulting oncoprotein. Consequently, this strategy could result in treatments that are cytotoxic toward cancer but display limited action against normal cells.

As a first step toward constraining the distribution of etoposide-induced DNA cleavage sites and developing sequence-specific topoisomerase II-targeting anticancer agents, the active core of etoposide, DEPT, was covalently coupled to oligonucleotides centered on a strong type II topoisomerase cleavage site in the *PML* gene[98, 99]. The initial sequence used for this OTI was identified as part of the translocation breakpoint of a patient with t-APL who had been treated with mitoxantrone for progressive multiple sclerosis[99]. Subsequent OTI sequences were derived from the observed t-APL breakpoint between *PML* and *RARA*. The proposed mechanism of action of OTIs can be seen in Figure 21.

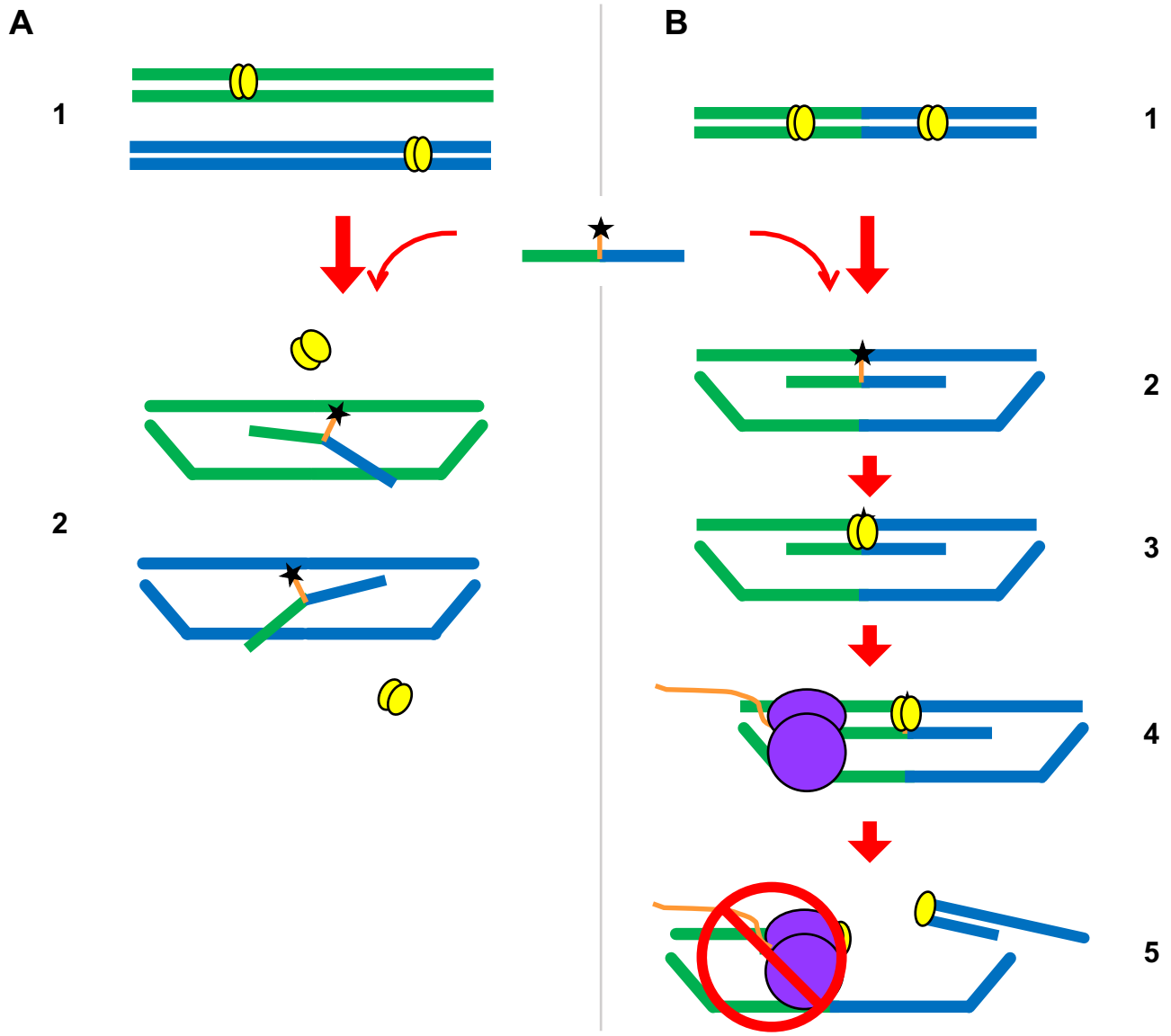

Figure 21. Proposed mechanism of action of OTIs. (**A**) In a population of non-cancer cells with WT parental genes (1, pair of green and pair of blue lines), an OTI (short green and blue line with black star, middle) designed to target a translocation would be unable to stabilize DNA cleavage by human type II topoisomerases (yellow ovals) on the WT parental genes (2). (**B**) In a population of cancer cells whose genomes contain the targeted translocation (pair of green/blue lines, 1), OTIs could hybridize to the target strand on the genome (2) such that if a type II topoisomerase bound at that site (3), it would stabilize enzyme-mediated DNA cleavage. Stable cleavage presents a danger to cells, as DNA processing systems (purple shapes, orange line, 4) like transcription machinery could collide with the cleavage complex (5), rendering the topoisomerase unable to religate the cleaved DNA[93, 101].

Results indicate that OTIs can be used to direct the sites of etoposide-induced DNA cleavage mediated by topoisomerase IIα and topoisomerase IIβ. Furthermore, OTIs directed against the *PML-RARA* breakpoint displayed cleavage specificity for oligonucleotides with the translocation sequence over those with sequences matching either parental gene. Finally, OTI duplexes containing a single mismatch were better able to stabilize DNA cleavage by both enzymes than free etoposide. This finding suggests that single-nucleotide polymorphisms (SNPs) are not appropriate targets for OTIs. Collectively, these studies demonstrate the feasibility of using oligonucleotides to direct topoisomerase II-mediated DNA cleavage to specific sites in the genome, especially those generated by chromosomal translocations.

Results

Structure-based Design of OTIs that Contain the Core of Etoposide

When cells are treated with etoposide, the drug induces topoisomerase II-mediated DNA cleavage at millions of sites throughout the human genome[81]. Therefore, in an effort to design an etoposide-based compound with specificity for cancer-associated DNA sequences, the active core of etoposide (DEPT) was covalently attached to a series of oligonucleotides by collaborators at GSK (Figures 8 and 11). DEPT was selected because it lacks the non-essential C4 sugar moiety of etoposide but retains a C4 hydroxyl group that can be activated for coupling reactions.

OTIs were designed to generate single-stranded, topoisomerase II-mediated cleavage on the strand opposite the etoposide core attachment site (Figure 11)[50]. To this end, crystal structures of human topoisomerase IIβ[136] and IIα[214] with two etoposide molecules and the bacterial *Staphylococcus aureus* DNA gyrase with one or two etoposide molecules[215] served as the basis for modeling studies (Figure 9). As a result of these studies, a linker consisting of a terminal alkyne moiety was attached to the C5 position of a cytosine or thymine residue and was

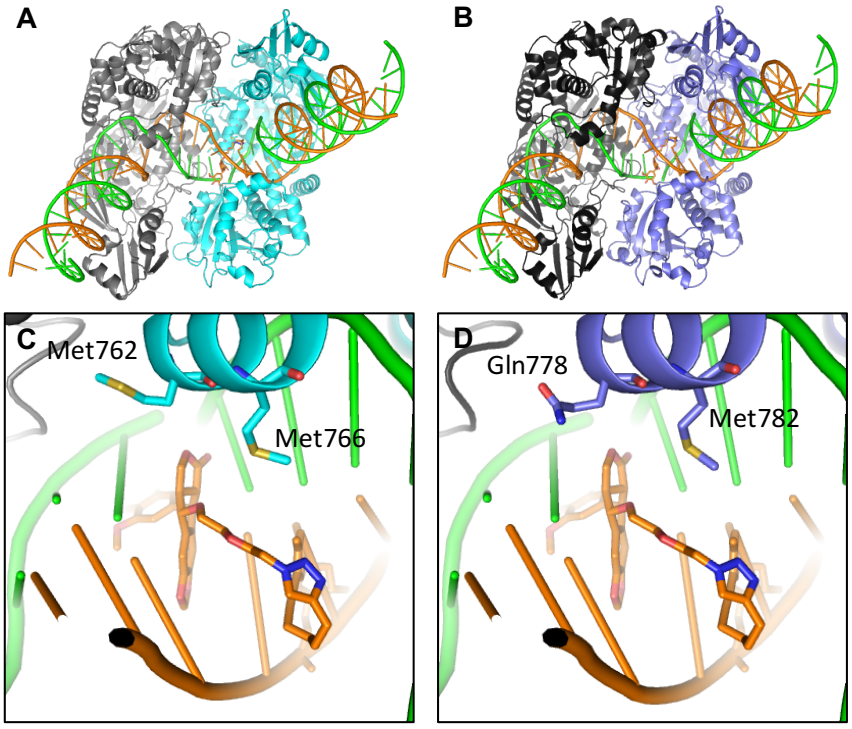

Figure 22. **Models of cleavage complexes of OTI28 with human topoisomerase IIα (left) and IIβ (right).** (**A,C**) Human topoisomerase IIα subunits (cyan and grey) are modeled in a single-stranded cleavage complex with OTI28 (orange) and target DNA (green). The target strand is cleaved at the 24-25 cleavage site. The crystal structure of a human topoisomerase IIα complex with etoposide (PDB code: 5GWK) was used in constructing the model. (**B,D**) Human topoisomerase IIβ subunits (blue and black) are modeled in a single-stranded cleavage complex with OTI28 (orange) and target DNA (green). The target strand is cleaved at the 24-25 cleavage site. The crystal structure of a human topoisomerase IIβ complex with etoposide (PDB code: 3QX3) was used in constructing the model. Note that in these cleavage complexes, the OTI linker does not come close to Met762 (topoisomerase IIα)/Gln778 (topoisomerase IIβ). These data were generated by collaborators at GSK.

coupled to a 4-azide-modified DEPT via copper-catalyzed click chemistry (Figure 8). The modeling studies indicated that the linked DEPT was capable of intercalating into a cleaved site on the opposite strand (shown for OTI28 in Figures 10, 11, 12, and 22).

An OTI Directed Against the PML *Gene Enhances DNA Cleavage Mediated by Human Type II Topoisomerases*

As a proof of concept that a covalently attached etoposide core can function as a sequence-specific topoisomerase II poison, an initial OTI (OTI28) was designed that utilized a DNA sequence spanning a strong drug-induced topoisomerase II cleavage hotspot within intron 6 of the *PML* gene (bases 1482-1489)[98]. This cleavage hotspot is also present in the t(15;17) translocation of a patient with APL who had been treated with mitoxantrone[99]. The interaction of an OTI that spanned the APL breakpoint sequence with topoisomerase II will be discussed in a later section.

The sequence of the central 30 nucleotides of the 50-base pair-oligonucleotide used for the initial experiments (bases 1461-1510) is shown in Figure 23A. When the unmodified oligonucleotide duplex (radiolabeled on its top/target strand) was treated with free etoposide in the presence of topoisomerase IIα, several strong DNA cleavage sites were observed (Figure 23B). The cleavage site between bases 24-25 (1484-1485) is also a strong site for mitoxantrone and is believed to be the hotspot that results in ~50% of the t(15;17) translocations observed in patients with therapy-related APLs following treatment with mitoxantrone[87, 98, 99, 177, 180].

To examine the effects of a linked drug on topoisomerase II-mediated DNA cleavage of this sequence, the active core of etoposide was covalently attached to cytosine 28 on the bottom strand (Figure 23A) through a flexible linker as described above. On the basis of modeling studies, the tethered drug moiety should be able to intercalate into the scissile bond between bases 24-25, stabilizing cleavage at that site (Figures 11 and 25A). As seen in Figure 23, this

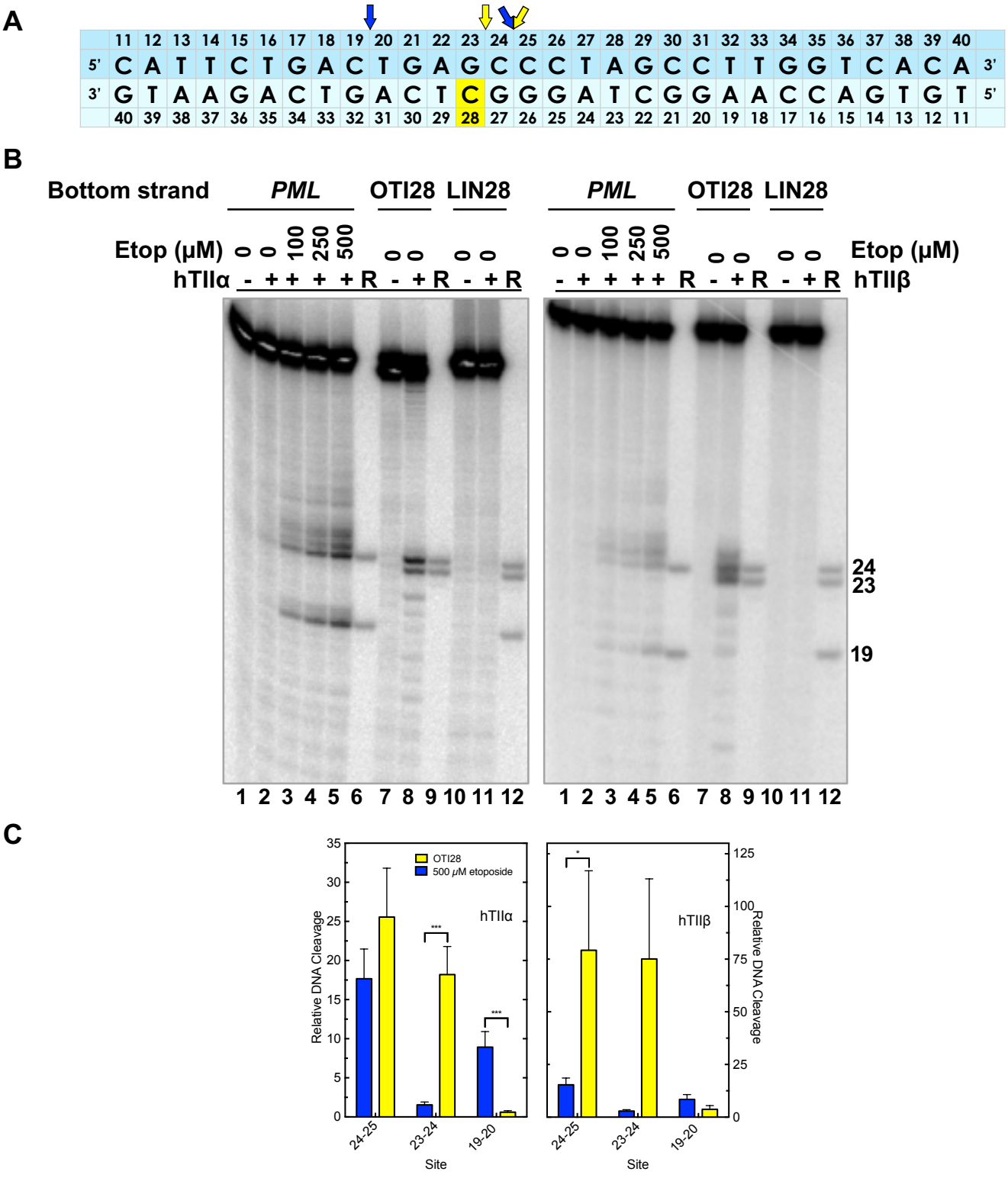

Figure 23. An oligonucleotide-linked etoposide core increases topoisomerase II-mediated DNA cleavage. Continued next page.

(**A**) The central 30 base pairs of a double stranded 50-mer oligonucleotide sequence corresponding to bases 1471-1500 (top strand) of *PML* intron 6. The yellow box denotes the position of the tethered etoposide core and linker moieties on OTI28 or LIN28. Arrows indicate sites of DNA cleavage induced by free etoposide (blue) or OTI28 (yellow). (**B**) Comparison of DNA cleavage mediated by human topoisomerase IIα (hTIIα, left) and topoisomerase IIβ (hTIIβ, right) of the radiolabeled, unmodified *PML* top strand hybridized to an unmodified *PML* bottom strand in the presence of free etoposide or hybridized to OTI28 (bottom strand). For each gel, lane 1 contains the unmodified *PML* oligonucleotide. Lanes 2-5 contain the unmodified *PML* duplex treated with 0-500 μM free etoposide. Lanes 7 and 8 contain the unmodified *PML* top strand hybridized with OTI28. Lanes 10 and 11 contain the unmodified top strand duplexed with LIN28 (bottom strand oligonucleotide that contains the linker at position 28 with no attached etoposide core). Lanes 6, 9, and 12 contain reference (R) oligonucleotides that were 24, 23, and 19 bases in length. Gels are representative of at least three independent experiments. (**C**) Quantification of the relative levels of DNA cleavage mediated by topoisomerase IIα (left) and topoisomerase IIβ (right). DNA cleavage at each site was normalized to the cleavage observed at site 24-25 in reactions containing unmodified duplex in the absence of etoposide (lane 2). Cleavage results of the unmodified duplex in the presence of 500 μM free etoposide are shown in blue (lane 5) and those with an unmodified top strand hybridized to OTI28 are shown in yellow (lane 8). Error bars represent the standard error of the mean of an average of two to five independent experiments. Significance was determined by paired t-tests. P-values are indicated by asterisks (*, $p < 0.05$; **, $p < 0.005$; ***, $p < 0.0005$).

was the case when the unmodified bottom strand was replaced with the drug-linked oligonucleotide (OTI28, bottom strand). Topoisomerase IIα cleaved at this position (between bases 24-25 on the top strand) at levels that were even higher than those observed in the unmodified duplex in the presence of 500 μM free etoposide. High enzyme-mediated cleavage was also observed one base away (between bases 23-24 on the top strand), although at slightly lower levels than at site 24-25. Drug insertion at this position is also supported by modeling studies (Figure 25B).

Four additional points should be noted regarding the data shown for topoisomerase IIα (Figure 23B,C; left): first, no DNA cleavage was observed in the absence of topoisomerase IIα (lane 1), indicating that the tethered etoposide core does not induce cleavage via a spontaneous chemical reaction. Second, OTI28 did not induce topoisomerase IIα-mediated cleavage at any of the other strong cleavage sites induced by free etoposide (compare lanes 8 and 5). This finding suggests that the specificity of the etoposide core can be constrained by its covalent attachment to an oligonucleotide. Third, some minor sites of topoisomerase IIα-mediated DNA cleavage with OTI28 were not predicted by our modeling studies (Figures 11 and 24). These sites were not related to the conditions utilized to anneal the OTIs to their complementary strand. Similar DNA cleavage patterns were observed when annealing temperatures were varied by 30 ˚C and cooling rates differed over an 8-fold range (Figure 24). These findings suggest that the presence of the drug may subtly alter the structure of the duplex that affects its interaction with topoisomerase IIα. Lastly, no enzyme-mediated DNA cleavage was observed when the bottom strand was replaced with an oligonucleotide that contained the linker alone (i.e., a linker with no attached drug moiety; lane 11). This provides strong evidence that it is the presence of the etoposide core rather than the linker alone on the oligonucleotide that enhances topoisomerase IIα-mediated DNA cleavage.

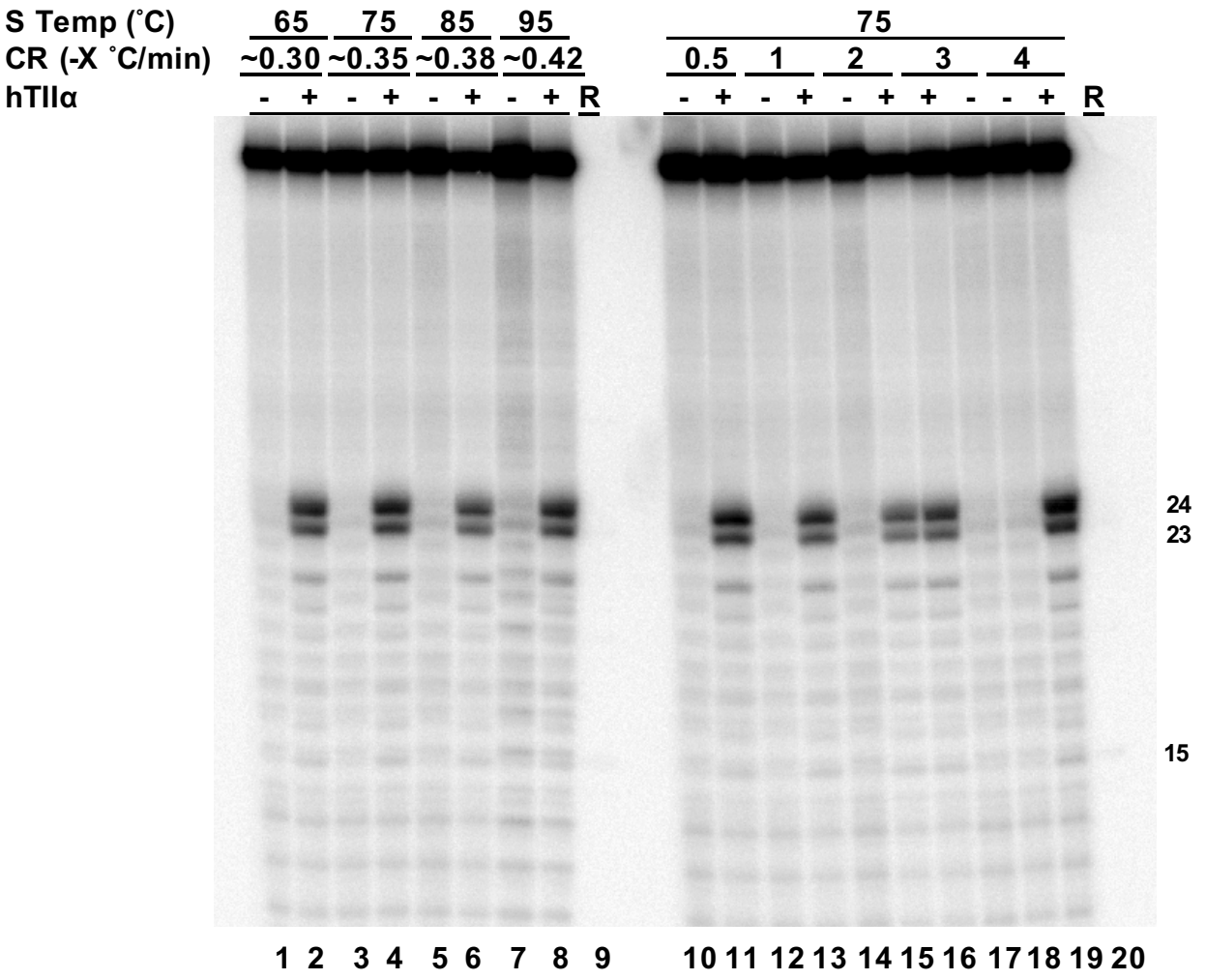

Figure 24. Changing annealing conditions does not change the topoisomerase IIα-mediated DNA cleavage pattern of OTI28. A comparison of the unmodified *PML* top strand hybridized to OTI28 under different annealing conditions in the absence (-hTIIα) and presence (+hTIIα) of human topoisomerase IIα is shown. Annealing conditions used in the study are shown in lanes 3 and 4 (10-min incubation at 75 ˚C followed by slow cooling on the benchtop to 30 ºC). The starting temperature (S Temp) was changed over a range of 30 ºC (from 65-95 ºC, lanes 1-8), and the cooling rate (CR) was varied by a factor of 8 (0.5-4 ºC/min, lanes 10-19) in a thermocycler. Lanes 9 and 20 contain reference (R) oligonucleotides that are 24, 23, and 15 bases in length. The gel is representative of three independent experiments.

Results similar to those with topoisomerase IIα also were observed with topoisomerase IIβ (Figure 23B,C; right). The same two strong sites of enzyme-mediated DNA cleavage were observed in a duplex containing OTI28. Once again, scission at both cleavage sites (24-25, 23-24) was higher than that seen in the unmodified duplex in the presence of 500 μM free etoposide (compare lanes 8 and 5). However, cleavage at 23-24 was similar to that seen at 24-25. Finally, as seen with the α isoform, topoisomerase IIβ did not cleave a duplex with a bottom strand that contained a linker but no tethered etoposide core at position 28 (lane 11).

To further characterize the mechanism of enzyme-mediated DNA cleavage induced by the OTI, the effects of the tethered etoposide core on rates of DNA ligation mediated by topoisomerase IIα were compared to those of free etoposide on an unmodified duplex oligonucleotide. Similar inhibition of religation was observed for both the tethered and the untethered drug (Figure 26A). Thus, like free etoposide, the OTI increases levels of cleavage complexes by inhibiting ligation of the cut DNA.

In addition, cleavage complexes formed with OTI28 versus free etoposide persisted for similar lengths of time (Figure 26B) following 20-fold dilution of the reaction mixtures. Therefore, the OTI appears to stabilize cleavage complexes to a comparable extent as the free etoposide. These findings further suggest that the effects of tethered etoposide core within the cleavage complex produce similar effects to the free drug.

DNA lesions have the capacity to act as topoisomerase II poisons. Abasic sites are among the most effective DNA lesions at inducing topoisomerase II-mediated DNA cleavage[153, 154, 157]. Thus, to provide further evidence that the effects of OTI28 were mediated by the tethered drug moiety as opposed to a distortion in the double helix, a new oligonucleotide was synthesized that replaced the cytosine-linker-etoposide core construct at position 28 with a tetrahydrofuran abasic site analog (AP28). DNA cleavage results are shown in Figure 27. The

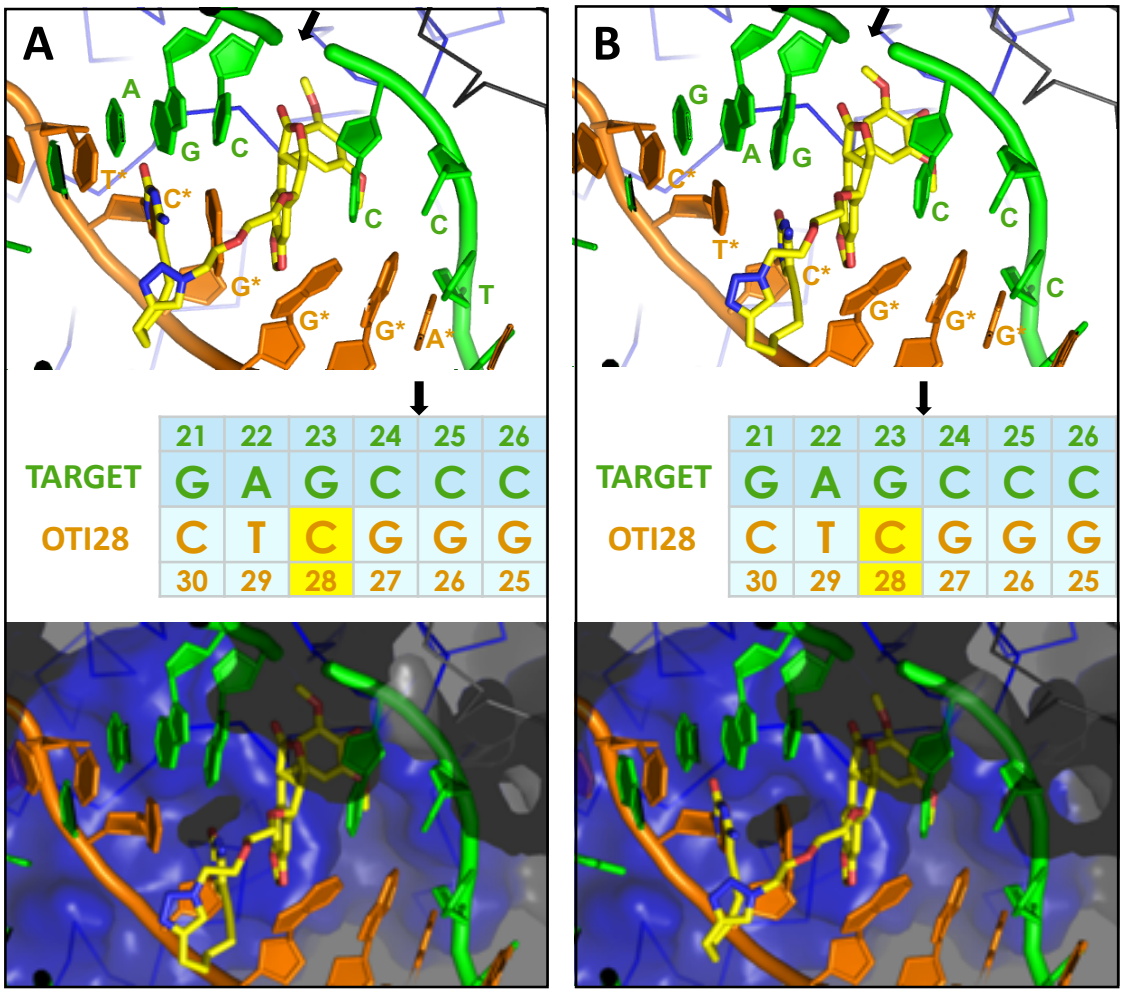

Figure 25. Molecular models of DNA cleavage complexes formed with OTI28. Models were based on the crystal structure of topoisomerase IIβ[215]. (**A**) Cleavage between bases 24-25 is depicted on the target (top) strand (green). (**B**) Cleavage between bases 23-24 is depicted on the target strand (green). The bottom (OTI) strand is shown in orange. The tethered etoposide core is shown in yellow (carbons, yellow; nitrogen, blue; oxygen, red). A Cα trace is shown for the two topoisomerase II subunits (blue and black lines) in the top panels. The bottom panels include a semi-transparent molecular surface, illustrating that the linker does not clash with the protein. The sequence diagram (middle) shows the position of the tethered etoposide core on OTI28 (yellow box). Black arrows indicate the cleavage sites. These data were generated by collaborators at GSK.

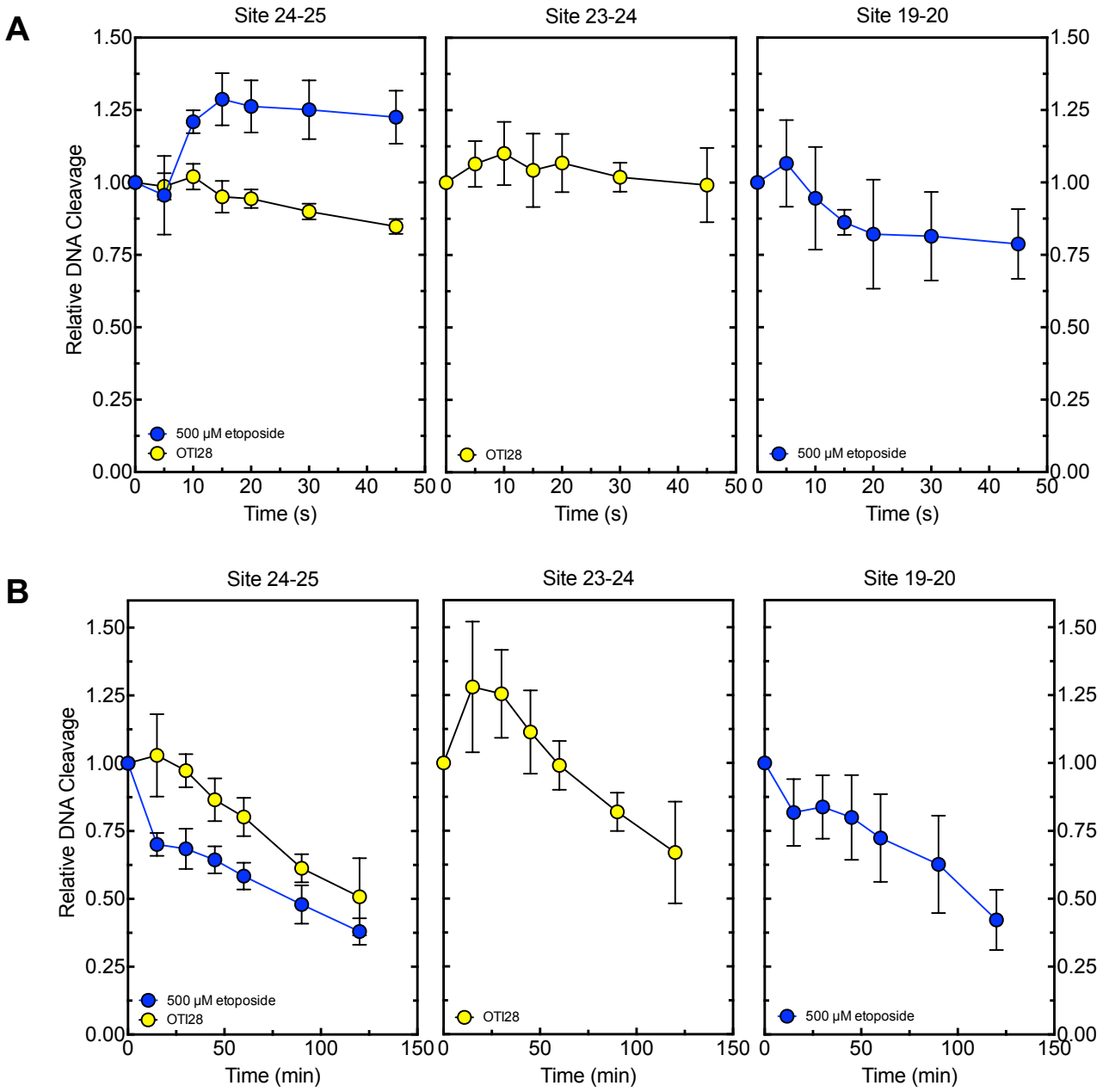

Figure 26. OTI28 inhibits DNA ligation and stabilizes cleavage complexes similarly to free etoposide. (**A**) Enzyme-mediated ligation of DNA. (**B**) Persistence of cleavage complexes. For both A and B, cleavage results of the unmodified *PML* duplex in the presence of 500 μM free etoposide are shown in blue and those with an unmodified *PML* top/target strand hybridized to OTI28 are shown in yellow. Error bars represent the standard deviation of at least three independent experiments.

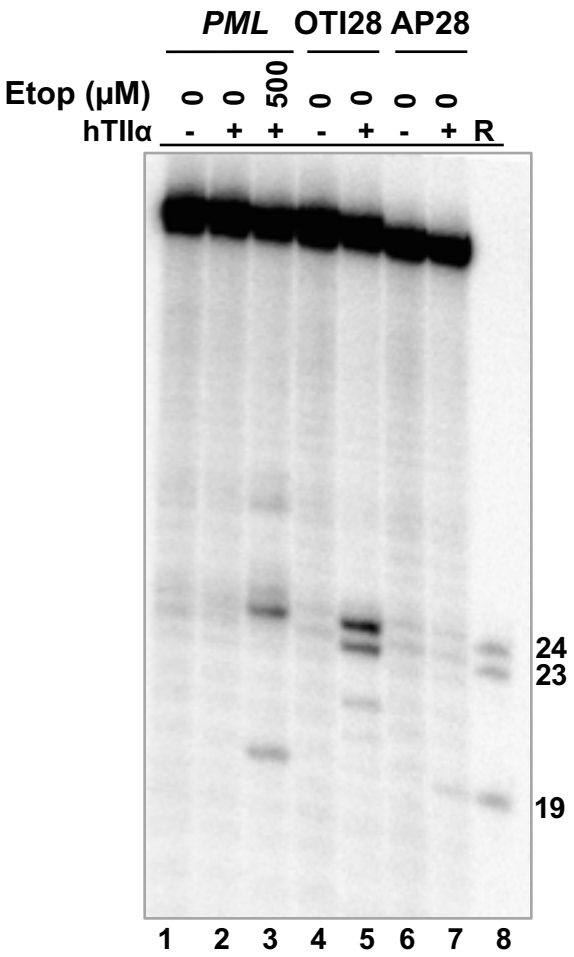

Figure 27. An oligonucleotide with an abasic site analog at position 28 generates a different DNA cleavage pattern than does OTI28. Lanes 1-3 contain a radiolabeled unmodified *PML* top/target strand hybridized to an unmodified *PML* bottom strand in the absence of enzyme, or in the presence of enzyme and 0-500 μM free etoposide. Lanes 4 and 5 contain a radiolabeled *PML* top strand hybridized with OTI28 (bottom strand). Lanes 6 and 7 contain a radiolabeled unmodified *PML* top strand hybridized to a bottom strand oligonucleotide containing an abasic site analog at position 28 (AP28). Lane 8 contains reference (R) oligonucleotides that are 24, 23, and 19 bases in length. The gel is representative of at least three independent experiments.

abasic site induced lower levels of cleavage than OTI28, with the major site of DNA cleavage (position 19-20) being five bases away from that of OTI28 (24-25) (compare lanes 7 to 5). The differences in the cleavage patterns obtained with AP28 and OTI28 provide additional strong evidence that DNA cleavage induced by OTI28 is due to the actions of the tethered etoposide core by type II topoisomerases and not to a distortion or lesion in the helix at the site of drug attachment.

Finally, the ability of OTI28 to induce DNA cleavage mediated by an etoposide-resistant type II topoisomerase was assessed. The yeast topoisomerase II H1011Y mutant[201] was used for these experiments for two reasons. First, target-based resistance to topoisomerase II-targeting drugs is generally associated with the loss of one enzyme allele or the deletion of nuclear localization signals[221, 222]. Consequently, point mutations that impart etoposide resistance to human type II topoisomerases have not been well described or characterized. Second, yeast topoisomerase II is highly sensitive to etoposide, and the H1011Y mutant is the only type II enzyme that has been shown to be etoposide resistant due to a reduced affinity for the drug[223]. As seen in Figure 28, yeast topoisomerase II H1011Y is ~4-fold resistant to the tethered etoposide core in OTI28 as compared to the wild-type enzyme. This result is consistent with the resistance of the mutant enzyme to free etoposide[201].

Taken together, the above experiments provide strong evidence that the DNA cleavage induced by OTI28 is due to the presence of the tethered etoposide core.

OTIs Enhance Topoisomerase II-mediated DNA Cleavage in a Sequence-dependent Manner

As described above, the major site of topoisomerase II-mediated DNA cleavage on the top/target strand induced by OTI28 was located at a position two bases away and opposite the tethered etoposide core (site 24-25). To determine whether OTIs generate a predictable pattern of cleavage, the location of the tethered etoposide core was shifted to three additional locations

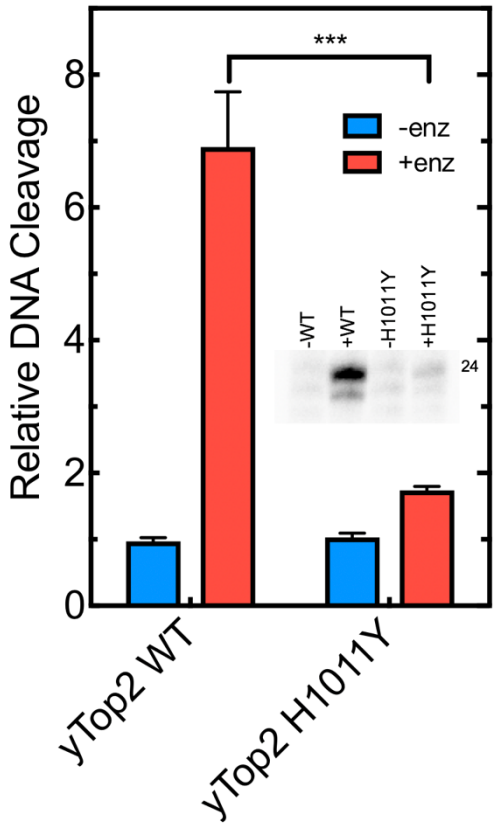

Figure 28. OTI28 induces lower levels of DNA cleavage mediated by an etoposide-resistant mutant yeast topoisomerase II as compared to wild-type yeast topoisomerase II. Quantification of the relative levels of enzyme-mediated DNA cleavage at site 24-25 (indicated as the band labeled 24 in the inset) mediated by wild-type (yTop2WT) and H1011Y mutant (yTop2H1011Y) yeast topoisomerase II on an unmodified *PML* top strand hybridized to OTI28 (graph: +enz, red; inset: +WT, +H1011Y). DNA cleavage is normalized to background levels of DNA when no enzyme is present (graph: -enz, blue; inset: -WT, -H1011Y). Error bars represent the standard deviation of three independent experiments. Significance was determined by a paired t-test. P-values are indicated by asterisks (***, $p < 0.0005$).

along the sequence of the bottom oligonucleotide: positions 29 (OTI29), 33 (OTI33), and 23 (OTI23) (Figure 29A). These locations were selected to determine if it was possible to move the major site of DNA cleavage to the second-strongest site of scission induced by OTI28 (site 23-24), to the site of secondary DNA cleavage induced when free etoposide was added to an unmodified duplex (site 19-20), and to a site that was not cleaved in the presence of free etoposide (site 29-30), respectively.

In all three cases, strong topoisomerase IIα-mediated DNA cleavage induced by the new OTIs was observed two bases away opposite the drug location at the predicted sites described above (Figure 29B; left). As with OTI28, some of the new OTIs also induced DNA scission at sites that were not predicted by our modeling studies (Figures 11 and 25). However, these sites were all in the vicinity of the predicted sites of cleavage. Similar sites of DNA cleavage were obtained with these OTIs and topoisomerase IIβ (Figure 29B; right).

Two important conclusions can be drawn from these studies. First, OTIs can be used to induce DNA cleavage, at least in part, in a predictable manner. Second, sites of cleavage can be moved to sequences not normally associated with the actions of free etoposide (Figures 23 and 29). Thus, the use of OTIs is not restricted to pre-existing etoposide-induced sites of cleavage, implying that it may be possible to design OTIs against almost any patient sequence associated with a cancer mutation or chromosomal breakpoint.

OTIs Can Be Directed Against a t(15;17) Translocation Breakpoint Seen in a Patient with t-APL

One of the goals in characterizing OTIs is to determine if it would be possible to target them to cancer-specific sequences present in malignant cells. Therefore, having established the proof of principle that OTIs can be used to direct the location of etoposide-induced topoisomerase II-mediated DNA cleavage, an OTI was designed against a t(15;17) chromosomal translocation

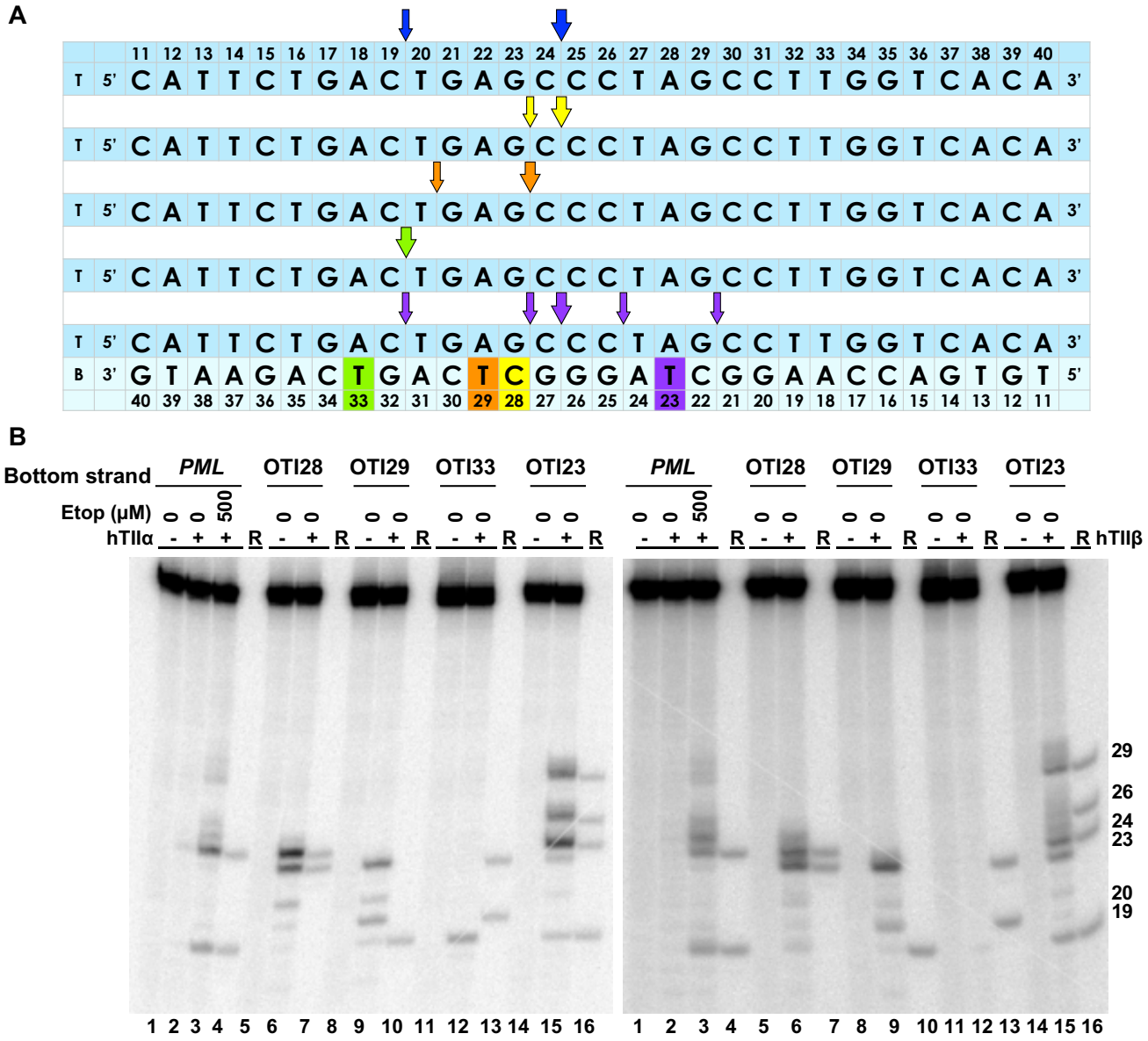

Figure 29. Moving the position of the linked etoposide core on the bottom strand OTI sequence alters the topoisomerase II-mediated cleavage pattern of the top strand. (**A**) Sequences of the top/target and bottom *PML* strands. The different-colored boxes indicate the position of the tethered etoposide core in each OTI (bottom strand), including OTI28 (yellow), OTI29 (orange), OTI33 (green), and OTI23 (purple). Arrows indicate the cleavage sites induced by each OTI (shown by corresponding colors). Blue arrows indicate cleavage sites induced by free etoposide. The size of the arrows is indicative of the relative strength of cleavage. T and B (first column) indicate top and bottom strands, respectively. (**B**) Comparison of DNA cleavage mediated by human topoisomerase IIα (hTIIα, left) and topoisomerase IIβ (hTIIβ, right) of the radiolabeled, unmodified *PML* top strand hybridized to an unmodified PML bottom strand in the presence of 0-500 μM free etoposide (lanes 2-3) or hybridized to the bottom strands OTI28 (lanes 5-6), OTI29 (lanes 8-9), OTI33 (lanes 11-12), or OTI23 (lanes 14-15). For each gel, lane 1 contains an unmodified *PML* duplex. Reference (R) oligonucleotides are 24, 23, 20, and 19 bases long. Gels are representative of at least three independent experiments.

(breakpoint at 1484-1485 in *PML* and 12034-12035 in *RARA*) in a patient with t-APL (Figure 30A)[99]. This sequence was chosen because it encompasses the site of cleavage in the *PML* gene induced by OTI28 (Figure 23). Initial studies with the translocation sequence utilized a 50-base pair oligonucleotide that was comprised of bases 1461-1488 of intron 6 of *PML* (Figure 30A; green) and 12039-12060 of intron 2 of *RARA* (Figure 30A; orange).

First, the unmodified breakpoint oligonucleotide duplex was treated with free etoposide (0-500 μM) in the presence of topoisomerase IIα, and several cleavage sites were observed (Figure 30B,C; left). The strongest of these sites were observed at positions 24-25, 25-26, and 19-20 on the top strand (lane 5), in order of decreasing strength of cleavage.

Second, the unmodified target strand was hybridized with a complementary 50-base OTI in which the tethered etoposide core was located at the equivalent position in the *PML* gene as OTI29 (Figure 30A). As predicted, this OTI induced strong cleavage at position 23-24 (lane 8), at a site two bases away and opposite the tethered drug. Strong cleavage was also observed at sites 20-21 and 24-25 (lane 8).

Human type II topoisomerases display a DNA length-dependence for scission. The enzyme cleaves a 50-mer duplex oligonucleotide considerably better than it does a 40-mer, and little cleavage is seen with oligonucleotides shorter than a 30-mer[92]. However, when one of the two strands is maintained at a 50-base length, levels of enzyme-mediated DNA cleavage remain relatively high until the length of the complementary strand is reduced to ~20 bases[92]. Therefore, to see if shorter OTIs could still be used to induce high levels of topoisomerase IIα-mediated DNA cleavage in the translocation sequence, I tested a 30-mer version of the breakpoint OTI in which 10 bases were removed from each terminus (Figure 30A). High levels of cleavage were maintained at sites 23-24 and 19-20; however, cleavage disappeared from site 24-25 (Figure 30B,C; lane 12). As predicted, when the breakpoint OTI was further reduced in length to a 20-mer version, DNA cleavage levels dropped precipitously (Figure 30B,C; lane 14).

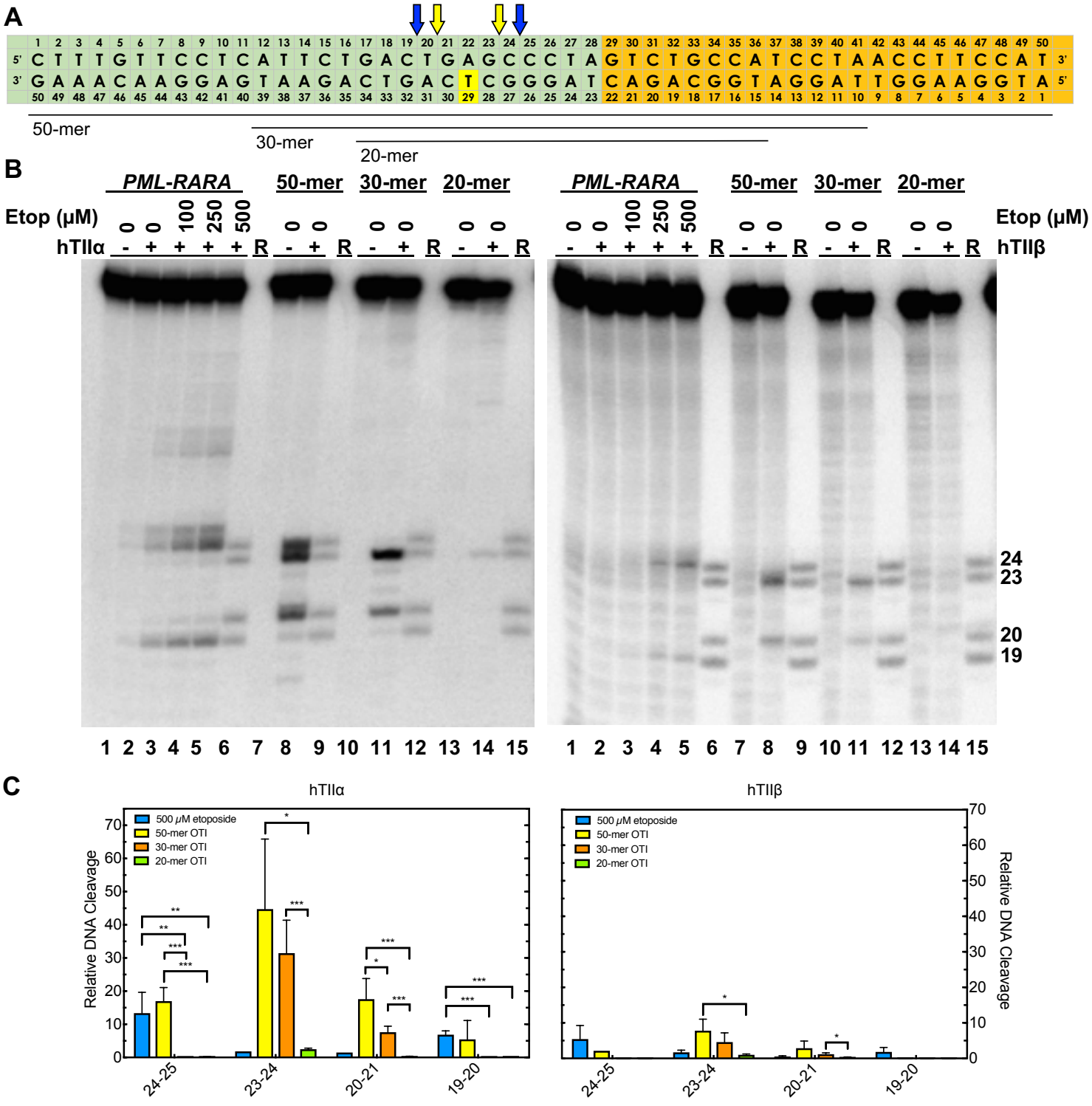

Figure 30. OTIs designed against a patient-observed *PML-RARA* translocation increase DNA cleavage mediated by human type II topoisomerases. (**A**) Sequences of the top and bottom strands of each *PML-RARA* duplex are shown. The blue portion corresponds to the segment derived from the *PML* gene, and the orange portion corresponds to the segment derived from the *RARA* gene. Continued next page.

The yellow box indicates the position of the tethered etoposide core on each OTI (bottom strand). The OTIs were 50, 30, or 20 bases in length (black lines below the diagram). Arrows indicate sites of DNA cleavage induced by free etoposide (blue) and the translocation OTIs (yellow). (**B**) Comparison of DNA cleavage mediated by human topoisomerase IIα (hTIIα, left) and topoisomerase IIβ (hTIIβ, right) of the radiolabeled, unmodified *PML-RARA* top/target strand hybridized to an unmodified *PML-RARA* bottom strand in the presence of free etoposide or of the radiolabeled *PML-RARA* top strand hybridized to a 50-mer, 30-mer, or 20-mer *PML-RARA* OTI bottom strand. Lanes 1-5 contain the unmodified *PML-RARA* duplex in the absence of enzyme, or in the presence of enzyme and 0-500 μM free etoposide. Lanes 7 and 8 contain the unmodified *PML-RARA* top strand hybridized with the 50-mer OTI. Lanes 10 and 11 contain the unmodified top strand hybridized with the 30-mer OTI. Lanes 13 and 14 contain the unmodified top strand hybridized with the 20-mer OTI. Lanes 6, 10, 13, and 15 contain reference (R) oligonucleotides 24, 23, 20, and 19 bases in length. Gels are representative of at least three independent experiments. (**C**) Quantification of the relative levels of enzyme-mediated DNA cleavage. DNA cleavage at each site is normalized to the cleavage observed at site 24-25 in reactions containing an unmodified duplex in the absence of etoposide (lane 2). Results with unmodified *PML-RARA* duplex in the presence of 500 μM free etoposide (blue) or with unmodified top strand hybridized with 50-mer OTI (yellow). 30-mer OTI (orange), or 20-mer OTI (green) bottom strand are shown. Error bars represent the standard deviation of at least three independent experiments. Significance was determined by paired t-tests. P-values are indicated by asterisks (*, $p < 0.05$; **, $p < 0.005$; ***, $p < 0.0005$).

In all respects, results obtained with topoisomerase IIβ and the chromosomal translocation model oligonucleotides (with either a free or a tethered etoposide core) were similar to those obtained with topoisomerase IIα (Figure 30B,C; right).

Finally, to determine whether the breakpoint OTIs displayed specificity for the translocation over the parental *PML* and *RARA* sequences, the 50-mer, 30-mer, and 20-mer breakpoint OTIs were hybridized to 50-mer top strands of each parental gene. Very low levels of DNA cleavage were generated by either topoisomerase IIα (Figure 31A) or topoisomerase IIβ (Figure 31B) in the *PML* oligonucleotide (lanes 8, 10, and 12) and no cleavage was observed in the *RARA* oligonucleotide with any of the breakpoint OTIs (lanes 18, 20, 22). This finding suggests that OTIs could potentially be directed to cancer-specific breakpoints without generating significant levels of DNA cleavage in the wild-type parental sequences.

OTIs Induce DNA Cleavage Mediated by Human Type II Topoisomerases on Duplexes Containing a Mismatch

Cancers can arise from a variety of mechanisms and are not limited to chromosomal translocations[224-229]. Therefore, I sought to determine if OTIs could be used to target SNPs such as might be present in a driver oncogene. In such a situation, OTIs could be used to induce enzyme-mediated DNA cleavage on the SNP-containing sequence (wherein the OTI would form a fully complementary duplex with its target sequence on the cancer genome) but not on the WT parental sequence (which would contain a one-base mismatch when hybridized to the OTI). To test this possibility, I designed six new oligonucleotides (C19G, G23A, C24G, C24A, C24T, and C25G) that shared the sequence of the WT *PML* top strand but differed by a single-base. These "mismatch oligonucleotides" were hybridized to WT *PML* or OTI bottom strands. To investigate the full potential of OTIs in targeting SNPs, I designed the mismatch oligonucleotides to generate the greatest amount of disruption in the double helix in the hopes of maximizing the interference with topoisomerase IIα and IIβ. This is representative of the best-case scenario in which an OTI

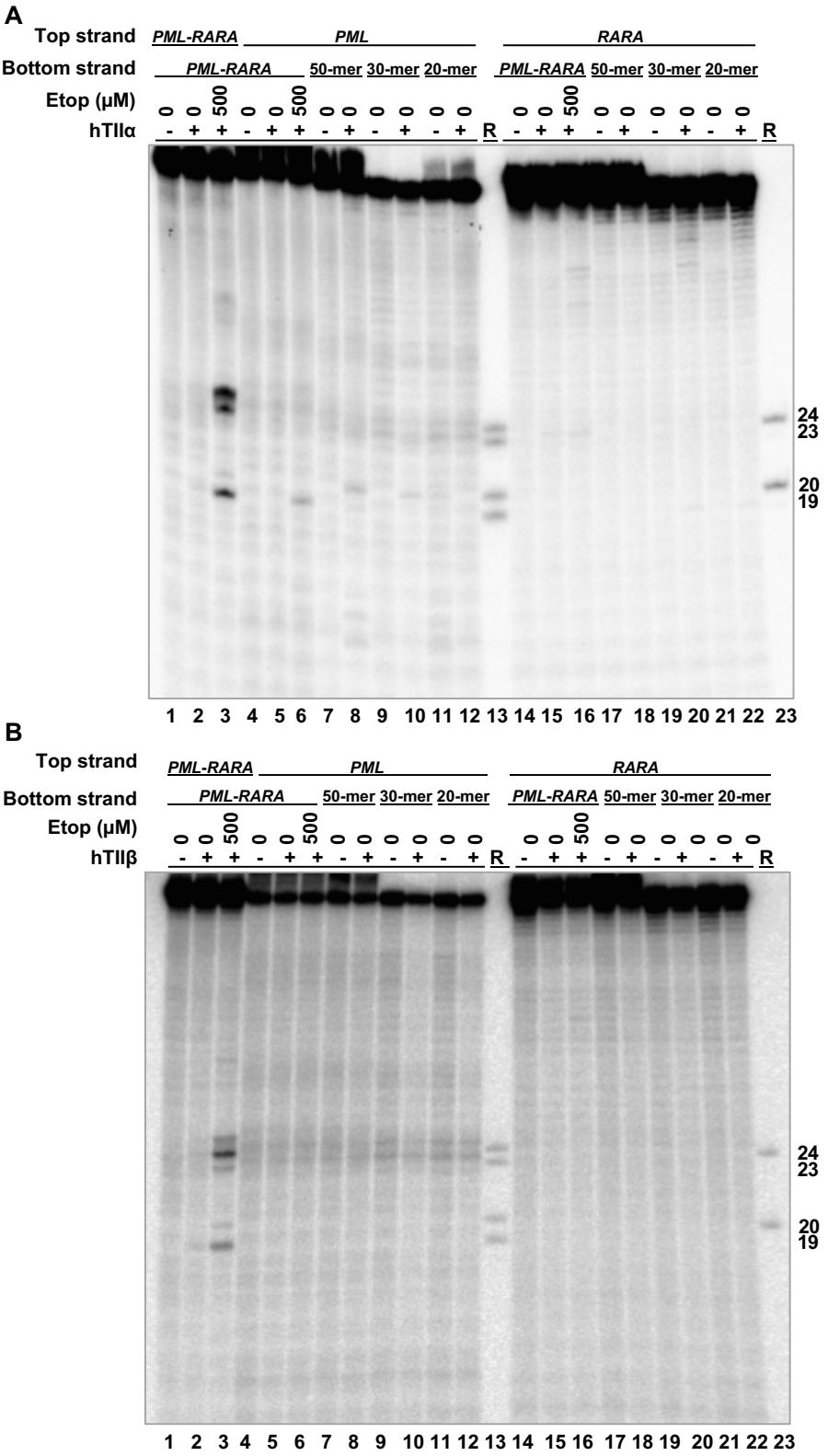

Figure 31. OTIs that incorporate an APL patient-derived *PML-RARA* translocation sequence do not increase DNA cleavage mediated by human type II topoisomerases when they are hybridized with the parental *PML* or *RARA* sequences. Continued next page.

Comparison of DNA cleavage mediated by human topoisomerase IIα (hTIIα) (**A**) and topoisomerase IIβ (hTIIβ) (**B**) of the radiolabeled top strand of an unmodified *PML-RARA* duplex in the presence of free etoposide, a radiolabeled, unmodified *PML* or *RARA* top strand hybridized to a *PML-RARA* bottom strand in the presence of free etoposide, or a radiolabeled, unmodified *PML* or *RARA* top strand hybridized to a 50-mer OTI, a 30-mer OTI, or a 20-mer *PML-RARA* OTI bottom strand. For each gel, lanes 1-3 contain unmodified *PML-RARA* top/target strand hybridized to the unmodified 50-mer *PML-RARA* bottom strand, in the absence of enzyme, or in the presence of enzyme and 0-500 μM etoposide. Lanes 4-6 contain unmodified parental *PML* top/target strand hybridized to the unmodified 50-mer *PML-RARA* bottom strand, in the absence of enzyme, or in the presence of enzyme and 0-500 μM etoposide. Lanes 7-12 contain the unmodified parental *PML* top strand hybridized to the 50-mer, 30-mer, or 20-mer *PML-RARA* OTI bottom strand in the absence or presence of enzyme. Lanes 14-16 contain unmodified parental *RARA* top strand hybridized to the 50-mer *PML-RARA* bottom strand, in the absence of enzyme, or in the presence of enzyme and 0-500 μM etoposide. Lanes 17-22 contain the unmodified parental *RARA* top strand hybridized to the 50-mer, 30-mer, or 20-mer *PML-RARA* OTI bottom strand in the absence or presence of enzyme. Lanes 13 and 23 contain a combination of reference (R) oligonucleotides 24, 23, 20, and 19 bases in length. Gels are representative of at least three independent experiments.

targeting a SNP is subjected to the highest possible amount of disruption when attempting to bind/stabilize enzyme-mediated cleavage on the WT sequence. The locations of the mismatches were selected on the basis of their proximity to the observed cleavage sites at 19-20, 23-24, and 24-25 (Figure 23), and the mismatched base in each one was designed to generate the highest amount of DNA breathing[204]. In one instance, all three possible base mutations were generated for a position (C24G, C24A, C24T).

In addition to probing the potential use of OTIs against SNPs, generating mismatch oligonucleotide duplexes allowed me to explore whether or not changing the bases that flank scissile bonds affects the ability of topoisomerase IIα to cleave the DNA within the context of the OTI-attached DEPT. Human type II topoisomerases interact with DNA in a sequence-dependent manner[149, 230], but the sequence requirement changes based on the presence or absence of a topoisomerase II poison (Table 2)[149, 231-235]. For example, human topoisomerase IIα has a strong preference for sequences with a C at the -1 position (the base that is 5' of the scissile bond) in the absence of drug and when incubated with etoposide[230], but displays a preference for A when incubated with doxorubicin[231] or a preference for T when incubated with amsacrine[232, 233]. It is important to note that although topoisomerases have sequence preferences, they do not necessarily cut at every site that displays the preferred sequences. Furthermore, type II topoisomerases display little or no DNA cleavage in the absence or presence of drug when there are mismatches at the -1, -2, -3, and -4 positions relative to a scissile bond, but mismatches at +1 or +2 may increase cleavage[236]. As OTIs contain a covalently linked topoisomerase II poison, they allow for the exploration of whether the sequence requirement for etoposide can be bypassed by having the drug "hardwired" into the system, and whether mismatches can affect the ability of the enzymes to cleave OTI-containing duplexes.

To examine these issues, I incubated topoisomerase IIα and IIβ with unmodified duplexes containing a radiolabeled mismatch oligonucleotide top strand and a WT *PML* bottom strand in

Enzyme/ drug	Nucleotide position													
	-5	-4	-3	-2	-1	+1	+2	+3	+4	+5	+6	+7	+8	+9
hTIIα	No A	No T	A, no C	-	C, no A	-	-	-	-	No T	-	T, no G	C, no A	-
hTIIβ	-	-	No C	G	-	T	-	-	-	No T	-	T, no G	C	-
Etop.					C, (T)									
Doxo.				T	A									
Mitox.					C, T		G							
Amsa					T	A								

Table 2. Sequence preferences for human topoisomerase IIα and topoisomerase IIβ in the absence and presence of topoisomerase II poisons. Nucleotides in parentheses indicate a secondary preference. Nucleotide position is relative to a scissile bond, where (-) indicates a position 5' bond and (+) indicates a position 3' to the bond. Hyphens indicate no preference. Gray shading indicates no data are available[149, 230-235]. hTIIα, human topoisomerase IIα; hTIIβ, human topoisomerase IIβ; Etop, etoposide; Doxo, doxorubicin; Mitox., mitoxantrone; Amsa, amsacrine.

the presence of 0-500 μM etoposide (Figure 32); each duplex is heretofore referred to by the name of its top strand. Compared to the WT duplex with 500 μM etoposide (lanes 1-3, both gels), cleavage of the mismatch-containing oligonucleotides dropped precipitously at most sites. Notice, for example, the low levels of cleavage observed on C24G (lanes 11, top gel, and 15, bottom gel) and C24A (lanes 23, top gel, and 19, bottom gel) when incubated with either enzyme and free etoposide. These data suggest that a mismatch proximal to a cleavage site precludes the formation of the proper ternary drug-enzyme-DNA complex that is necessary for stabilization of cleavage by the topoisomerase II poisons. There were, however, clear increases in drug-induced enzyme-mediated cleavage at sites distal to the mismatch. These locations were site 24-25 on C19G (lanes 19, top gel, and 7, bottom gel) and site 19-20 on G23A (lanes 7, top gel, and 11) and on C24T (lanes 27, top gel, and 23, bottom gel). It is not immediately apparent why cleavage increases distally to the mismatches, but it is possible that local changes in structure are translated down the double helix such that the distal cleavage sites facilitate the formation of the ternary complex[204]. Overall levels of cleavage were lower in reactions containing topoisomerase IIα versus topoisomerase IIβ.

Following these initial experiments, I tested whether OTIs could affect the amount of cleavage observable at the three primary cleavage sites observed in Figure 23. Topoisomerase IIα- and IIβ-mediated cleavage at 24-25 was monitored on duplexes containing either WT *PML*, C24G, C24A, C24T, or C25G as top strand and WT *PML*, OTI28, or OTI29 as the bottom strand (Figure 33). The results in Figure 33B suggest that mismatches 5’ to the cleavage site (C24G, C24A, C24T) tend to maintain lower levels of cleavage mediated by both enzymes compared to mismatches 3’ to the cleavage site (C25G). Similar results were observed at site 23-24 (Figure 34), although the effect was less pronounced. Cleavage 5’ to site 19-20 (Figure 35) was also lower in C19G/OTI33 duplexes. Generally, OTIs induced higher levels of enzyme-mediated cleavage (yellow and orange bars, Figures 33 and 34) on duplexes containing mismatches

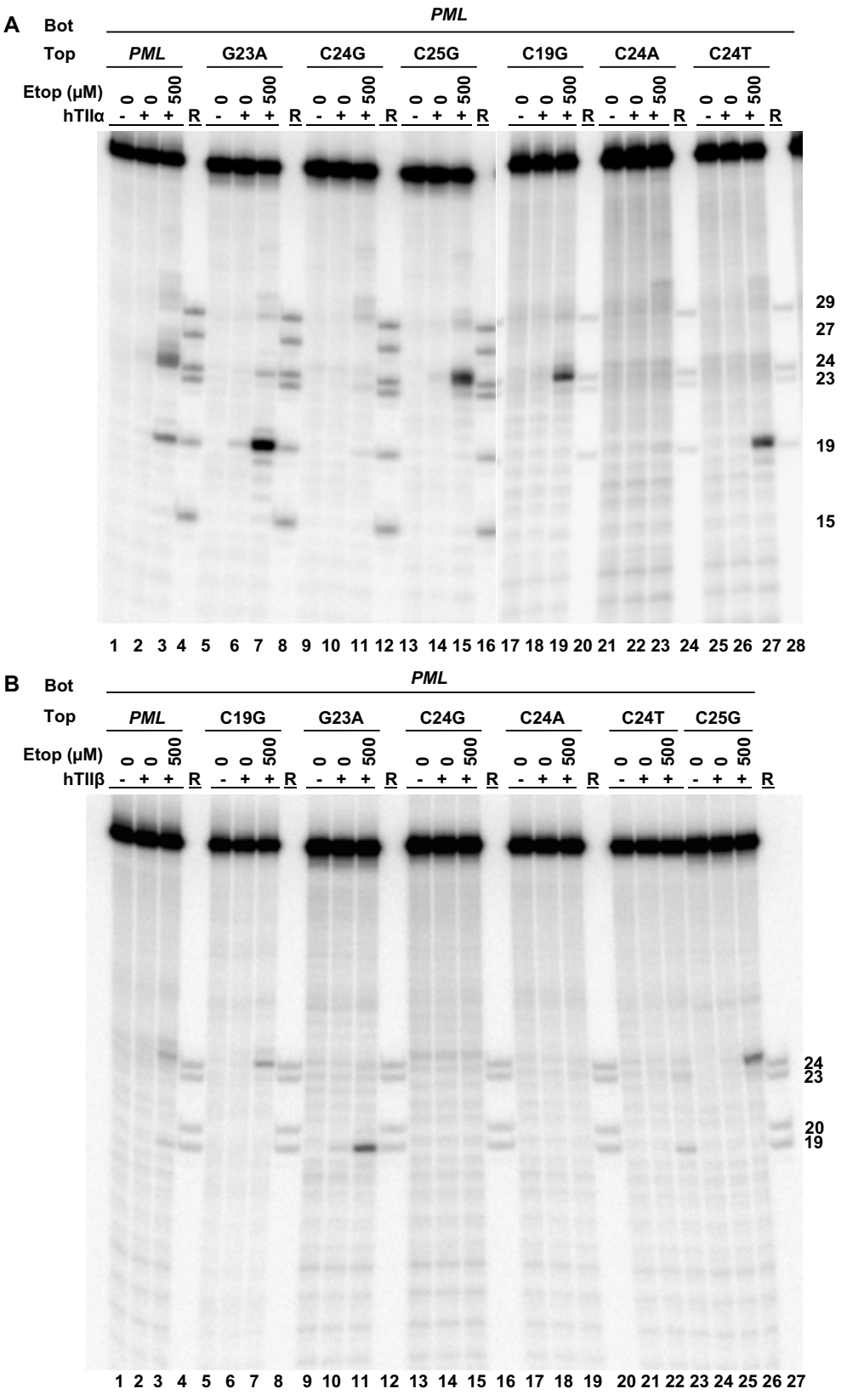

Figure 32. **Duplexes containing a single mismatch did not generally stabilize cleavage by topoisomerase IIα or IIβ in the presence of free etoposide.** Continued next page.

Comparison of DNA cleavage mediated by human topoisomerase IIα (hTIIα) (**A**) and topoisomerase IIβ (hTIIβ) (**B**) of the radiolabeled *PML* or radiolabeled mismatch oligonucleotide top strand hybridized to a *PML* bottom strand in the presence of free etoposide (Etop). For each gel, lanes 1-3 contain a *PML* top strand hybridized to a *PML* bottom strand, in the absence of enzyme, or in the presence of enzyme and 0-500 μM etoposide. Each gel also shows the cleavage products of reactions containing a *PML* bottom strand annealed to a radiolabeled C19G (lanes 17-19 [**A**] and 5-7 [**B**]), G23A (lanes 5-7 [**A**] and 9-11 [**B**]), C24G (lanes 9-11 [**A**] and13-15 [**B**]), C24A (lanes 21-23 [**A**] and 13-15 [**B**]), C24T (lanes 25-27 [**A**] and 21-23 [**B**]), or C25G (lanes 13-15 [**A**] and 24-26 [**B**]) top strand in the absence of enzyme or in the presence of 0-500 μM etoposide. Lanes 4, 8, 12, and 16 of (**A**) contain a combination of reference (R) oligonucleotides 29, 27, 24, 23, 20, 19, and 15 bases in length. Lanes 20, 24, and 28 of (**A**) contain a combination of reference oligonucleotides 29, 27, 24, 23, 20, and 19 bases in length. Lanes 4, 8, 12, 16, 20, and 27 of (**B**) contain a combination of reference oligonucleotides 24, 23, 20, and 19 bases in length. Gels are representative of at least three independent experiments.

compared to similar duplexes in the presence of free etoposide (blue bars, Figures 33 and 34). Cleavage on duplexes containing C24T tended to be higher than the cleavage on duplexes containing the other two mismatch oligonucleotides, indicating that the identity of the specific mismatch plays a role in whether or not topoisomerase IIα or IIβ can stably cleave at that site or not. These results are unexpected in that G:A mismatches (as in C24A) are reported to induce less DNA breathing than the other G:X mismatches used here[204], but the levels of cleavage on C24A were lower than the levels on cleavage on C24T. It is clear that the convergence of mismatches, OTIs, and type II topoisomerases create a complicated interaction that warrants further study.

The results observed in Figures 33, 34, and 35 indicate, first and foremost, that OTIs can induce cleavage by both topoisomerase IIα and IIβ even when their cognate sequences contain a mismatch. This suggests that OTIs are not currently optimized to target SNPs. These results are promising, however, when considering that cancerous tumors can display startling genetic heterogeneity[225] and that can evolve over time. If a patient were to receive an OTI to target a particular sequence, these results indicate that it might retain its effectiveness against the target sequence and against any variations that might arise through mutations or that might exist in a heterogeneous population of cancer cells.

Discussion

Etoposide and other topoisomerase II-targeting drugs are important therapeutics for the treatment of cancer[8, 18, 86, 87, 106, 237]. Unfortunately, the induction of topoisomerase II-mediated DNA cleavage throughout the genome, coupled with the lack of specificity toward cancer cells, limits the safe usage of these drugs. Among the most insidious of toxicities related with treatment with topoisomerase II poisons is the development of secondary leukemias[87, 162, 180, 238]. Indeed, as many as 3% of patients treated with etoposide or doxorubicin develop

t-AMLs with translocations at chromosomal band 11q23[163, 239] or treated with mitoxantrone develop t-APLs with t(15;17) translocations[98, 240].

One approach to providing anticancer agents with reduced toxicities is to develop drugs that specifically inhibit the activity of driver oncoproteins. An example is imatinib, which targets the TK domain of the *bcr-abl* fusion tyrosine kinase that is generated by the chromosomal translocation in chronic myelogenous leukemia[241]. An alternative approach would be to target the chromosomal translocation itself by specifically cleaving the DNA in the vicinity of the translocation site. This could lead to disruption of the oncogene or interference with its transcription. If either occurred, it ultimately could rob the cell of the oncoprotein that drives malignant tumor growth. Potentially, a cocktail of OTIs that target a variety of sites on a cancer genome (at oncogene super-enhancers[242] or the genomic loci of long non-coding RNA[243], for example) or even within a single oncogene could be generated, thus compounding the negative effect of the transcriptional interference.

Previous attempts to impart specificity to topoisomerase-targeting drugs were based on the attachment of either camptothecin[244] or etoposide derivatives[245] to the ends of triplex-forming oligonucleotides. The attached camptothecin induced topoisomerase I-mediated DNA scission at sites that were consistent with the location of the linked drug[244]. However, cleavage appeared to be constrained to pre-existing cleavage sites[244]. In contrast, the attachment of etoposide to the end of a triplex-forming oligonucleotide induced DNA cleavage at locations that were approximately 10 base pairs away from sites that could have come into physical contact with the drug based on the length of the drug and linkers employed[245]. Thus, the basis for etoposide-induced DNA cleavage that resulted from the triplex-forming oligonucleotides could not be determined[245].

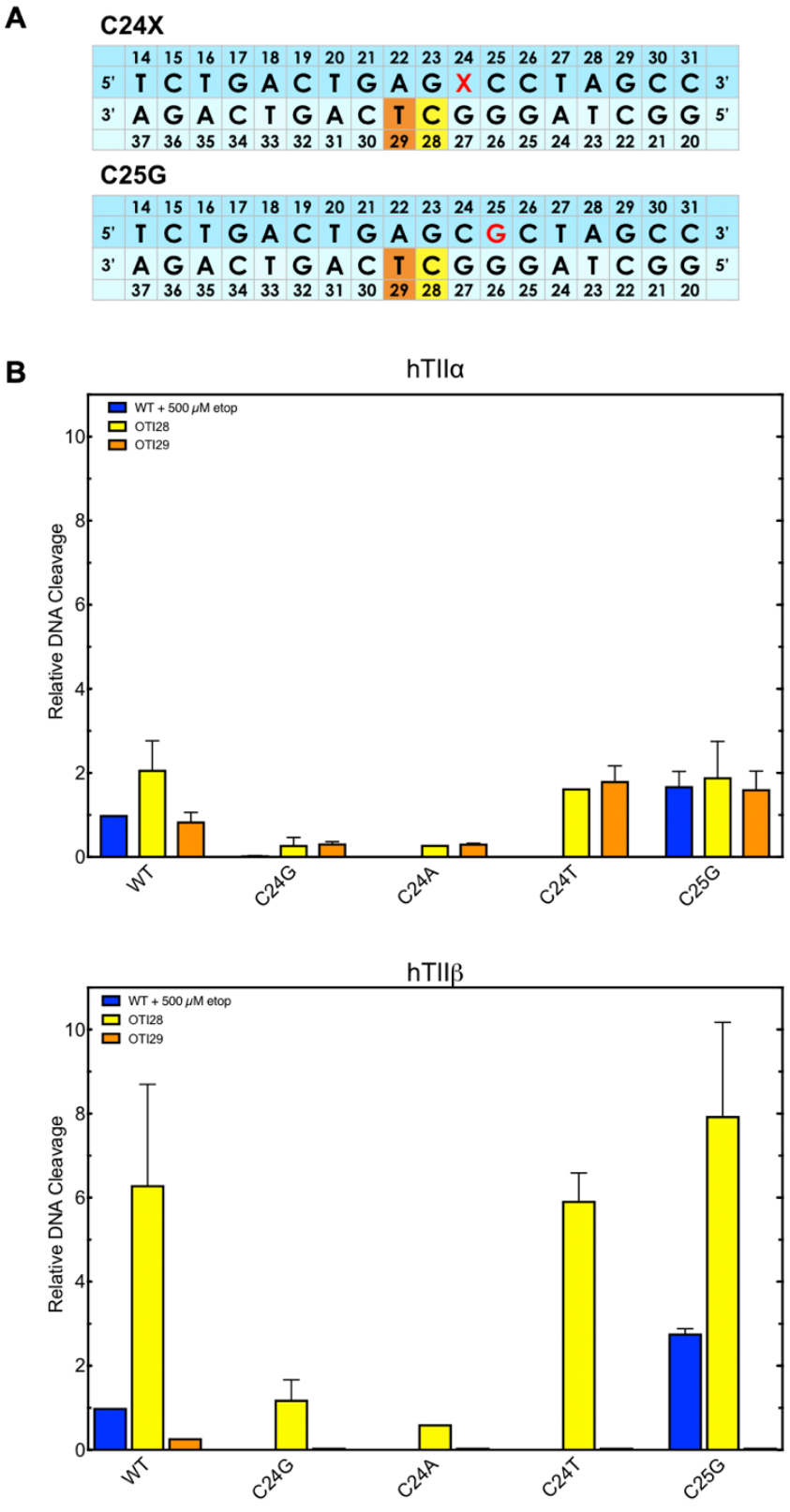

Figure 33. Cleavage patterns at 24-25 on duplexes containing a mismatch at a position flanking the cleavage site change compared to cleavage on duplexes containing no mismatch. Continued next page.

(**A**) Central 18 base pairs of the mismatch oligonucleotide duplexes used in these experiments. The changed base is indicated in red. X is a G, A, or T. Colored boxes indicate the position of the attached etoposide depending on whether OTI28 (yellow) or OTI29 (orange) was used. The WT sequence used can be found in Figure. (**B**) Quantification of the relative levels of DNA cleavage mediated by topoisomerase IIα (top) and topoisomerase IIβ (bottom). DNA cleavage at each site was normalized to the cleavage observed at site 24-25 in reactions containing unmodified duplex in the presence of 500 μM etoposide. WT *PML* or mismatch top strands were utilized in all reactions as indicated. Cleavage of duplexes where the bottom strand was a WT *PML* bottom strand in the presence of 500 μM free etoposide are shown in blue, where the bottom strand was OTI28 are shown in yellow, and where the bottom strand was OTI29 are shown in orange. Error bars represent the standard deviation of at least two independent experiments.

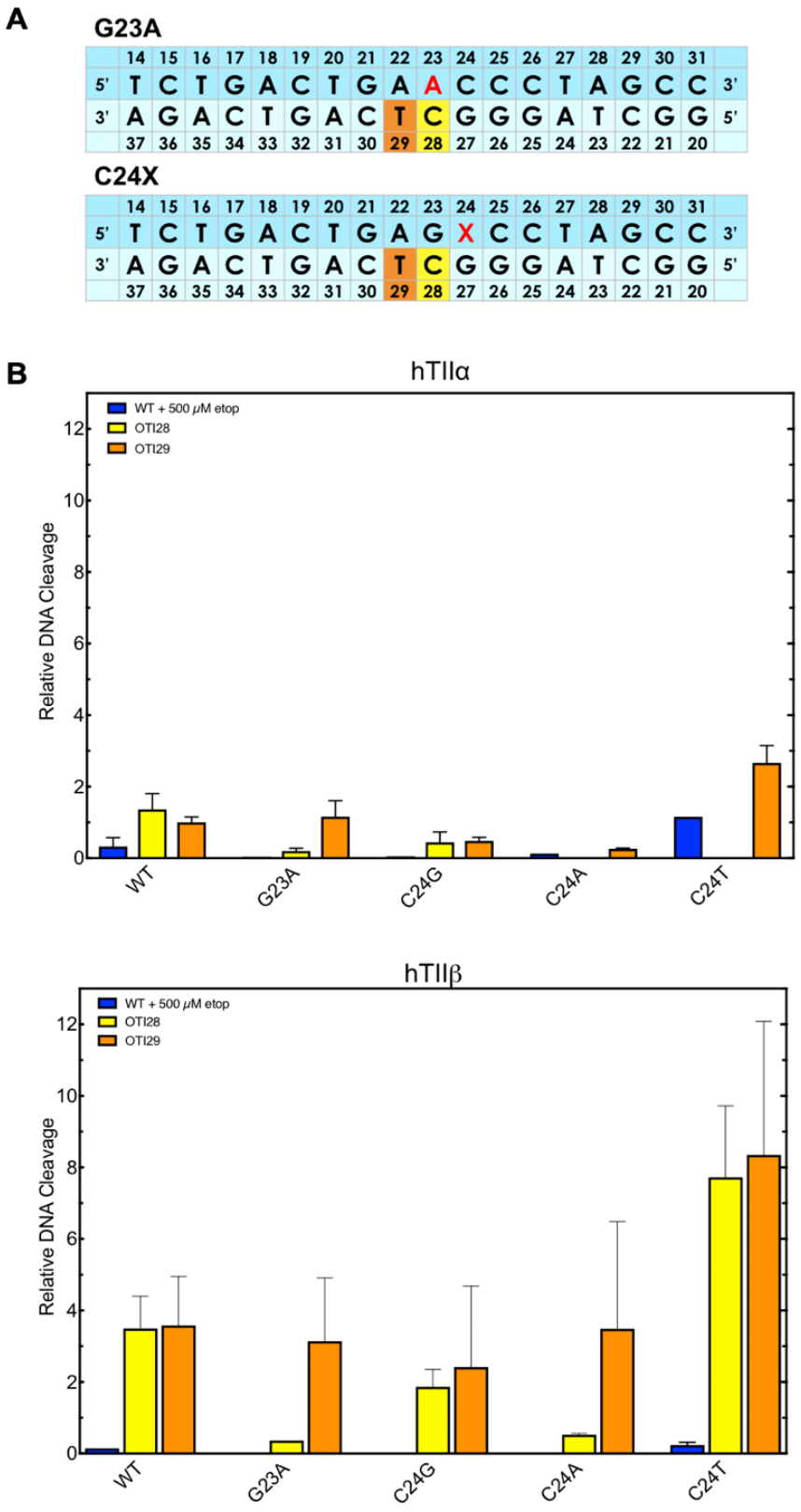

Figure 34. Cleavage patterns at 23-24 on duplexes containing a mismatch at a position flanking the cleavage site change compared to cleavage on duplexes containing no mismatch. Continued next page.

(**A**) Central 18 base pairs of the mismatch oligonucleotide duplexes used in these experiments. The changed base is indicated in red. X is a G, A, or T. Colored boxes indicate the position of the attached etoposide depending on whether OTI28 (yellow) or OTI29 (orange) was used. The WT sequence used can be found in Figure. (**B**) Quantification of the relative levels of DNA cleavage mediated by topoisomerase IIα (top) and topoisomerase IIβ (bottom). DNA cleavage at each site was normalized to the cleavage observed at site 24-25 in reactions containing unmodified duplex in the presence of 500 μM etoposide. WT *PML* or mismatch top strands were utilized in all reactions as indicated. Cleavage of duplexes where the bottom strand was a WT *PML* bottom strand in the presence of 500 μM free etoposide are shown in blue, where the bottom strand was OTI28 are shown in yellow, and where the bottom strand was OTI29 are shown in orange. Error bars represent the standard deviation of at least three independent experiments.

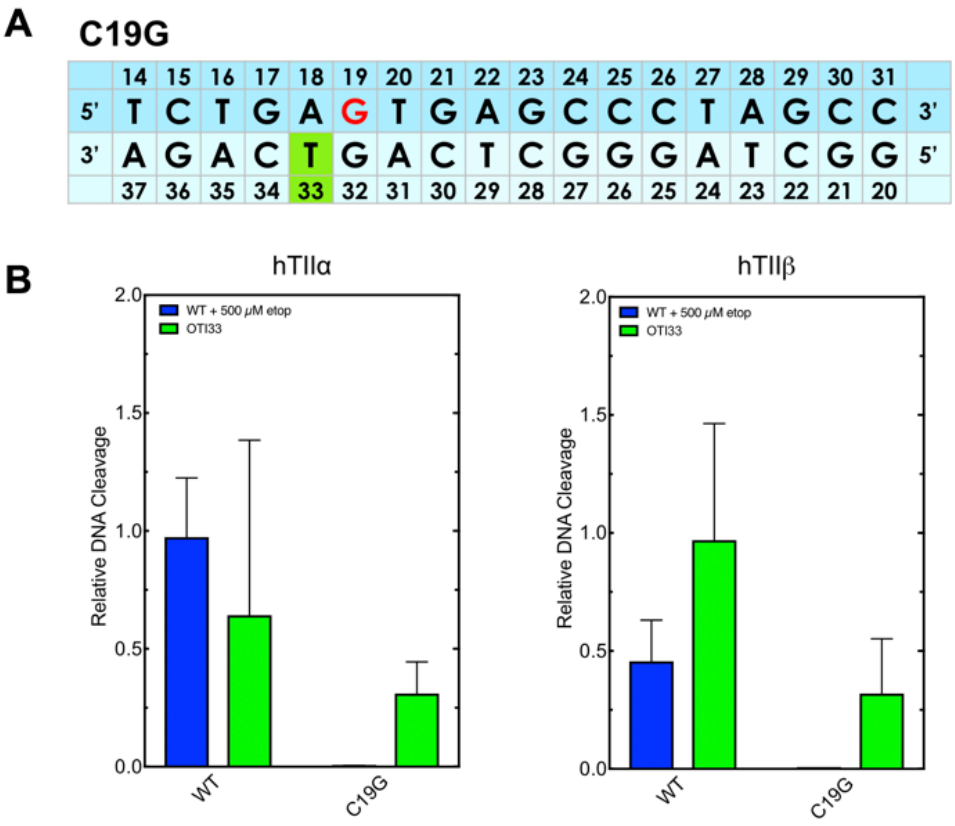

Figure 35. Cleavage patterns at 19-20 on duplexes containing a mismatch at a position 5' to the cleavage site decreases compared to cleavage on duplexes containing no mismatch. (**A**) Central 18 base pairs of the mismatch oligonucleotide duplexes used in these experiments. The changed base is indicated in red. A green box indicates the position of the attached etoposide when OTI33 is used as a bottom strand. The WT sequence used can be found in Figure. (**B**) Quantification of the relative levels of DNA cleavage mediated by topoisomerase IIα (left) and topoisomerase IIβ (right). DNA cleavage at each site was normalized to the cleavage observed at site 24-25 in reactions containing unmodified duplex in the presence of 500 μM etoposide. WT *PML* or mismatch top strands were utilized in all reactions as indicated. Cleavage of duplexes where the bottom strand was a WT *PML* bottom strand in the presence of 500 μM free etoposide are shown in blue and reactions where the bottom strand was OTI33 are shown in green. Error bars represent the standard deviation of at least two independent experiments.

Although the present study also utilized drug-linked oligonucleotides to enhance the specificity of etoposide-induced DNA cleavage, the approach was to design sequences that would form duplex (rather than triplex) structures at the proposed sites of cleavage. To this end, a series of oligonucleotides that contained a linked etoposide core (OTIs) was synthesized using a copper-catalyzed click chemistry scheme. OTIs were designed to take advantage of the following: 1. Etoposide acts by a known mechanism in which it enhances DNA cleavage mediated by type II topoisomerases[18, 49, 106]. 2. The type II enzymes are validated targets for chemotherapeutic agents[18, 86, 95, 106]. 3. Levels of type II topoisomerases are generally higher in malignant cells, which generates higher levels of DNA strand breaks in treated cells[246, 247]. 4. Cancer cells often have high metabolic rates, which results in more replication and transcription complexes that convert topoisomerase II-DNA cleavage complexes into permanent double-strand breaks[18, 81, 86].

Results indicate that the tethered etoposide core in OTIs acts against type II topoisomerases in a manner similar to that of the free drug, but with a specificity (at least for the major sites of cleavage) that is tied to its site of linkage on the oligonucleotide. Furthermore, the linked drug can induce enzyme-mediated DNA cleavage at sites of action of the free drug or at sites at which free drug does not act. This finding suggests that it might be possible to develop OTIs against a broad range of translocation-related sequences. Results further suggest that OTIs can be designed to have high activity against cancer-related translocations but display limited activity against the parental genes.

It is notable that in some cases, minor cleavage is observed at positions that were not predicted from modeling studies (Figures 10, 11, 22, and 25). Although the basis for cleavage at these minor sites is not obvious, it is possible that they are induced by distortions in the oligonucleotide caused by the presence of the OTI. Alternatively, an OTI attached to the transport helix could act in trans to induce cleavage within the gate helix (Figure 11A). However,

this seems unlikely, as cleavage patterns for these minor sites do not coincide with those observed in the presence of free etoposide (compare Figure 23 to Figure 29).

In contrast to their ability to target translocations over parental sequences, OTIs are less able to discern between parental sequences and sequences containing single mismatches, suggesting that they are not currently optimized to target SNPs. However, it does appear that OTIs can retain effectiveness against their target sequences even in the presence of mismatches, which could either arise as a result of mutation in a cancer cell lineage or could simply be present as variations in a heterogeneous population of cancer cells[225].

In order for OTIs to function in cells and block the expression of driver oncogenes, they would have to hybridize to their target sequence. It is envisioned that this could potentially take place when the two strands of the double helix are separated during replication or transcription (Figure 21). *In vitro* experiments suggest that single-stranded oligonucleotides as short as 24-mers can invade the double helix and form a D-loop[248]. Alternatively, invasion can be greatly enhanced by the presence of recombination proteins[249, 250].

The development of oligonucleotide-based therapeutics has been challenging[251]. However, improved chemistry and targeted delivery systems, together with the recent FDA approval of new RNA therapeutics[251], hold promise for the potential development of oligonucleotide-based agents. Modifying the chemical makeup of OTIs from deoxyribonucleic acids to a different backbone, such as peptide nucleic acids[252], could enhance their affinity for the cognate genomic sequence, possibly enhancing their efficiency and allowing for their use against SNPs.

Chapter 5: Conclusions and Future Directions

The material discussed in this dissertation aims to address the issue of target specificity in chemotherapeutic topoisomerase II poisons. Although this class of topoisomerase II-targeting drugs is efficacious against cancer cells for a variety of reasons (see Chapter 1), it also induces undesirable side effects[102].

First, considerable circumstantial evidence indicates that topoisomerase IIβ is the primary isoform associated with the toxic side effects associated with treatment with topoisomerase II poisons, such as leukemogenesis and cardiotoxicity[63, 86, 87, 184, 253-257]. Developing compounds that are more specific to the α isoform compared to the β isoform could help reduce topoisomerase II poison-related toxicities[258, 259]. However, given the high structural similarity of the isoforms, this task has proven to be difficult, and no truly isoform-specific compounds have been developed to date[18, 259]. Unfortunately, many of the compounds that have preferences for one isoform or the other tend to induce higher-fold increases in DNA cleavage mediated by topoisomerase IIβ rather than IIα[127, 129, 148, 190]. Given the problems associated with current topoisomerase II poisons, the exploration of new drug scaffolds could help identify new compounds that have the potential to be stronger topoisomerase II poisons than the currently used drugs and to be more specific for topoisomerase IIα.

The work in Chapter 3 explored the use of trifluoromethylated 9-amino-3,4-dihydroacridin-1(2H)-one derivatives (Figure 13) as topoisomerase II poisons. Initial experiments indicated that five of the seven derivatives tested were topoisomerase IIα poisons, but they were not nearly as potent as etoposide or amsacrine (Figure 15). By their CC_3 measures, the most potent derivative (compound 3) was 10 times less potent than amsacrine and about 2.6 times less potent than etoposide (Figure 15). As enhanced interactions with DNA can lead to greater drug activity against type II topoisomerases[113], the compounds were tested for their ability to intercalate

with DNA (Figure 16). Some of the derivatives were weak intercalators at best (such as compound 3), and a couple did not appear to intercalate into the DNA at all. Additional testing indicated that the trifluoromethylated 9-amino-3,4-dihydroacridin-1(2H)-one derivatives carried out their topoisomerase II-poisoning activity through a covalent poison mechanism (Table 1). This was suggested by a lack of inhibition of topoisomerase IIα-mediated religation (Figure 17), by the sharp reduction of compound activity after incubation with DTT (Figure 18), by a lack of activity against the catalytic core of the enzyme (Figure 19), and by the inhibition of enzyme-mediated DNA cleavage when the compounds were incubated with the enzyme prior to the addition of DNA (Figure 20).

Although many dietary poisons that are associated with chemoprevention are covalent poisons of topoisomerase II, all of the clinically relevant poisons act in a non-covalent manner by preventing religation of the DNA at the DNA-enzyme interface[94, 260]. Covalent topoisomerase poisons act by adducting (primarily to cysteines) their target enzyme, but they have the potential to interfere with the function of a plethora of other proteins. Thus, the current structures of the trifluoromethylated 9-amino-3,4-dihydroacridin-1(2H)-one derivatives explored in this dissertation are not promising for the development of new clinical compounds. It is worth noting that the 4'-amino-methane-sulfon-*m*-anisidide head group of amsacrine acts as a covalent topoisomerase II poison, yet the intact amsacrine molecule acts as an interfacial poison[113]. Coupling the trifluoromethylated 9-amino-3,4-dihydroacridin-1(2H)-one derivatives to a headgroup could change the nature of their interaction with DNA and with the enzyme. No tests were carried out with topoisomerase IIβ, but given the relatively high concentration of the derivatives required to enhance cleavage by topoisomerase IIα compared to etoposide and amsacrine, such testing is likely to be superfluous without modification of the skeleton of the trifluoromethylated 9-amino-3,4-dihydroacridin-1(2H)-ones. Future work in collaboration with the

laboratory of Dr. Cosmas Okoro at Tennessee State University intends to explore related compounds (with and without headgroups) against human type II topoisomerases.

A second source of topoisomerase II poison-related side effects is the ubiquitous nature of type II topoisomerases throughout the body[59, 87, 162, 181, 185]. Reduction of those side effects would result from better drug targeting of cancer cells. Current approaches include the use of nanoparticles[192-194], drug-polymer conjugates[189-191], drug-loaded hydrogels[195], receptor-based targeting[194], and antibody-drug conjugates[196] among others. Chapter 4 takes a DNA-targeting approach, as it explores the use of oligonucleotide-drug conjugates (OTIs) that are specific to DNA sequences present in cancer cells. The decreasing costs of genome sequencing[261, 262] suggest that OTIs use could be highly individualized.

OTIs are designed such that their oligonucleotide portion is complementary to cancer-specific DNA sequences. It is envisioned that OTIs, as currently designed, could bind to their complementary sequence when the double helix is opened during transcription or replication (Figure 21). Once bound to their target sequence, the linked topoisomerase II poisons could induce the formation of topoisomerase II cleavage complexes at that site that would then interfere with proper replication and transcription at that locus. As OTIs would be designed to target cancer-specific sequences, their effect on non-cancerous cells is expected to be minimal.

The current design of OTIs was informed by several factors. The chosen topoisomerase II poison was etoposide given that it has historically been well studied[50, 106, 115, 119, 121, 124, 223], and therefore any observed effects of the OTIs against type II topoisomerases could be interpreted within the context of previous knowledge. As the active core of etoposide, DEPT, shows similar levels of activity against topoisomerase II compared to the parent compound[123, 124], it was utilized in the synthesis of the OTIs. DEPT lacks the sugar moiety at C4, which allowed for the activation of the C4 hydroxyl group for coupling reactions.

Another factor affecting the design of the OTIs was the length of the linker that joined the DEPT to the oligonucleotide (Figure 8). Computational simulations with OTIs of different linker lengths (data not shown) indicated that the linker needed to be long enough to allow the DEPT to curve back into the DNA, as shorter linkers placed the DEPT outside of the bounds of the double helix (data not shown). Based on the simulations, the selected linker length allowed the DEPT to interact with the DNA on the opposing strand (Figures 11, 12, 22, and 25).

Finally, the sequence chosen for the initial OTIs was that of intron 6 of the *PML* gene, which contains a strong drug-induced topoisomerase II cleavage hotspot[84, 87, 98, 99]. Subsequent OTIs were synthesized with the sequence of a t(15;17) translocation observed in a t-APL patient treated with mitoxantrone for MS, which was also observed to be a strong site of mitoxantrone-induced cleavage *in vitro*[99].

The proof-of-principle experiments presented in Chapter 4 aimed to determine if OTIs could induce cleavage by type II topoisomerases, and whether said cleavage could be constrained by the sequence specificity of the employed OTI. Initial results with OTI28 indicated that (when hybridized to a complementary oligonucleotide) the OTI could induce higher levels of topoisomerase IIα- and IIβ-mediated DNA cleavage compared to free etoposide (Figure 23). Further testing suggested that the inclusion of the DEPT on the OTI was chemically necessary for its poisoning of type II topoisomerases, the other possibility being that the OTIs acted as DNA lesions that enhanced cleavage by the type II topoisomerases. A “precursor” version of OTI28 (an OTI with a modified nucleotide containing the linker but no DEPT), LIN28 (compound 6, Figure 8), did not lead to any enzyme-mediated DNA cleavage (Figure 23). The OTIs inhibited DNA religation and stabilized cleavage complexes on a similar timescale as free etoposide (Figure 26), results that would not be expected were the OTIs acting like DNA lesions. As lesions that act as topoisomerase II poisons act by enhancing the forward rate of cleavage instead of

inhibiting religation or stabilizing cleavage complexes[18, 92, 152-159], the effects of the OTIs are believed to be mediated by the tethered drug moiety as opposed to a distortion in the double helix. These results were supported by the decrease in cleavage enhancement observed when an OTI-containing double-stranded oligonucleotide was incubated with a mutant yeast topoisomerase II that was resistant to etoposide (Figure 28)[201].

To determine whether or not type II topoisomerases could be directed to cleave at specific sequences, three new OTIs were generated that varied in the position of the attached DEPT. The results observed in Figure 29 indicate that incubation of each OTI with the type II topoisomerases resulted in unique cleavage patterns. Two takeaway points can be gleaned from these data. First, OTIs can be used to induce DNA cleavage, at least in part, in a predictable manner, as strong topoisomerase IIα-mediated DNA cleavage induced by the new OTIs was observed two bases away opposite the drug location (Figure 29). Second, sites of cleavage can be moved to sequences not normally associated with the actions of free etoposide (Figures 23 and 29), suggesting that sequences generated by novel translocations in cancer cells could still be targeted even though they do not represent previously-observed topoisomerase II cleavage sites.

The key experiments demonstrating the potential of OTIs involved the incubation of topoisomerase IIα and IIβ with non-complementary duplexes. No DNA cleavage was observed when either enzyme was incubated with a *PML* top strand or a *RARA* top strand and a *PML-RARA* bottom strand in the presence of free etoposide, nor when either top strand was annealed to an OTI that was 50, 30, or 20 nucleotides long (Figure 31). Results demonstrated that the 50-mer and 30-mer OTIs, but not the 20-mer OTI, were able to increase enzyme-mediated DNA cleavage when annealed to complementary *PML-RARA* oligonucleotides (Figure 30), which suggests that OTIs could target their complementary sequence without inducing cleavage of the

parental sequences. A 26-mer OTI annealed to a complementary *PML-RARA* oligonucleotide demonstrated similar cleavage as the 30-mer OTI at site 20-21, but markedly reduced cleavage at 23-24 (data not shown). As the longer OTIs (50-mer and 30-mer) maintained high levels of cleavage at both sites compared to shorter OTIs (20-mer and 26-mer)(Figure 30, data not shown), these results suggest that the minimum effective length for the tested OTIs is somewhere between 27 and 30 nucleotides long, although the length might depend on the specific OTI.

The final section of Chapter 4 explored the effects of mismatches on the ability of OTIs to induce topoisomerase II-mediated DNA cleavage. The reasons for testing DNA duplexes containing a mismatch are two-fold. First, although the results with the *PML* and *RARA* oligonucleotides suggest that OTIs can target translocation sequences, they do not speak to the ability of OTIs to target other types of cancer-specific sequences, like SNPs. Second, they can afford us mechanistic information as to how the drug-enzyme-DNA ternary complex interacts. Type II topoisomerases have a sequence preference for where they cleave[149, 230], and this preference changes depending on the presence of different topoisomerase II poisons (Table 2)[149, 231-235]. OTIs can help us determine if the cleavage site preferences of the enzymes change considering that the drug is fixed or “hardwired” into the system.

Cleavage data on the mismatch oligonucleotides indicates that both type II topoisomerase isoforms are capable of inducing DNA cleavage when the substrate includes an OTI (Figures 33, 34, and 35), but not when the substrate was an unmodified duplex incubated in the presence of free etoposide (Figure 32). These data suggest that OTIs are not specific enough for type II topoisomerases to discern between a fully complementary sequence and a sequence that contains a single mismatch. The implications of these results are that SNPs are not optimal targets for OTIs, but imply that OTIs can retain their effectiveness against their target even if

new mutations arise at that locus, or if there is genetic variation among a population of cancer cells[225].

Figure 32 shows that mismatch-containing, non-OTI oligonucleotide duplexes tend to decrease cleavage even in the presence of free etoposide, especially when the mismatch is located 5' to a site of cleavage. There were some exceptions, however, which are likely attributed to mismatch-induced distortions that are translated down the duplex and that facilitate cleavage at other sites[204]. In contrast, data from Figures 33, 34, and 35 suggest that, when OTIs are part of the substrate, mismatches 5' to the cleavage sites tend to maintain lower levels of cleavage mediated by both enzymes compared to mismatches 3' to the cleavage site. Cleavage on OTI-containing duplexes was observed even when the cleavage sites had bases at the -1 position that are not normally preferred either by topoisomerase IIα (A) nor by type II topoisomerases in the presence of etoposide (not C or T)[149, 230-235]. Collectively, these data suggest that the attachment of the etoposide core onto the OTI is enough to overcome some of the physical constraints[121] that normally would prevent a fruitful interaction between the enzyme, the drug, and the DNA.

The experiments described in Chapter 4 provide a promising first look into the use and potential of OTIs, but also leave several questions unanswered. OTIs can function in *in vitro* systems where they are annealed to complementary oligonucleotides, but future experiments must explore the function of OTIs in situations that are more representative of the cellular environment in which their target is double stranded. *In vitro* experiments suggest that single-stranded oligonucleotides as short as 24-mers can spontaneously invade the double helix and form a D-loop[248]. Results from Figure 30 suggest that OTIs 20 nucleotides long do not induce strong levels of cleavage at their target sites, so it is therefore conceivable that the shortest effective OTIs could similarly invade the double helix. The strand invasion ability of OTIs could

be investigated by incubating them with a modified plasmid bearing a 319-bp segment of *PML*. If no strand invasion is observed, Rad51 could be added into the reactions[249, 250]. Rad51 has a major role in homologous recombination, as it helps facilitate the invasion of a ssDNA strand into a complementary DNA duplex[249, 250]; thus, Rad51 might facilitate the invasion of an OTI into the DNA duplex that contains the OTI target sequence.

Further, experiments exploring the ability of OTIs to interfere with DNA processing systems such as transcription and replication are necessary before transitioning into a cellular system. To begin, *in vitro* transcription reactions could be set up to monitor transcription on the *PML*-modified plasmid. Monitoring of the products by northern blot analysis would indicate whether a OTIs can inhibit the production of the RNA product. Investigations of the effect of OTIs on DNA replication could be carried out in *Xenopus laevis* egg extracts in collaboration with Vanderbilt University Department of Biochemistry faculty Dr. James Dewar. His laboratory employs a cell-free *Xenopus* egg extract system that promotes sequence non-specific replication of DNA that would allow for the use of the *PML*-modified plasmid[20]. Monitoring the appearance of replication products in the presence and absence of an OTI would provide information on whether or not the OTIs are capable of interfering with DNA replication. Results of these experiments can be compared to those of similar experiments that contain free etoposide but no OTI to help discern if the OTIs interfere with replication by acting as topoisomerase II poisons or if they interfere by virtue of base pairing with their target. Collectively, the above experiments would also inform on whether it is necessary for the DNA duplex to be open for the OTIs to exert their function, or whether the OTIs have the capability to invade their target duplexes.

It is important to note that all of the conducted and proposed experiments thus far are proof of concept. OTIs in their current design have two main problems that preclude their use in patients or even in cells. First, OTIs have a deoxyribonucleic acid backbone, which makes them

immensely susceptible to degradation inside cells[263, 264]. Second, although there have been great strides in the development and delivery of RNA and other nucleic acid-based therapies[243, 265], there has not been much research into nucleic acid transfection into nuclei considering that these technologies tend to target RNAs in the cytosol[243].

To address the first issue, there are different modifications that change the structure of the backbone that still allow the OTIs to retain sequence specificity for their target, or that could delay or prevent their degradation. Peptide nucleic acids (PNA), for example, are non-natural analogs of DNA with a *N*-(2-aminoethyl)glycine backbone that is linked through peptide bonds instead of phosphodiester bonds[252]. The nucleobases in PNA retain their spatial arrangement, which allows them to base pair with DNA, RNA, and PNA. The peptide backbone of PNA affords several advantages over DNA. First, it is not susceptible to enzymatic degradation. Second, it is neutral, which reduces the repulsion the DNA backbone has to itself (facilitates packaging for drug delivery) and with the opposing strand (enhances hybridization strength)[252]. In fact, the hybridization strength of PNA oligomers to complementary PNA and DNA is greater than that of DNA to DNA[252]. Thus, PNA-OTIs would likely have a higher affinity for their target DNA sequence than the target strand would have to its genomic complement.

A second possible oligomer structure involves the use of locked nucleic acids (LNA)[243]. This type of modification is mainly used in antisense technologies that target RNAs, and is characterized by a methylene bridge connecting the 2′-oxygen and the 4′-carbon atoms in the furanose ring of ribonucleic acids[243, 266]. Despite being ribonucleotide analogs, LNAs can bind to DNA with higher affinity than DNA has to itself[266, 267]. A number of other options are available, including nucleic acid analogs with phosphorothioate linkages instead of the canonical phosphodiester bonds[243, 265, 268], 2′-*O*-methoxyethyl-modified oligonucleotides (2′-MOE)[243, 268], and 2’-*O*-constrained ethyl-modified (cEt) nucleotides[267].

Research on nucleic acid modifications such as the ones described above has come hand-in-hand with developments in cell delivery methods[192, 193, 243, 252, 266, 268-270]. Modified nucleic acids have been introduced into cells through a variety of mechanisms, including encapsulation in nanoparticles[192-194], loading of drugs into hydrogels[195], or through receptor-based targeting[194] or antibody-drug conjugation[196] among others. Although most of the work to date has focused on drug delivery into cells, there is evidence that some modified oligonucleotides, such as LNA, localize to nuclei following transfection[266].

The initial experiments with OTIs contained herein demonstrate that they are effective at inducing topoisomerase II-mediated DNA cleavage in a sequence-specific manner. Developments in oligonucleotide therapies open up the way for further exploration of OTIs beyond the current *in vitro* systems.

References

1. Hershey, A.D. and M. Chase, *Independent functions of viral protein and nucleic acid in growth of bacteriophage.* J. Gen. Physiol., 1952. **36**(1): p. 39-56.
2. Watson, J.D. and F.H. Crick, *Molecular structure of nucleic acids; A structure for deoxyribose nucleic acid.* Nature, 1953. **171**(4356): p. 737-738.
3. Watson, J.D. and F.H. Crick, *Genetical implications of the structure of deoxyribonucleic acid.* Nature, 1953. **171**(4361): p. 964-967.
4. Kanaar, R. and N.R. Cozzarelli, *Roles of supercoiled DNA structure in DNA transactions.* Curr. Opin. Struct. Biol., 1992. **2**(3): p. 369-379.
5. Wang, J.C., *DNA topoisomerases.* Annu. Rev. Biochem., 1996. **65**: p. 635-692.
6. Wang, J.C., *Cellular roles of DNA topoisomerases: A molecular perspective.* Nat. Rev. Mol. Cell. Biol., 2002. **3**(6): p. 430-440.
7. Bates, A.D. and A. Maxwell, *DNA Topology*. 2005: Oxford University Press.
8. Deweese, J.E., M.A. Osheroff, and N. Osheroff, *DNA topology and topoisomerases: Teaching a "knotty" subject.* Biochem. Mol. Biol. Educ., 2008. **37**(1): p. 2-10.
9. Espeli, O. and K.J. Marians, *Untangling intracellular DNA topology.* Mol. Microbiol., 2004. **52**(4): p. 925-31.
10. Travers, A. and G. Muskhelishvili, *A common topology for bacterial and eukaryotic transcription initiation?* EMBO Rep., 2007. **8**(2): p. 147-151.
11. Falaschi, A., et al., *Molecular and structural transactions at human DNA replication origins.* Cell Cycle, 2007. **6**(14): p. 1705-1712.
12. Schvartzman, J.B. and A. Stasiak, *A topological view of the replicon.* EMBO Rep., 2004. **5**(3): p. 256-261.
13. Mirkin, S.M., *DNA Topology: Fundamentals*, in *eLS*. 2001, John Wiley & Sons, Ltd.
14. Champoux, J.J., *DNA topoisomerases: Structure, function, and mechanism.* Ann. Rev. Biochem., 2001. **70**: p. 369-413.
15. Meselson, M. and F.W. Stahl, *The Replication of DNA in Escherichia Coli.* Proc. Natl. Acad. Sci. U.S.A., 1958. **44**(7): p. 671-82.
16. Hirt, B., *Evidence for semiconservative replication of circular polyoma DNA.* Proc. Natl. Acad. Sci. U.S.A., 1966. **55**(4): p. 997-1004.
17. Gross, N.J. and M. Rabinowitz, *Synthesis of new strands of mitochondrial and nuclear deoxyribonucleic acid by semiconservative replication.* J. Biol. Chem., 1969. **244**(6): p. 1563-6.
18. Deweese, J.E. and N. Osheroff, *The DNA cleavage reaction of topoisomerase II: Wolf in sheep's clothing.* Nucleic Acids Res., 2009. **37**(3): p. 738-748.
19. Nitiss, J.L., *DNA topoisomerase II and its growing repertoire of biological functions.* Nat. Rev. Cancer, 2009. **9**(5): p. 327-337.
20. Dewar, J.M., M. Budzowska, and J.C. Walter, *The mechanism of DNA replication termination in vertebrates.* Nature, 2015. **525**(7569): p. 345-50.
21. Pommier, Y., et al., *Roles of eukaryotic topoisomerases in transcription, replication and genomic stability.* Nat. Rev. Mol. Cell Biol., 2016. **17**(11): p. 703-721.
22. Wasserman, S.A. and N.R. Cozzarelli, *Biochemical topology: applications to DNA recombination and replication.* Science, 1986. **232**(4753): p. 951-60.
23. Shishido, K., N. Komiyama, and S. Ikawa, *Increased production of a knotted form of plasmid pBR322 DNA in Escherichia coli DNA topoisomerase mutants.* J. Mol. Biol., 1987. **195**(1): p. 215-8.

24. Rybenkov, V.V., N.R. Cozzarelli, and A.V. Vologodskii, *Probability of DNA knotting and the effective diameter of the DNA double helix.* Proc. Natl. Acad. Sci. U.S.A., 1993. **90**(11): p. 5307-11.
25. Vos, S.M., et al., *All tangled up: How cells direct, manage and exploit topoisomerase function.* Nat. Rev. Mol. Cell. Biol., 2011. **12**(12): p. 827-841.
26. Chen, S.H., N.-L. Chan, and T.-S. Hsieh, *New mechanistic and functional insights into DNA topoisomerases.* Ann. Rev. Biochem., 2013. **82**(1): p. 139-170.
27. Kikuchi, A. and K. Asai, *Reverse gyrase--a topoisomerase which introduces positive superhelical turns into DNA.* Nature, 1984. **309**(5970): p. 677-81.
28. Hsieh, T.S. and J.L. Plank, *Reverse gyrase functions as a DNA renaturase: annealing of complementary single-stranded circles and positive supercoiling of a bubble substrate.* J. Biol. Chem., 2006. **281**(9): p. 5640-7.
29. Bizard, A.H., et al., *TopA, the Sulfolobus solfataricus topoisomerase III, is a decatenase.* Nucleic Acids Res., 2018. **46**(2): p. 861-872.
30. Koster, D.A., et al., *Friction and torque govern the relaxation of DNA supercoils by eukaryotic topoisomerase IB.* Nature, 2005. **434**(7033): p. 671-4.
31. Bush, N.G., K. Evans-Roberts, and A. Maxwell, *DNA Topoisomerases.* EcoSal Plus, 2015. **6**(2).
32. Taneja, B., et al., *Structure of the N-terminal fragment of topoisomerase V reveals a new family of topoisomerases.* EMBO J., 2006. **25**(2): p. 398-408.
33. Zhang, H., J.C. Wang, and L.F. Liu, *Involvement of DNA topoisomerase I in transcription of human ribosomal RNA genes.* Proc. Natl. Acad. Sci. U.S.A., 1988. **85**(4): p. 1060-4.
34. Kretzschmar, M., M. Meisterernst, and R.G. Roeder, *Identification of human DNA topoisomerase I as a cofactor for activator-dependent transcription by RNA polymerase II.* Proc. Natl. Acad. Sci. U.S.A., 1993. **90**(24): p. 11508-12.
35. Zhang, H., et al., *Human mitochondrial topoisomerase I.* Proc. Natl. Acad. Sci. U.S.A., 2001. **98**(19): p. 10608-13.
36. Hiasa, H., R.J. DiGate, and K.J. Marians, *Decatenating activity of Escherichia coli DNA gyrase and topoisomerases I and III during oriC and pBR322 DNA replication in vitro.* J. Biol. Chem., 1994. **269**(3): p. 2093-9.
37. Harmon, F.G., R.J. DiGate, and S.C. Kowalczykowski, *RecQ helicase and topoisomerase III comprise a novel DNA strand passage function: a conserved mechanism for control of DNA recombination.* Mol. Cell, 1999. **3**(5): p. 611-20.
38. Swuec, P. and A. Costa, *Molecular mechanism of double Holliday junction dissolution.* Cell Biosci., 2014. **4**: p. 36.
39. Goto-Ito, S., et al., *Structural basis of the interaction between Topoisomerase IIIβ and the TDRD3 auxiliary factor.* Sci. Rep., 2017. **7**: p. 42123.
40. Ahmad, M., et al., *Topoisomerase 3β is the major topoisomerase for mRNAs and linked to neurodevelopment and mental dysfunction.* Nucleic Acids Res., 2017. **45**(5): p. 2704-2713.
41. Stoll, G., et al., *Deletion of TOP3β, a component of FMRP-containing mRNPs, contributes to neurodevelopmental disorders.* Nat. Neurosci., 2013. **16**(9): p. 1228-1237.
42. Xu, D., et al., *Top3β is an RNA topoisomerase that works with fragile X syndrome protein to promote synapse formation.* Nat. Neurosci., 2013. **16**(9): p. 1238-47.
43. Lee, M.P., et al., *DNA topoisomerase I is essential in Drosophila melanogaster.* Proc. Natl. Acad. Sci. U.S.A., 1993. **90**(14): p. 6656-60.

44. Morham, S.G., et al., *Targeted disruption of the mouse topoisomerase I gene by camptothecin selection.* Mol. Cell Biol., 1996. **16**(12): p. 6804-9.
45. Miao, Z.H., et al., *Nonclassic functions of human topoisomerase I: genome-wide and pharmacologic analyses.* Cancer Res., 2007. **67**(18): p. 8752-61.
46. Gellert, M., et al., *DNA gyrase: an enzyme that introduces superhelical turns into DNA.* Proc. Natl. Acad. Sci. U.S.A., 1976. **73**(11): p. 3872-6.
47. Bergerat, A., et al., *An atypical topoisomerase II from Archaea with implications for meiotic recombination.* Nature, 1997. **386**(6623): p. 414-7.
48. Gadelle, D., et al., *DNA topoisomerase VIII: a novel subfamily of type IIB topoisomerases encoded by free or integrated plasmids in Archaea and Bacteria.* Nucleic Acids Res., 2014. **42**(13): p. 8578-91.
49. Osheroff, N., *Effect of antineoplastic agents on the DNA cleavage/religation reaction of eukaryotic topoisomerase II: inhibition of DNA religation by etoposide.* Biochemistry, 1989. **28**(15): p. 6157-60.
50. Bromberg, K.D., A.B. Burgin, and N. Osheroff, *A two-drug model for etoposide action against human topoisomerase IIα.* J. Biol. Chem., 2003. **278**(9): p. 7406-12.
51. Deweese, J.E. and N. Osheroff, *The use of divalent metal ions by type II topoisomerases.* Metallomics, 2010. **2**(7): p. 450-9.
52. Levine, C., H. Hiasa, and K.J. Marians, *DNA gyrase and topoisomerase IV: biochemical activities, physiological roles during chromosome replication, and drug sensitivities.* Biochim. Biophys. Acta, 1998. **1400**(1-3): p. 29-43.
53. Sissi, C. and M. Palumbo, *In front of and behind the replication fork: bacterial type IIA topoisomerases.* Cell. Mol. Life Sci., 2010. **67**(12): p. 2001-24.
54. Cole, S.T., et al., *Deciphering the biology of Mycobacterium tuberculosis from the complete genome sequence.* Nature, 1998. **393**(6685): p. 537-44.
55. Aubry, A., et al., *First functional characterization of a singly expressed bacterial type II topoisomerase: the enzyme from Mycobacterium tuberculosis.* Biochem. Biophys. Res. Commun., 2006. **348**(1): p. 158-65.
56. Ashley, R.E., et al., *Recognition of DNA Supercoil Geometry by Mycobacterium tuberculosis Gyrase.* Biochemistry, 2017. **56**(40): p. 5440-5448.
57. Wendorff, T.J., et al., *The structure of DNA-bound human topoisomerase IIα: Conformational mechanisms for coordinating inter-subunit interactions with DNA cleavage.* J. Mol. Biol., 2012. **424**(3-4): p. 109-124.
58. Lindsey, R.H., et al., *Catalytic core of human topoisomerase IIα: Insights into enzyme–DNA interactions and drug mechanism.* Biochemistry, 2014. **53**(41): p. 6595-6602.
59. McClendon, A.K. and N. Osheroff, *DNA topoisomerase II, genotoxicity, and cancer.* Mutat. Res., 2007. **623**(1-2): p. 83-97.
60. Lee, I., K.C. Dong, and J.M. Berger, *The role of DNA bending in type IIA topoisomerase function.* Nucleic Acids Res., 2013. **41**(10): p. 5444-56.
61. Vologodskii, A.V., et al., *Mechanism of topology simplification by type II DNA topoisomerases.* Proc. Natl. Acad. Sci. U.S.A., 2001. **98**(6): p. 3045-9.
62. Dong, K.C. and J.M. Berger, *Structural basis for gate-DNA recognition and bending by type IIA topoisomerases.* Nature, 2007. **450**(7173): p. 1201-1205.
63. Delgado, J.L., et al., *Topoisomerases as anticancer targets.* Biochem. J., 2018. **475**(2): p. 373-398.
64. Schmidt, B.H., et al., *A novel and unified two-metal mechanism for DNA cleavage by type II and IA topoisomerases.* Nature, 2010. **465**(7298): p. 641-4.

65. Schmidt, B.H., N. Osheroff, and J.M. Berger, *Structure of a topoisomerase II-DNA-nucleotide complex reveals a new control mechanism for ATPase activity.* Nat. Struct. Mol. Biol., 2012. **19**(11): p. 1147-54.
66. Mueller-Planitz, F. and D. Herschlag, *Coupling between ATP binding and DNA cleavage by DNA topoisomerase II: A unifying kinetic and structural mechanism.* J. Biol. Chem., 2008. **283**(25): p. 17463-17476.
67. Lindsley, J.E. and J.C. Wang, *On the coupling between ATP usage and DNA transport by yeast DNA topoisomerase II.* J. Biol. Chem., 1993. **268**(11): p. 8096-8104.
68. Tsai-Pflugfelder, M., et al., *Cloning and sequencing of cDNA encoding human DNA topoisomerase II and localization of the gene to chromosome region 17q21-22.* Proc. Natl. Acad. Sci. U.S.A., 1988. **85**(19): p. 7177-7181.
69. Chung, T.D., et al., *Characterization and immunological identification of cDNA clones encoding two human DNA topoisomerase II isozymes.* Proc. Natl. Acad. Sci. U.S.A., 1989. **86**(23): p. 9431-9435.
70. Austin, C.A. and L.M. Fisher, *Isolation and characterization of a human cDNA clone encoding a novel DNA topoisomerase II homologue from HeLa cells.* FEBS Lett., 1990. **266**(1-2): p. 115-7.
71. Tan, K.B., et al., *Topoisomerase IIα and topoisomerase IIβ genes: Characterization and mapping to human chromosomes 17 and 3, respectively.* Cancer Res., 1992. **52**(1): p. 231-234.
72. Jenkins, J.R., et al., *Isolation of cDNA clones encoding the β isozyme of human DNA topoisomerase II and localisation of the gene to chromosome 3p24.* Nucleic Acids Res., 1992. **20**(21): p. 5587-92.
73. Drake, F.H., et al., *Purification of topoisomerase II from amsacrine-resistant P388 leukemia cells. Evidence for two forms of the enzyme.* J. Biol. Chem., 1987. **262**(34): p. 16739-16747.
74. Drake, F.H., et al., *Biochemical and pharmacological properties of p170 and p180 forms of topoisomerase II.* Biochemistry, 1989. **28**(20): p. 8154-8160.
75. Woessner, R.D., et al., *Proliferation- and cell cycle-dependent differences in expression of the 170 kilodalton and 180 kilodalton forms of topoisomerase II in NIH-3T3 cells.* Cell Growth Differ., 1991. **2**(4): p. 209-214.
76. Tiwari, V.K., et al., *Target genes of Topoisomerase IIβ regulate neuronal survival and are defined by their chromatin state.* Proc. Natl. Acad. Sci. U.S.A., 2012. **109**(16): p. E934-43.
77. Bollimpelli, V.S., P.S. Dholaniya, and A.K. Kondapi, *Topoisomerase IIβ and its role in different biological contexts.* Arch. Biochem. Biophys., 2017. **633**: p. 78-84.
78. Watanabe, M., et al., *Differential expressions of the topoisomerase IIα and IIβ mRNAs in developing rat brain.* Neurosci. Res., 1994. **19**(1): p. 51-7.
79. Ju, B.G., et al., *A topoisomerase IIβ-mediated dsDNA break required for regulated transcription.* Science, 2006. **312**(5781): p. 1798-1802.
80. Ju, B.G. and M.G. Rosenfeld, *A breaking strategy for topoisomerase IIβ/PARP-1-dependent regulated transcription.* Cell Cycle, 2006. **5**(22): p. 2557-60.
81. Yu, X., et al., *Genome-wide TOP2A DNA cleavage is biased toward translocated and highly transcribed loci.* Genome Res., 2017. **27**(7): p. 1238-1249.
82. Yang, X., et al., *DNA topoisomerase IIβ and neural development.* Science, 2000. **287**: p. 131-134.

83. Lyu, Y.L. and J.C. Wang, *Aberrant lamination in the cerebral cortex of mouse embryos lacking DNA topoisomerase IIß.* Proc. Natl. Acad. Sci. U.S.A., 2003. **100**(12): p. 7123-8.
84. Felix, C.A., *Secondary leukemias induced by topoisomerase-targeted drugs.* Biochim. Biophys. Acta, 1998. **1400**(1-3): p. 233-55.
85. Anderson, V.E. and N. Osheroff, *Type II topoisomerases as targets for quinolone antibacterials: turning Dr. Jekyll into Mr. Hyde.* Curr. Pharm. Des., 2001. **7**(5): p. 337-53.
86. Nitiss, J.L., *Targeting DNA topoisomerase II in cancer chemotherapy.* Nat. Rev. Cancer, 2009. **9**(5): p. 338-350.
87. Pendleton, M., et al., *Topoisomerase II and leukemia.* Ann. N.Y. Acad. Sci., 2014. **1310**(1): p. 98-110.
88. Berger, J.M., et al., *Structure and mechanism of DNA topoisomerase II.* Nature, 1996. **379**(6562): p. 225-232.
89. Fortune, J.M. and N. Osheroff, *Topoisomerase II as a target for anticancer drugs: When enzymes stop being nice*, in *Progress in Nucleic Acid Research and Molecular Biology*, K. Moldave, Editor. 2000, Elsevier. p. 221-253.
90. Schoeffler, A.J. and J.M. Berger, *Recent advances in understanding structure-function relationships in the type II topoisomerase mechanism.* Biochem. Soc. Trans., 2005. **33**(Pt 6): p. 1465-1470.
91. Bender, R. and N. Osheroff, *DNA Topoisomerases as Targets for the Chemotherapeutic Treatment of Cancer*, in *Checkpoint Responses in Cancer Therapy*, W. Dai, Editor. 2008, Humana Press.
92. Deweese, J.E., A.B. Burgin, and N. Osheroff, *Using 3'-bridging phosphorothiolates to isolate the forward DNA cleavage reaction of human topoisomerase IIα.* Biochemistry, 2008. **47**(13): p. 4129-40.
93. Howard, M.T., et al., *Disruption of a topoisomerase-DNA cleavage complex by a DNA helicase.* Proc. Natl. Acad. Sci. U.S.A., 1994. **91**(25): p. 12031-5.
94. Pommier, Y. and C. Marchand, *Interfacial inhibitors: Targeting macromolecular complexes.* Nat. Rev. Drug. Discov., 2012. **11**(1): p. 25-36.
95. Pommier, Y., *Drugging topoisomerases: Lessons and challenges.* ACS Chem. Biol., 2013. **8**(1): p. 82-95.
96. Felix, C.A. and B.J. Lange, *Leukemia in infants.* Oncologist, 1999. **4**(3): p. 225-240.
97. Felix, C.A., *Leukemias related to treatment with DNA topoisomerase II inhibitors.* Med. Pediatr. Oncol., 2001. **36**(5): p. 525-535.
98. Mistry, A.R., et al., *DNA topoisomerase II in therapy-related acute promyelocytic leukemia.* N. Engl. J. Med., 2005. **352**(15): p. 1529-1538.
99. Hasan, S.K., et al., *Molecular analysis of t(15;17) genomic breakpoints in secondary acute promyelocytic leukemia arising after treatment of multiple sclerosis.* Blood, 2008. **112**(8): p. 3383-3390.
100. Ezoe, S., *Secondary leukemia associated with the anti-cancer agent, etoposide, a topoisomerase II inhibitor.* Int. J. Environ. Res. Public Health, 2012. **9**(7): p. 2444-2453.
101. Holm, C., et al., *Differential requirement of DNA replication for the cytotoxicity of DNA topoisomerase I and II inhibitors in Chinese hamster DC3F cells.* Cancer Res., 1989. **49**(22): p. 6365-8.
102. Gibson, E.G. and J.E. Deweese, *Covalent poisons of topoisomerase II.* J. Curr. Top. Pharmacol., 2013. **17**: p. 1-12.
103. Puigvert, J.C., K. Sanjiv, and T. Helleday, *Targeting DNA repair, DNA metabolism and replication stress as anti-cancer strategies.* FEBS J., 2016. **283**(2): p. 232-45.

104. Murai, J., *Targeting DNA repair and replication stress in the treatment of ovarian cancer.* Int. J. Clin. Oncol., 2017. **22**(4): p. 619-628.
105. Pommier, Y., et al., *DNA topoisomerases and their poisoning by anticancer and antibacterial drugs.* Chem. Biol., 2010. **17**(5): p. 421-433.
106. Baldwin, E.L. and N. Osheroff, *Etoposide, topoisomerase II and cancer.* Curr. Med. Chem. Anticancer Agents, 2005. **5**(4): p. 363-372.
107. PubChem. *Etoposide*. [cited 2018 Nov. 29]; Available from: https://pubchem.ncbi.nlm.nih.gov/compound/36462.
108. PubChem. *Doxorubicin*. [cited 2018 Nov. 29]; Available from: https://pubchem.ncbi.nlm.nih.gov/compound/31703.
109. PubChem. *Mitoxantrone*. [cited 2018 Nov. 29]; Available from: https://pubchem.ncbi.nlm.nih.gov/compound/4212.
110. Lallana, E.C. and C.E. Fadul, *Toxicities of immunosuppressive treatment of autoimmune neurologic diseases.* Curr. Neuropharmacol., 2011. **9**(3): p. 468-77.
111. PubChem. *Amsacrine*. [cited 2018 Nov. 29]; Available from: https://pubchem.ncbi.nlm.nih.gov/compound/amsacrine.
112. Nelson, E.M., K.M. Tewey, and L.F. Liu, *Mechanism of antitumor drug action: poisoning of mammalian DNA topoisomerase II on DNA by 4'-(9-acridinylamino)-methanesulfon-m-anisidide.* Proc. Natl. Acad. Sci. U.S.A., 1984. **81**(5): p. 1361-1365.
113. Ketron, A.C., et al., *Amsacrine as a topoisomerase II poison: Importance of drug-DNA interactions.* Biochemistry, 2012. **51**(8): p. 1730-1739.
114. Gamage, S.A., et al., *Structure-activity relationships for substituted bis(acridine-4-carboxamides): a new class of anticancer agents.* J. Med. Chem., 1999. **42**(13): p. 2383-93.
115. Hande, K.R., *Etoposide: Four decades of development of a topoisomerase II inhibitor.* Eur. J. Cancer, 1998. **34**(10): p. 1514-1521.
116. Greenspan, E.M., J. Leiter, and M.J. Shear, *Effect of alpha-peltatin, beta-peltatin, podophyllotoxin on lymphomas and other transplanted tumors.* J. Natl. Cancer Inst., 1950. **10**(6): p. 1295-1333.
117. Cortese, F., B. Bhattacharyya, and J. Wolff, *Podophyllotoxin as a probe for the colchicine binding site of tubulin.* J. Biol. Chem., 1977. **252**(4): p. 1134-40.
118. Stahelin, H.F. and A. von Wartburg, *The chemical and biological route from podophyllotoxin glucoside to etoposide: ninth Cain memorial Award lecture.* Cancer Res., 1991. **51**(1): p. 5-15.
119. Meresse, P., et al., *Etoposide: discovery and medicinal chemistry.* Curr. Med. Chem., 2004. **11**(18): p. 2443-66.
120. Loike, J.D. and S.B. Horwitz, *Effects of podophyllotoxin and VP-16-213 on microtubule assembly in vitro and nucleoside transport in HeLa cells.* Biochemistry, 1976. **15**(25): p. 5435-43.
121. Burden, D.A., et al., *Topoisomerase II-Etoposide interactions direct the formation of drug-induced enzyme-DNA cleavage complexes.* J. Biol. Chem., 1996. **271**(46): p. 29238-29244.
122. Wilstermann, A.M. and N. Osheroff, *Stabilization of eukaryotic topoisomerase II-DNA cleavage complexes.* Curr. Top. Med. Chem., 2003. **3**: p. 1349-1364.
123. Wilstermann, A.M., et al., *Topoisomerase II-drug interaction domains: Identification of substituents on etoposide that interact with the enzyme.* Biochemistry, 2007. **46**(28): p. 8217-8225.

124. Bender, R.P., et al., *Substituents on etoposide that interact with human topoisomerase IIα in the binary enzyme-drug complex: Contributions to etoposide binding and activity.* Biochemistry, 2008. **47**(15): p. 4501-4509.
125. Austin, C.A., et al., *Site-specific DNA cleavage by mammalian DNA topoisomerase II induced by novel flavone and catechin derivatives.* Biochem. J., 1992. **282 (Pt 3)**: p. 883-9.
126. Bandele, O.J. and N. Osheroff, *(-)-Epigallocatechin gallate, a major constituent of green tea, poisons human type II topoisomerases.* Chem. Res. Toxicol., 2008. **21**(4): p. 936-43.
127. Bandele, O.J. and N. Osheroff, *Bioflavonoids as poisons of human topoisomerase IIα and IIβ.* Biochemistry, 2007. **46**(20): p. 6097-6108.
128. Ketron, A.C., et al., *Oxidative metabolites of curcumin poison human type II topoisomerases.* Biochemistry, 2013. **52**(1): p. 221-227.
129. Vann, K.R., et al., *Effects of olive metabolites on DNA cleavage mediated by human type II topoisomerases.* Biochemistry, 2015. **54**(29): p. 4531-4541.
130. Ashley, R.E. and N. Osheroff, *Natural products as topoisomerase II poisons: Effects of thymoquinone on DNA cleavage mediated by human topoisomerase IIα.* Chem. Res. Toxicol., 2014. **27**(5): p. 787-793.
131. Ketron, A.C. and N. Osheroff, *Phytochemicals as anticancer and chemopreventive topoisomerase II poisons.* Phytochem. Rev., 2014. **13**(1): p. 19-35.
132. Kandaswami, C., et al., *The antitumor activities of flavonoids.* In Vivo, 2005. **19**(5): p. 895-909.
133. Barnes, S., T.G. Peterson, and L. Coward, *Rationale for the use of genistein-containing soy matrices in chemoprevention trials for breast and prostate cancer.* J. Cell. Biochem. Suppl., 1995. **22**: p. 181-7.
134. Spector, L.G., et al., *Maternal diet and infant leukemia: the DNA topoisomerase II inhibitor hypothesis: a report from the children's oncology group.* Cancer Epidemiol. Biomarkers Prev., 2005. **14**(3): p. 651-5.
135. Puumala, S.E., et al., *Epidemiology of childhood acute myeloid leukemia.* Pediatr. Blood Cancer, 2013. **60**(5): p. 728-33.
136. Wu, C.C., et al., *Structural basis of type II topoisomerase inhibition by the anticancer drug etoposide.* Science, 2011. **333**(6041): p. 459-462.
137. Mondrala, S. and D.A. Eastmond, *Topoisomerase II inhibition by the bioactivated benzene metabolite hydroquinone involves multiple mechanisms.* Chem. Biol. Interact., 2010. **184**(1-2): p. 259-68.
138. Wang, H., et al., *Stimulation of topoisomerase II-mediated DNA damage via a mechanism involving protein thiolation.* Biochemistry, 2001. **40**(11): p. 3316-3323.
139. Bender, R.P. and N. Osheroff, *Mutation of cysteine residue 455 to alanine in human topoisomerase IIα confers hypersensitivity to quinones: Enhancing DNA scission by closing the N-terminal protein gate.* Chem. Res. Toxicol., 2007. **20**(6): p. 975-981.
140. Lin, R.K., et al., *Dietary isothiocyanate-induced apoptosis via thiol modification of DNA topoisomerase IIα.* J. Biol. Chem., 2011. **286**(38): p. 33591-33600.
141. Srinivasan, A., L.W. Robertson, and G. Ludewig, *Sulfhydryl binding and topoisomerase inhibition by PCB metabolites.* Chem. Res. Toxicol., 2002. **15**(4): p. 497-505.
142. Bender, R.P., et al., *Polychlorinated biphenyl quinone metabolites poison human topoisomerase IIα: Altering enzyme function by blocking the N-terminal protein gate.* Biochemistry, 2006. **45**(33): p. 10140-10152.

143. Bender, R.P., A.J. Ham, and N. Osheroff, *Quinone-induced enhancement of DNA cleavage by human topoisomerase IIα: Adduction of cysteine residues 392 and 405.* Biochemistry, 2007. **46**(10): p. 2856-2864.
144. Lindsey, R.H., Jr., et al., *1,4-Benzoquinone is a topoisomerase II poison.* Biochemistry, 2004. **43**(23): p. 7563-7574.
145. Bender, R.P., et al., *N-acetyl-p-benzoquinone imine, the toxic metabolite of acetaminophen, is a topoisomerase II poison.* Biochemistry, 2004. **43**(12): p. 3731-3739.
146. Lindsey, R.H., Jr., R.P. Bender, and N. Osheroff, *Effects of benzene metabolites on DNA cleavage mediated by human topoisomerase IIα: 1,4-hydroquinone is a topoisomerase II poison.* Chem. Res. Toxicol., 2005. **18**(4): p. 761-770.
147. Jacob, D.A., et al., *Etoposide quinone is a redox-dependent topoisomerase II poison.* Biochemistry, 2011. **50**(25): p. 5660-5667.
148. Smith, N.A., et al., *Etoposide quinone is a covalent poison of human topoisomerase IIβ.* Biochemistry, 2014. **53**(19): p. 3229-36.
149. Capranico, G. and M. Binaschi, *DNA sequence selectivity of topoisomerases and topoisomerase poisons.* Biochim. Biophys. Acta, 1998. **1400**(1-3): p. 185-194.
150. Pommier, Y. and C. Marchand, *Interfacial inhibitors of protein-nucleic acid interactions.* Curr. Med. Chem. Anticancer Agents, 2005. **5**(4): p. 421-429.
151. Chen, G.L., et al., *Nonintercalative antitumor drugs interfere with the breakage-reunion reaction of mammalian DNA topoisomerase II.* J .Biol. Chem., 1984. **259**(21): p. 13560-13566.
152. Kingma, P.S. and N. Osheroff, *Apurinic sites are position-specific topoisomerase II poisons.* J. Biol. Chem., 1997. **272**(2): p. 1148-55.
153. Kingma, P.S., C.A. Greider, and N. Osheroff, *Spontaneous DNA lesions poison human topoisomerase IIα and stimulate cleavage proximal to leukemic 11q23 chromosomal breakpoints.* Biochemistry, 1997. **36**(20): p. 5934-5939.
154. Kingma, P.S. and N. Osheroff, *The response of eukaryotic topoisomerases to DNA damage.* Biochim. Biophys. Acta, 1998. **1400**(1-3): p. 223-32.
155. Cline, S.D. and N. Osheroff, *Cytosine arabinoside lesions are position-specific topoisomerase II poisons and stimulate DNA cleavage mediated by the human type II enzymes.* J. Biol. Chem., 1999. **274**(42): p. 29740-3.
156. Cline, S.D., et al., *DNA abasic lesions in a different light: solution structure of an endogenous topoisomerase II poison.* Biochemistry, 1999. **38**(47): p. 15500-7.
157. Sabourin, M. and N. Osheroff, *Sensitivity of human type II topoisomerases to DNA damage: stimulation of enzyme-mediated DNA cleavage by abasic, oxidized and alkylated lesions.* Nucleic Acids Res., 2000. **28**(9): p. 1947-54.
158. Khan, Q.A., et al., *Position-specific trapping of topoisomerase II by benzo[a]pyrene diol epoxide adducts: implications for interactions with intercalating anticancer agents.* Proc. Natl. Acad. Sci. U.S.A., 2003. **100**(21): p. 12498-503.
159. Velez-Cruz, R., et al., *Exocyclic DNA lesions stimulate DNA cleavage mediated by human topoisomerase IIα in vitro and in cultured cells.* Biochemistry, 2005.
160. Wilstermann, A.M. and N. Osheroff, *Base excision repair intermediates as topoisomerase II poisons.* J. Biol. Chem., 2001. **276**(49): p. 46290-6.
161. Baguley, B.C. and L.R. Ferguson, *Mutagenic properties of topoisomerase-targeted drugs.* Biochim. Biophys. Acta, 1998. **1400**(1-3): p. 213-22.
162. Felix, C.A., C.P. Kolaris, and N. Osheroff, *Topoisomerase II and the etiology of chromosomal translocations.* DNA Repair, 2006. **5**(9-10): p. 1093-1108.

163. DeVore, R., et al., *Therapy-related acute nonlymphocytic leukemia with monocytic features and rearrangement of chromosome 11q.* Ann. Intern. Med., 1989. **110**(9): p. 740-2.
164. Pui, C.H., et al., *Acute myeloid leukemia in children treated with epipodophyllotoxins for acute lymphoblastic leukemia.* N. Engl. J. Med., 1991. **325**(24): p. 1682-7.
165. Smith, M.A., L. Rubinstein, and R.S. Ungerleider, *Therapy-related acute myeloid leukemia following treatment with epipodophyllotoxins: estimating the risks.* Med. Pediatr. Oncol., 1994. **23**(2): p. 86-98.
166. Smith, M.A., et al., *Secondary leukemia or myelodysplastic syndrome after treatment with epipodophyllotoxins.* J. Clin. Oncol., 1999. **17**(2): p. 569-77.
167. Le Deley, M.C., et al., *Risk of secondary leukemia after a solid tumor in childhood according to the dose of epipodophyllotoxins and anthracyclines: a case-control study by the Societe Francaise d'Oncologie Pediatrique.* J. Clin. Oncol., 2003. **21**(6): p. 1074-81.
168. De Kouchkovsky, I. and M. Abdul-Hay, *'Acute myeloid leukemia: a comprehensive review and 2016 update'.* Blood Cancer J., 2016. **6**(7): p. e441.
169. Felix, C.A., et al., *Chromosome band 11q23 translocation breakpoints are DNA topoisomerase II cleavage sites.* Cancer Res., 1995. **55**: p. 4287-4292.
170. Milne, T.A., et al., *MLL targets SET domain methyltransferase activity to Hox gene promoters.* Mol. Cell, 2002. **10**(5): p. 1107-17.
171. Cowell, I.G., et al., *Model for MLL translocations in therapy-related leukemia involving topoisomerase IIß-mediated DNA strand breaks and gene proximity.* Proc. Natl. Acad. Sci. U.S.A., 2012. **109**(23): p. 8989-94.
172. Lovett, B.D., et al., *Etoposide metabolites enhance DNA topoisomerase II cleavage near leukemia-associated MLL translocation breakpoints.* Biochemistry, 2001. **40**(5): p. 1159-70.
173. Robinson, B.W., et al., *Prospective tracing of MLL-FRYL clone with low MEIS1 expression from emergence during neuroblastoma treatment to diagnosis of myelodysplastic syndrome.* Blood, 2008. **111**(7): p. 3802-12.
174. Lovett, B.D., et al., *Near-precise interchromosomal recombination and functional DNA topoisomerase II cleavage sites at MLL and AF-4 genomic breakpoints in treatment-related acute lymphoblastic leukemia with t(4;11) translocation.* Proc. Natl. Acad. Sci. U.S.A., 2001. **98**(17): p. 9802-7.
175. Whitmarsh, R.J., et al., *Reciprocal DNA topoisomerase II cleavage events at 5'-TATTA-3' sequences in MLL and AF-9 create homologous single-stranded overhangs that anneal to form der(11) and der(9) genomic breakpoint junctions in treatment-related AML without further processing.* Oncogene, 2003. **22**(52): p. 8448-59.
176. Cowell, I.G. and C.A. Austin, *Mechanism of generation of therapy related leukemia in response to anti-topoisomerase II agents.* Int. J. Environ. Res. Public Health, 2012. **9**(6): p. 2075-2091.
177. Joannides, M., et al., *Molecular pathogenesis of secondary acute promyelocytic leukemia.* Mediterr. J. Hematol. Infect. Dis., 2011. **3**(1): p. e2011045.
178. Ellis, R., S. Brown, and M. Boggild, *Therapy-related acute leukaemia with mitoxantrone: four years on, what is the risk and can it be limited?* Mult. Scler., 2015. **21**(5): p. 642-5.
179. Reiter, A., et al., *Genomic anatomy of the specific reciprocal translocation t(15;17) in acute promyelocytic leukemia.* Genes Chromosomes Cancer, 2003. **36**(2): p. 175-88.
180. Joannides, M. and D. Grimwade, *Molecular biology of therapy-related leukaemias.* Clin. Transl. Oncol., 2010. **12**(1): p. 8-14.

181. Azarova, A.M., et al., *Roles of DNA topoisomerase II isozymes in chemotherapy and secondary malignancies.* Proc. Natl. Acad. Sci. U.S.A., 2007. **104**(26): p. 11014-9.
182. Papantonis, A. and P.R. Cook, *Transcription factories: genome organization and gene regulation.* Chem. Rev., 2013. **113**(11): p. 8683-705.
183. Lyu, Y.L., et al., *Topoisomerase IIβ mediated DNA double-strand breaks: implications in doxorubicin cardiotoxicity and prevention by dexrazoxane.* Cancer Res., 2007. **67**(18): p. 8839-8846.
184. Menna, P., E. Salvatorelli, and G. Minotti, *Cardiotoxicity of antitumor drugs.* Chem. Res. Toxicol., 2008. **21**(5): p. 978-989.
185. Sehested, M., et al., *Antagonistic effect of the cardioprotector (+)-1,2-bis(3,5-dioxopiperazinyl-1-yl)propane (ICRF-187) on DNA breaks and cytotoxicity induced by the topoisomerase II directed drugs daunorubicin and etoposide (VP-16).* Biochem. Pharmacol., 1993. **46**(3): p. 389-93.
186. Pellettieri, J. and A. Sanchez Alvarado, *Cell turnover and adult tissue homeostasis: from humans to planarians.* Annu. Rev. Genet., 2007. **41**: p. 83-105.
187. Bachrach, U. and N. Seiler, *Formation of acetylpolyamines and putrescine from spermidine by normal and transformed chick embryo fibroblasts.* Cancer Res., 1981. **41**(3): p. 1205-8.
188. Barret, J.M., et al., *F14512, a potent antitumor agent targeting topoisomerase II vectored into cancer cells via the polyamine transport system.* Cancer Res., 2008. **68**(23): p. 9845-53.
189. Kruczynski, A., et al., *Preclinical activity of F14512, designed to target tumors expressing an active polyamine transport system.* Invest. New Drugs, 2011. **29**(1): p. 9-21.
190. Oviatt, A.A., et al., *Polyamine-containing etoposide derivatives as poisons of human type II topoisomerases: Differential effects on topoisomerase IIα and IIβ.* Bioorg. Med. Chem. Lett., 2018. **28**(17): p. 2961-2968.
191. Khan, J., et al., *Exploring the role of polymeric conjugates toward anti-cancer drug delivery: Current trends and future projections.* Int. J. Pharm., 2018. **548**(1): p. 500-514.
192. King, M.R. and Z.J. Mohamed, *Dual nanoparticle drug delivery: the future of anticancer therapies?* Nanomedicine, 2017. **12**(2): p. 95-98.
193. Kamath, P.R. and D. Sunil, *Nano-Chitosan Particles in Anticancer Drug Delivery: An Up-to-Date Review.* Mini Rev. Med. Chem., 2017. **17**(15): p. 1457-1487.
194. Singh, S.K., et al., *Drug delivery approaches for breast cancer.* Int. J. Nanomedicine, 2017. **12**: p. 6205-6218.
195. Bastiancich, C., et al., *Anticancer drug-loaded hydrogels as drug delivery systems for the local treatment of glioblastoma.* J. Control Release, 2016. **243**: p. 29-42.
196. Abdollahpour-Alitappeh, M., et al., *Antibody-drug conjugates (ADCs) for cancer therapy: Strategies, challenges, and successes.* J. Cell. Physiol., 2018.
197. Infante Lara, L., et al., *Novel trifluoromethylated 9-amino-3,4-dihydroacridin-1(2H)-ones act as covalent poisons of human topoisomerase IIα.* Bioorg. Med. Chem. Lett., 2017. **27**(3): p. 586-589.
198. Infante Lara, L., et al., *Coupling the core of the anticancer drug etoposide to an oligonucleotide induces topoisomerase II-mediated cleavage at specific DNA sequences.* Nucleic Acids Res., 2018. **46**(5): p. 2218-2233.
199. Worland, S.T. and J.C. Wang, *Inducible overexpression, purification, and active site mapping of DNA topoisomerase II from the yeast Saccharomyces cerevisiae.* J. Biol. Chem., 1989. **264**(8): p. 4412-4416.

200. Wasserman, R.A., et al., *Use of yeast in the study of anticancer drugs targeting DNA topoisomerases: Expression of a functional recombinant human DNA topoisomerase IIα in yeast.* Cancer Res., 1993. **53**(15): p. 3591-3596.
201. Elsea, S.H., et al., *A yeast type II topoisomerase selected for resistance to quinolones. Mutation of histidine 1012 to tyrosine confers resistance to nonintercalative drugs but hypersensitivity to ellipticine.* J. Biol. Chem., 1995. **270**(4): p. 1913-20.
202. Byl, J.A., et al., *DNA topoisomerase II as the target for the anticancer drug TOP-53: mechanistic basis for drug action.* Biochemistry, 2001. **40**(3): p. 712-8.
203. Liu, Q. and J.C. Wang, *Identification of active site residues in the "GyrA" half of yeast DNA topoisomerase II.* J. Biol. Chem., 1998. **273**(32): p. 20252-60.
204. Rossetti, G., et al., *The structural impact of DNA mismatches.* Nucleic Acids Res., 2015. **43**(8): p. 4309-21.
205. Fortune, J.M. and N. Osheroff, *Merbarone inhibits the catalytic activity of human topoisomerase IIα by blocking DNA cleavage.* J. Biol. Chem., 1998. **273**(28): p. 17643-17650.
206. Fortune, J.M., et al., *DNA topoisomerases as targets for the anticancer drug TAS-103: DNA interactions and topoisomerase catalytic inhibition.* Biochemistry, 1999. **38**(47): p. 15580-15586.
207. Byl, J.A., et al., *DNA topoisomerases as targets for the anticancer drug TAS-103: Primary cellular target and DNA cleavage enhancement.* Biochemistry, 1999. **38**(47): p. 15573-15579.
208. Bromberg, K.D., et al., *DNA ligation catalyzed by human topoisomerase IIα.* Biochemistry, 2004. **43**(42): p. 13416-23.
209. Bandele, O.J. and N. Osheroff, *The efficacy of topoisomerase II-targeted anticancer agents reflects the persistence of drug-induced cleavage complexes in cells.* Biochemistry, 2008. **47**(45): p. 11900-11908.
210. Cui, B., et al., *Synthesis of enaminones in aqueous media using catalytic dilute HCl.* Synth. Commun., 2011. **41**(7): p. 1064-1070.
211. Shutske, G.M., et al., *9-Amino-1,2,3,4-tetrahydroacridin-1-ols. Synthesis and evaluation as potential Alzheimer's disease therapeutics.* J. Med. Chem., 1989. **32**(8): p. 1805-1813.
212. Emsley, P., *Tools for ligand validation in Coot.* Acta. Crystallogr. D. Struct. Biol., 2017. **73**(Pt 3): p. 203-210.
213. ULC, C.C.G., *Molecular Operating Environment (MOE)*. 2017: Sherbooke St. West, Suite #910, Montreal, QC, Canada.
214. Wang, Y.R., et al., *Producing irreversible topoisomerase II-mediated DNA breaks by site-specific Pt(II)-methionine coordination chemistry.* Nucleic Acids Res., 2017. **45**(18): p. 10861-10871.
215. Chan, P.F., et al., *Structural basis of DNA gyrase inhibition by antibacterial QPT-1, anticancer drug etoposide and moxifloxacin.* Nat. Commun., 2015. **6**: p. 10048.
216. Fadeyi, O.O., et al., *Novel fluorinated acridone derivatives. Part 1: Synthesis and evaluation as potential anticancer agents.* Bioorg. Med. Chem. Lett., 2008. **18**(14): p. 4172-4176.
217. Baranello, L., et al., *DNA break mapping reveals topoisomerase II activity genome-wide.* Int. J. Mol. Sci., 2014. **15**(7): p. 13111-22.
218. Rowley, J.D., *Letter: A new consistent chromosomal abnormality in chronic myelogenous leukaemia identified by quinacrine fluorescence and Giemsa staining.* Nature, 1973. **243**(5405): p. 290-3.

219. Barreca, A., et al., *Anaplastic lymphoma kinase in human cancer.* J. Mol. Endocrinol., 2011. **47**(1): p. R11-23.
220. Stenman, G., *Fusion oncogenes in salivary gland tumors: molecular and clinical consequences.* Head Neck Pathol., 2013. **7 Suppl 1**: p. S12-9.
221. Matsumoto, Y., et al., *Incidence of mutation and deletion in topoisomerase IIα mRNA of etoposide and mAMSA-resistant cell lines.* Jpn. J. Cancer Res., 2001. **92**(10): p. 1133-7.
222. Kanagasabai, R., et al., *Alternative RNA Processing of Topoisomerase IIα in Etoposide-Resistant Human Leukemia K562 Cells: Intron Retention Results in a Novel C-Terminal Truncated 90-kDa Isoform.* J. Pharmacol. Exp. Ther., 2017. **360**(1): p. 152-163.
223. Kingma, P.S., D.A. Burden, and N. Osheroff, *Binding of etoposide to topoisomerase II in the absence of DNA: decreased affinity as a mechanism of drug resistance.* Biochemistry, 1999. **38**(12): p. 3457-61.
224. Cordon-Cardo, C., et al., *p53 mutations in human bladder cancer: genotypic versus phenotypic patterns.* Int. J. Cancer, 1994. **56**(3): p. 347-53.
225. Lawrence, M.S., et al., *Mutational heterogeneity in cancer and the search for new cancer-associated genes.* Nature, 2013. **499**(7457): p. 214-218.
226. Zhao, H., et al., *Somatic Mutation of the SNP rs11614913 and Its Association with Increased MIR 196A2 Expression in Breast Cancer.* DNA Cell Biol., 2016. **35**(2): p. 81-7.
227. Aoi, T., *Biology of lung cancer: genetic mutation, epithelial-mesenchymal transition, and cancer stem cells.* Gen. Thorac. Cardiovasc. Surg., 2016. **64**(9): p. 517-23.
228. Benafif, S. and R. Eeles, *Genetic predisposition to prostate cancer.* Br. Med. Bull., 2016. **120**(1): p. 75-89.
229. Minotti, L., et al., *SNPs and Somatic Mutation on Long Non-Coding RNA: New Frontier in the Cancer Studies?* High Throughput, 2018. **7**(4).
230. Strumberg, D., et al., *Molecular analysis of yeast and human type II topoisomerases. Enzyme-DNA and drug interactions.* J. Biol. Chem., 1999. **274**(40): p. 28246-55.
231. Capranico, G., K.W. Kohn, and Y. Pommier, *Local sequence requirements for DNA cleavage by mammalian topoisomerase II in the presence of doxorubicin.* Nucleic Acids Res., 1990. **18**(22): p. 6611-9.
232. Pommier, Y., et al., *Local base sequence preferences for DNA cleavage by mammalian topoisomerase II in the presence of amsacrine or teniposide.* Nucleic Acids Res., 1991. **19**(21): p. 5973-80.
233. Capranico, G., et al., *Effects of base mutations on topoisomerase II DNA cleavage stimulated by mAMSA in short DNA oligomers.* Biochemistry, 1993. **32**(1): p. 145-52.
234. Capranico, G., et al., *Similar sequence specificity of mitoxantrone and VM-26 stimulation of in vitro DNA cleavage by mammalian DNA topoisomerase II.* Biochemistry, 1993. **32**(12): p. 3038-46.
235. Capranico, G., et al., *Conformational drug determinants of the sequence specificity of drug-stimulated topoisomerase II DNA cleavage.* J. Mol. Biol., 1994. **235**(4): p. 1218-30.
236. Bigioni, M., et al., *Position-specific effects of base mismatch on mammalian topoisomerase II DNA cleaving activity.* Biochemistry, 1996. **35**(1): p. 153-9.
237. Bender, R.P. and N. Osheroff, *DNA topoisomerases as targets for the chemotherapeutic treatment of cancer*, in *Checkpoint Responses in Cancer Therapy*, W. Dai, Editor. 2008, Humana Press: Totowa, New Jersey. p. 57-91.
238. Mays, A.N., et al., *Evidence for direct involvement of epirubicin in the formation of chromosomal translocations in t(15;17) therapy-related acute promyelocytic leukemia.* Blood, 2010. **115**(2): p. 326-30.

239. Ratain, M.J., et al., *Acute nonlymphocytic leukemia following etoposide and cisplatin combination chemotherapy for advanced non-small-cell carcinoma of the lung.* Blood, 1987. **70**(5): p. 1412-7.
240. Ramkumar, B., et al., *Acute promyelocytic leukemia after mitoxantrone therapy for multiple sclerosis.* Cancer Genet. Cytogenet., 2008. **182**(2): p. 126-9.
241. Druker, B.J., et al., *Effects of a selective inhibitor of the Abl tyrosine kinase on the growth of Bcr-Abl positive cells.* Nat. Med., 1996. **2**(5): p. 561-6.
242. Mansour, M.R., et al., *Oncogene regulation. An oncogenic super-enhancer formed through somatic mutation of a noncoding intergenic element.* Science, 2014. **346**(6215): p. 1373-7.
243. Adams, B.D., et al., *Targeting noncoding RNAs in disease.* J. Clin. Invest., 2017. **127**(3): p. 761-771.
244. Arimondo, P.B., et al., *Exploring the cellular activity of camptothecin-triple-helix-forming oligonucleotide conjugates.* Mol. Cell Biol., 2006. **26**(1): p. 324-33.
245. Duca, M., et al., *Molecular basis of the targeting of topoisomerase II-mediated DNA cleavage by VP16 derivatives conjugated to triplex-forming oligonucleotides.* Nucleic Acids Res., 2006. **34**(6): p. 1900-11.
246. Davies, S.M., et al., *Nuclear topoisomerase II levels correlate with the sensitivity of mammalian cells to intercalating agents and epipodophyllotoxins.* J. Biol. Chem., 1988. **263**(33): p. 17724-9.
247. Coutts, J., et al., *Expression of topoisomerase IIα and β in an adenocarcinoma cell line carrying amplified topoisomerase IIα and retinoic acid receptor alpha genes.* Br. J. Cancer, 1993. **68**(4): p. 793-800.
248. Necasova, I., et al., *Basic domain of telomere guardian TRF2 reduces D-loop unwinding whereas Rap1 restores it.* Nucleic Acids Res., 2017. **45**(21): p. 12170-12180.
249. Li, X., et al., *PCNA is required for initiation of recombination-associated DNA synthesis by DNA polymerase delta.* Mol. Cell, 2009. **36**(4): p. 704-13.
250. Bower, B.D. and J.D. Griffith, *TRF1 and TRF2 differentially modulate Rad51-mediated telomeric and nontelomeric displacement loop formation in vitro.* Biochemistry, 2014. **53**(34): p. 5485-95.
251. Kaczmarek, J.C., P.S. Kowalski, and D.G. Anderson, *Advances in the delivery of RNA therapeutics: from concept to clinical reality.* Genome Med., 2017. **9**(1): p. 60.
252. Anstaett, P. and G. Gasser, *Peptide nucleic acid - an opportunity for bio-nanotechnology.* Chimia, 2014. **68**(4): p. 264-8.
253. Withoff, S., et al., *Differential expression of DNA topoisomerase IIα and β in P-gp and MRP-negative VM26, mAMSA and mitoxantrone-resistant sublines of the human SCLC cell line GLC4.* Br. J. Cancer, 1996. **74**(12): p. 1869-76.
254. Dereuddre, S., C. Delaporte, and A. Jacquemin-Sablon, *Role of topoisomerase IIβ in the resistance of 9-OH-ellipticine-resistant Chinese hamster fibroblasts to topoisomerase II inhibitors.* Cancer Res., 1997. **57**(19): p. 4301-8.
255. Herzog, C.E., et al., *Absence of topoisomerase IIβ in an amsacrine-resistant human leukemia cell line with mutant topoisomerase IIα.* Cancer Res., 1998. **58**(23): p. 5298-300.
256. Errington, F., et al., *Murine transgenic cells lacking DNA topoisomerase IIβ are resistant to acridines and mitoxantrone: analysis of cytotoxicity and cleavable complex formation.* Mol. Pharmacol., 1999. **56**(6): p. 1309-1316.

257. Zhang, S., et al., *Identification of the molecular basis of doxorubicin-induced cardiotoxicity.* Nat. Med., 2012. **18**(11): p. 1639-1642.
258. Chen, W., J. Qiu, and Y.M. Shen, *Topoisomerase IIα, rather than IIβ, is a promising target in development of anti-cancer drugs.* Drug. Discov. Ther., 2012. **6**(5): p. 230-7.
259. Mariani, A., et al., *Differential Targeting of Human Topoisomerase II Isoforms with Small Molecules.* J. Med. Chem., 2015. **58**(11): p. 4851-6.
260. Vann, K.R., et al., *Inhibition of human DNA topoisomerase IIα by two novel ellipticine derivatives.* Bioorg. Med. Chem. Lett., 2016.
261. van Nimwegen, K.J., et al., *Is the $1000 Genome as Near as We Think? A Cost Analysis of Next-Generation Sequencing.* Clin Chem, 2016. **62**(11): p. 1458-1464.
262. Plothner, M., M. Frank, and J.G. von der Schulenburg, *Cost analysis of whole genome sequencing in German clinical practice.* Eur J Health Econ, 2017. **18**(5): p. 623-633.
263. Medzhitov, R., *Recognition of microorganisms and activation of the immune response.* Nature, 2007. **449**(7164): p. 819-26.
264. Li, T. and Z.J. Chen, *The cGAS-cGAMP-STING pathway connects DNA damage to inflammation, senescence, and cancer.* J. Exp. Med., 2018. **215**(5): p. 1287-1299.
265. Jain, H.V., D. Verthelyi, and S.L. Beaucage, *Amphipathic trans-acting phosphorothioate DNA elements mediate the delivery of uncharged nucleic acid sequences in mammalian cells.* RSC Adv., 2015. **5**: p. 65245–65254.
266. Lundin, K.E., et al., *Biological activity and biotechnological aspects of locked nucleic acids*, in *Advances in Genetics*, T. Friedmann, J.C. Dunlap, and S.F. Goodwin, Editors. 2013, Elsevier. p. 47-107.
267. Seth, P.P., et al., *Short antisense oligonucleotides with novel 2'-4' conformationaly restricted nucleoside analogues show improved potency without increased toxicity in animals.* J. Med. Chem., 2009. **52**(1): p. 10-3.
268. Paton, D.M., *Nusinersen: antisense oligonucleotide to increase SMN protein production in spinal muscular atrophy.* Drugs Today, 2017. **53**(6): p. 327-337.
269. Koppelhus, U. and P.E. Nielsen, *Cellular delivery of peptide nucleic acid (PNA).* Adv. Drug Deliv. Rev., 2003. **55**(2): p. 267-80.
270. Douglas, A.G. and M.J. Wood, *Splicing therapy for neuromuscular disease.* Mol. Cell. Neurosci., 2013. **56**: p. 169-85.